INVESTIGATION OF THE EFFECT OF PHASE-CHANGE MATERIALS ON THE PERFORMANCE OF HOUSEHOLD REFRIGERATORS

A Thesis Submitted to
the Graduate School of Engineering and Science of
İzmir Institute of Technology
in Partial Fulfillment of the Requirements for the Degree of

MASTER OF SCIENCE

in Mechanical Engineering

by
Çağlar COŞKUN

July 2014
İZMİR

We approve the thesis of **Çağlar COŞKUN**.

Examining Committee Members:

_____

Assist. Prof. Dr. Ünver ÖZKOL
Department of Mechanical Engineering
İzmir Institute of Technology

_____

Assoc. Prof. Dr. Moghtada MOBEDİ
Department of Mechanical Engineering
İzmir Institute of Technology

_____

Assoc. Prof. Dr. Tahsin BAŞARAN
Department of Architecture
İzmir Institute of Technology

9 July 2014

_____

Assist. Prof. Dr. Ünver ÖZKOL
Supervisor, Department of Mechanical Engineering
İzmir Institute of Technology

_____

Prof. Dr. Metin TANOĞLU
Head of the Department of
Mechanical Engineering

_____

Prof. Dr. R. Tuğrul SENGER
Dean of the Graduate School of
Engineering and Sciences

ACKNOWLEDGMENTS

This thesis is dedicated to my family members, Ali Münif COŞKUN, Meral COŞKUN, Uygar COŞKUN and Barış COŞKUN, who always encouraged and supported me even the most difficult times during my studies.

I would like to thank all the professors and colleagues in ME department, who never denied their assistances, especially my advisor, Dr. Ünver ÖZKOL, who gave me the opportunity to complete my studies under his valuable guidance.

I would also like to thank to Gürcan DURMAZ for his helps and supports, and other R&D department employees of INDESIT Company.

Lastly, I would like to thank all of my friends with whom I always have good time together, especially my present and previous lab. friends, Yusufcan UZ, Ömer Buğra KANARGI, Veysel Egemen AĞAKAY and Serdar MALAK, for their precious office fellowship.

ABSTRACT

INVESTIGATION OF THE EFFECT OF PHASE-CHANGE MATERIALS ON THE PERFORMANCE OF HOUSEHOLD REFRIGERATORS

The main problem that this study deals with is the issues of thermal effectiveness of phase change materials (or PCM) application to household refrigerators and investigating the performance improvement with numerical methods. PCMs are materials that store thermal energy in latent heat form between its solidus and liquidus points. By this way, these materials can store large amount of heat in a narrow temperature range, which made them to gain popularity in recent years. By exploiting this feature of PCMs, it is thought that using these materials in household refrigerators could increase the energy efficiency, thus energy class of a refrigerator. Because, keeping the cold energy inside the refrigerated space as latent heat will decrease the number of stop and start cycles of the compressor. Decreasing the number of stop and start cycles is beneficial since the distribution of refrigerant fluid in the refrigeration cycle breaks down every time compressor is stopped and established again on the next start, which is the main inefficiency source.

In this study, at first, the steady temperature contours are extracted by steady state numerical simulations to see the possible locations for the application of PCMs. Then, transient simulations are conducted to understand the transient thermal behavior of the refrigerated space and these transient results are validated with experimental data. In the light of these steady and transient thermal pictures, PCMs having proper phase change temperatures are placed in appropriate places on the walls of the refrigerator and transient simulations are conducted to see the effects of PCMs. Since radiative heat transfer cannot be ignored in household refrigerators, all simulations are conducted with and without radiation and effects of radiation are also presented.

The well – known commercial computational fluid dynamics (CFD) code, FLUENT is employed for the numerical simulations.

ÖZET

FAZ DEĞİŞKEN MALZEMELERİN EV TİPİ BUZDOLAPLARININ PERFORMANSINA OLAN ETKİSİNİN İNCELENMESİ

Bu çalışmanın ele aldığı ana problem, ev tipi bir buzdolabında faz değişken malzemelerin (FDM) uygulanmasının ısıl yönden yararlılığı ve bu uygulamanın getirdiği performans artışının nümerik yöntemlerle incelenmesidir. FDM'ler, ısıl enerjiyi katı ve sıvı faz değişim sıcaklığı aralığında gizli ısı olarak depolayan malzemelere denmektedir. Bu malzemeler yüksek miktarda ısıyı dar bir sıcaklık aralığında depolayabilmektedirler ve bu özelliklerinden dolayı son yıllarda artan bir popülariteye sahiptirler. FDM'lerin bu özelliklerinden faydalanarak, onların ev tipi buzdolaplarında uygulanmasının buzdolabının enerji verimliliğini ve enerji sınıfını arttıracağı düşünülmektedir. Çünkü, buzdolabındaki soğuk enerjiyi gizli ısı olarak depolayarak, kompresörün çalışma ve durma döngü sayısı azaltılabilir. Kompresörün çalışma ve durma sıklığını azaltmak şu yönden yararlıdır; kompresör her durduğunda, soğutma çevrimi içerisindeki soğutucu akışkan dağılımı bozulur ve bir sonraki çalışmada tekrar oluşur ve bu durum genel verimsizlik kaynağıdır.

Bu çalışmada, öncelikle, FDM uygulanmasının yapılabileceği olarsı yerleri görmek amacıyla, kararlı simülasyonlar gerçekleştirilerek kararlı sıcaklık dağılımları çıkartılmıştır. Daha sonra, soğutucu bölmedeki ısıl durumunun zamana bağlı davranışını anlamak amacıyla zamana bağlı analizler gerçekleştirilmiş ve sonuçlar deneysel verilerle doğrulanmıştır. Elde edilen bu kararlı ve zamana bağlı ısıl görüntülerin ışığında, uygun faz değişim sıcaklığına sahip FDM'ler, buzdolabı duvarlarında uygun yerlere yerleştirilerek zamana bağlı analizler FDM'lerin etkisini görmek üzere tekrarlanmıştır. Ev tipi buzdolaplarında radyasyonlu ısı transferinin etkileri ihmal edilemeyecğinden dolayı, tüm analizler radyason açık ve kapalı olarak yapılmış ve radyasyonun etkileri sunulmuştur.

Nümerik analizlerde, bilinen bir ticari hesaplamalı akışkanlar dinamiği (HAD) paket programı olan FLUENT kullanılmıştır.

TABLE OF CONTENTS

LIST OF FIGURES

LIST OF TABLES

Table **Page**

LIST OF SYMBOLS

T_L	Absolute Temperature of Refrigerated Space	^oC
a	Absorption Coefficient	1/m
COP	Coefficient of Performance	
CFD	Computational Fluid Dynamics	
CAD	Computer Aided Drawing	
h_c	Convective Heat Transfer Coefficient	$W/m^2.K$
ρ	Density	kg/m^3
$\vec{s}$	Direction Vector	
μ	Dynamic Viscosity	kg/m.s
H	Enthalpy	J
g	Gravitational Acceleration	m/s^2
Q	Heat	W
C	Heat Capacity	W/kg
$\dot{Q}_H$	Heat Rejected to Ambient	W
$\dot{Q}_L$	Heat Transferred from Refrigerated Space	W
H	Height	m
ν	Kinematic Viscosity	m^2/s
L	Length	m
β	Liquid Fraction	
m	Mass	kg
s_P	Path Length	m
PCM	Phase Change Material	
ϕ	Phase Function	
$\vec{r}$	Position Vector	
P	Pressure	Pa
I	Radiation Intensity	W/sr
h_r	Radiative Heat Transfer Coefficient	
n	Refractive Index	
σ_s	Scattering Coefficient	1/m
$\vec{s}'$	Scattering Direction Vector	

Ω	Solid Angle	
$\tilde{v}$	Spalart – Allmaras Variable	
h	Specific Enthalpy	kJ/kg
s	Specific Entropy	kJ/kg.K
c_p	Specific Heat at Constant Pressure	kJ/kg.K
σ	Stefan – Boltzmann Coefficient	W/m^2K^4
T	Temperature	^oC
k	Thermal Conductivity	W/m.K
α	Thermal Diffusivity	
TES	Thermal Energy Storage	
η	Thermal Expansion Coefficient	1/K
k_T	Turbulence Kinetic Energy	J
μ_T	Turbulence Viscosity	kg/m.s
UDF	User Defined Function	
$\dot{W}_{IN}$	Work İnput to the Compressor	W

Subscripts

∞	Ambient
$evap$	Evaporator
fus	Fusion
$liquidus$	Liqudius Temperature
$melt$	Melting
ref	Reference
$solidus$	Solidus Temperature
w	Wall

Dimensionless Numbers

Nu	Nusselt Number
Pr	Prandtl Number
Ra	Rayleigh Number

CHAPTER 1

INTRODUCTION

Throughout the history, food preservation has always been one of oldest problems to survive in every culture. In old times before the invention of mechanical refrigeration systems, people keep their food and beverage by some primitive ways, such as by cooling in well preserved caves or in cold water wells, or by drying under the sun or in salt baths or by smoking. Smoking and salting are applied especially to the food which is susceptible to spoilage, such as meat or fish.

The milestones in cooling can be summarized as follows: At 1000 B.C., people in China are able to cut and store ice. Around 500 B.C., Chinese and Indian people are able to make ice in cold nights by putting water inside pots and keeping the pot wet. In England, at the beginning of 18^{th} century, ice can be collected in winter and put into icehouses to use them in summer. At 19^{th} century, portable ice boxes are started to be used.

The first artificial refrigeration were proposed and demonstrated by a Scotsman, Dr. William Cullen at mid – 1700s. He created a vacuum using a pump over a container filled by diethyl ether, which caused a sudden boiling and absorbing heat from the surroundings. Dr. William Cullen's demonstration is followed by the works of Oliver Evans, Jacob Perkins and Michael Faraday. At the beginning of 1800s, Michael Faraday liquefied ammonia to create a cooling effect. Oliver Evans designed the first refrigeration machine, which employs a compression cycle similar to the today's modern vapor compression cycle, but that machine is never built. Lately, his design is modified and built by Jacob Perkins and he patented his invention with the title "Apparatus and means for producing ice, and in cooling fluids." By his patent, Jacob Perkins is known as the father of refrigeration. German engineer, Carl von Linden is also a notable inventor in the history of refrigeration. He invented and patented not a refrigeration machine, but an improved method for continuous process of liquefying gases, such as ammonia, sulphur dioxide and methyl chloride for cooling purposes. In 1873, he developed a refrigerator whose working fluid is dimethyl ether. Later, he improved his invention with a more reliable working fluid, ammonia and built a

refrigerator based on ammonia in 1876. Today, ammonia is still used in industrial refrigeration systems.

1.1. Mechanical Refrigeration Systems

Refrigeration can be described as keeping a space cooler than ambient by transferring heat from that space to the ambient. It is a general term that is used for both space cooling for thermal comfort (air conditioning), and food cooling to delay the spoilage time. In more specific words, refrigeration is the science which deals with the process of reducing and maintaining the temperature of a media below the temperature of its surroundings (Dossat, 1961). The devices that employing a mechanical cycle for refrigeration are called refrigerators, and the process or cycle that refrigerators are based on are called refrigeration cycle. In any refrigeration cycle, the agent fluid that absorbs heat from the refrigerated space is called refrigerant.

Commonly used refrigerants are R600a, R134, R12 and ammonia. These fluids boil at about -18^{o}C to -20^{o}C in the evaporator of a refrigeration system (where the pressure is about 0.9 – 1 bar, which is close to normal ambient pressures) so that the evaporator and refrigerated space temperatures are maintained at acceptable limits if the refrigerator is working properly (M.M. Farid, 2010).

The main objective of refrigeration cycle is like moving water from one place to another with sponge. When a dry sponge is allowed to absorb water in a puddle and the wetted sponge is squeezed to a container, you exert an amount of energy much like to the compressor in a refrigeration cycle does (Whitman, Johnson, & Tomczyk, 2005).

In refrigeration systems, since heat flows from high temperature media to the low temperature media naturally and refrigeration system does the opposite, there is a need for thermal insulation in order to preserve the cooled space from getting hotter again.

1.2. Vapor – Compression Refrigeration Cycle

The main goal of a refrigeration system, which has the reverse effect of a heat engine is, removing the heat from a low level temperature media (refrigerated space)

and transfer this heat to a media that has higher temperature (warm environment) (Dincer & Kanoglu, 2011). In vapor – compression cycle, which is the most commonly used refrigeration cycle, there are four basic units which are evaporator, compressor, condenser and expansion valve. Each of these units completes different thermal processes. The schematic view of a vapor – compression cycle, is shown in Figure 1.1 with all of its equipment.

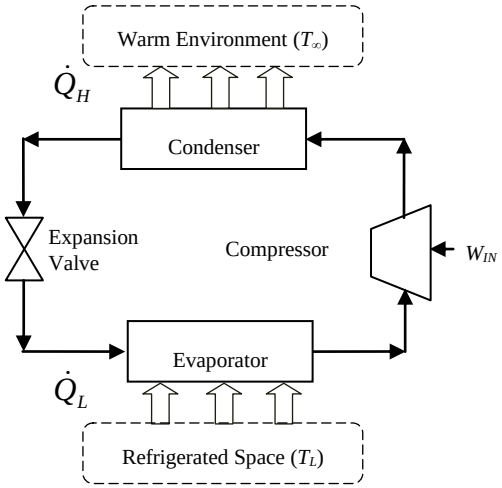

Figure 1.1. A vapor compression cycle with its basic components

Cycle parameters in Figure 1.1. can be defined as follows, the absolute temperature of refrigerated space is T_L, and the transferred heat to ambient from this refrigerated space is $\dot{Q}_L$. At the warm environment, the absolute temperature is T_∞ and the amount of heat rejected is $\dot{Q}_H$. These heat removal and reject processes are done by the work input to the compressor, $\dot{W}_{IN}$. The first law of thermodynamics can be applied to the continuous operation of this cycle.

1.2.1. P – h and T – s Diagrams

For a better understaning of this thermodynamic cyclic process explained above, $P - h$ (Pressure – enthalpy) and $T - s$ (Temperature – entropy) diagrams can be drawn for the ideal refrigeration cycle, and they are shown in Figure 1.2.

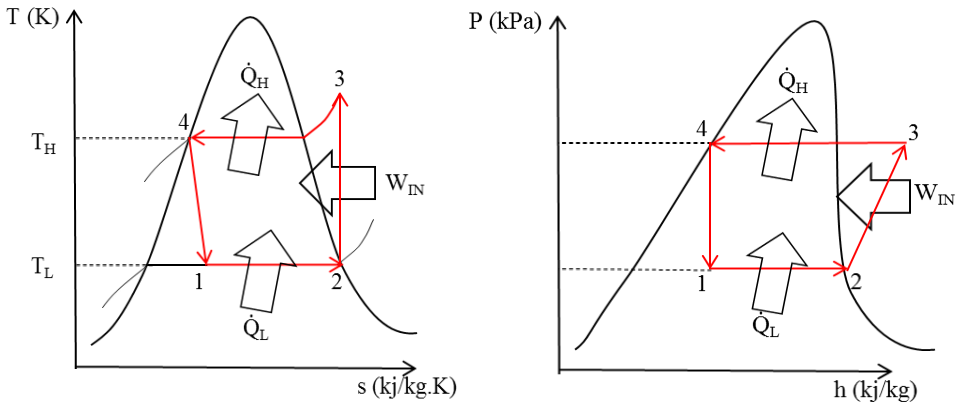

Figure 1.2. T – s diagram (a) and P – h diagram (b) of a vapor - compression refrigeration cycle

In these plots, process 1 – 2 expresses the reversible heat absorption at constant pressure from the refrigerated space by the evaporator ($\dot{Q}_L$). In this process, the refrigerant boils, thus provides a cooling effect. Process 2 – 3 expresses the reversible adiabatic compression by the compressor ($\dot{W}_{IN}$), increasing the pressure and temperature of refrigerant. Process 3 – 4 shows the reversible heat rejection at constant pressure from the condenser to warm environment ($\dot{Q}_H$), and finally process 4 – 1 expresses the irreversible expansion of refrigerant at constant enthalpy from an expansion device, such as expansion valve. At the end of this process, refrigerant becomes a low quality low pressure saturated mixture and reenters to the evaporator.

1.2.2. Components of Vapor – Compression Refrigeration Cycle

The components of vapor – compression refrigeration cycle, which are evaporators, compressors, condensers and expansion valves are explained in detail in the following sections with their descriptions and types.

1.2.2.1. Evaporators

Evaporation is escaping of liquid molecules from a liquid gas interface into the gas phase when they receive extra energy. This extra energy is usually in the form of

heat. Therefore, liquids can evaporate at any temperature if there is no necessary energy to bond the molecules in the liquid form. The rate of evaporation increases at higher temperatures.

The duty of evaporator in a vapor compression cycle is to remove the heat from the refrigerated space. This can be accomplished by evaporating the low-quality and low pressure saturated refrigerant that is in contact with the space to be refrigerated. Therefore, it must satisfy to keep the overall heat transfer coefficient (U – factor) at a desired level under all working scenarios. After evaporation, refrigerant becomes a low-pressure saturated vapor.

Evaporators are manufactured in different types, according to their area of usage. They are divided into two general categories, flooded and dry expansion evaporators.

1.2.2.1.1. Flooded Evaporators

Flooded evaporators are suitable for water cooling and chilling applications. In these type of evaporators, the tubes of heat exchanger is always filled with liquid refrigerant, which is fed from the bottom and the evaporation occurs on the free surface at outside. The vaporized and accumulated refrigerant is drawn to the compressor. The level of liquid refrigerant at outside is controlled by a valve. Water being chilled passes through the tubes. Flow of refrigerant fluid in the tubes is provided by gravitational force. The schematic view of a flooded evaporator can be seen in Figure 1.3.

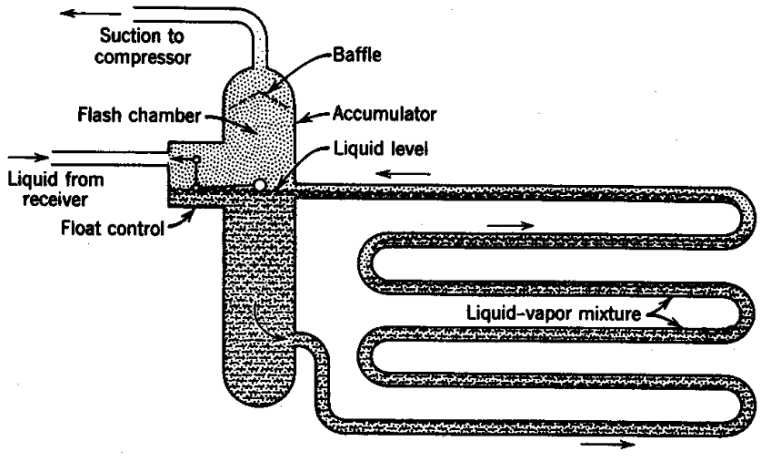

Figure 1.3. Schematic view of a flooded evaporator
(Source: Dossat, 1961)

1.2.2.1.2. Dry Expansion Evaporators

In dry – expansion evaporators, which are proper for air and gas cooling, the refrigerant fluid boils as it flows through the tubes of the evaporator. The evaporator is fed by an expansion valve with the refrigerant in liquid form. Rate of refrigerant flow is controlled by some types of expansion valves to ensure that all the liquid vaporizes and only refrigerant gas exits from the tubes (Whitman et al., 2005).

Flooded and dry expansion evaporators explained above can be constructed in various ways for different areas of usage. The most common evaporator types according to their construction are as follows; bare tube, plate surface and finned.

The most basic one is the bare tube evaporator, which is formed by coiling the evaporator tube and circulating the refrigerant fluid. The surface of the evaporator is completely in contact with the refrigerant and there is not any other secondary heat transfer surface to increase the heat transfer rate. In Figure 1.4., various bare tube evaporators can be seen.

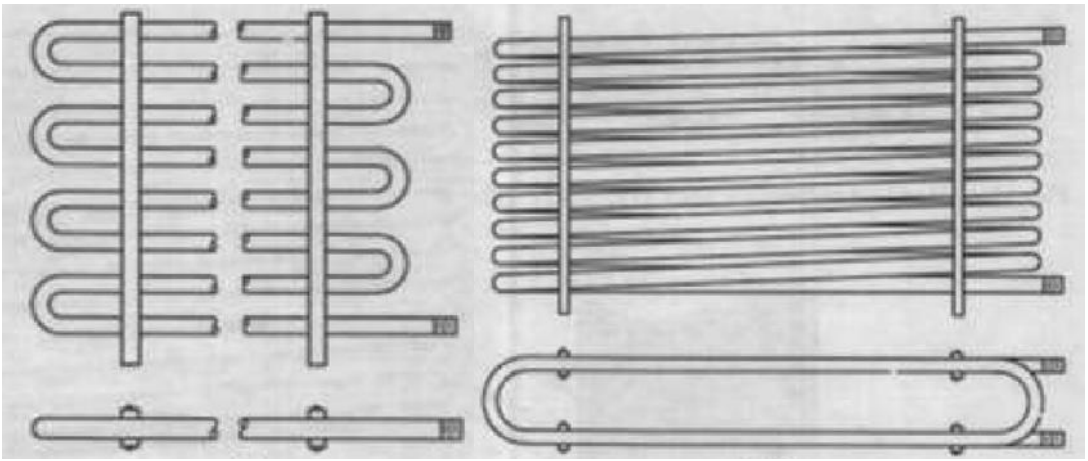

a b

Figure 1.4. Some designs of bare – tube evaporators, (a) flat zig – zag, (b) oval trombone coil (Source: Dossat, 1961).

In plate – surface (or stamped) evaporators, two plates are embossed and welded together and the refrigerant flows in the path between the plates. By this way, heat transfer area is increased slightly. Since their manufacturing is easy and they are also easy to clean, they are broadly used in household refrigerators and freezers (Dossat, 1961). In Figure 1.5., some plate surface evaporator installed in a refrigeration system can be seen.

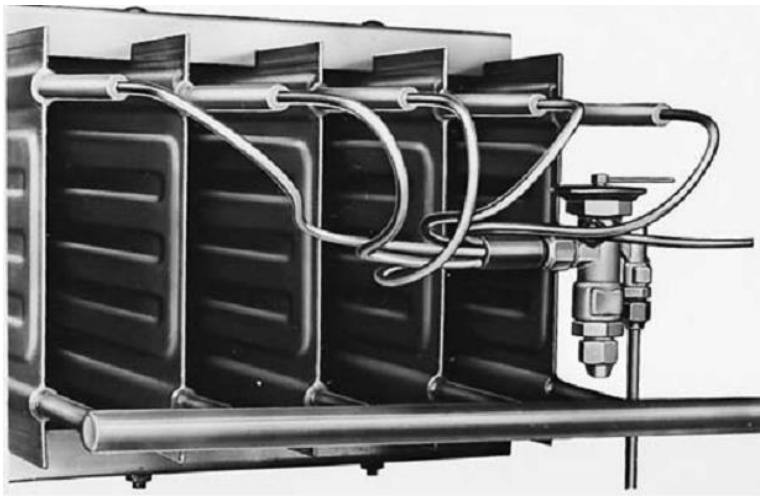

Figure 1.5. A plate surface evaporator
(Source: Whitman et al., 2005).

Finned evaporator is actually a bare tube evaporator with fins. These fins are in good contact with the tube and enhance the heat transfer rate much. They are used extensively in refrigeration applications because of their high efficiency. In Figure 1.6., a finned evaporator can be seen.

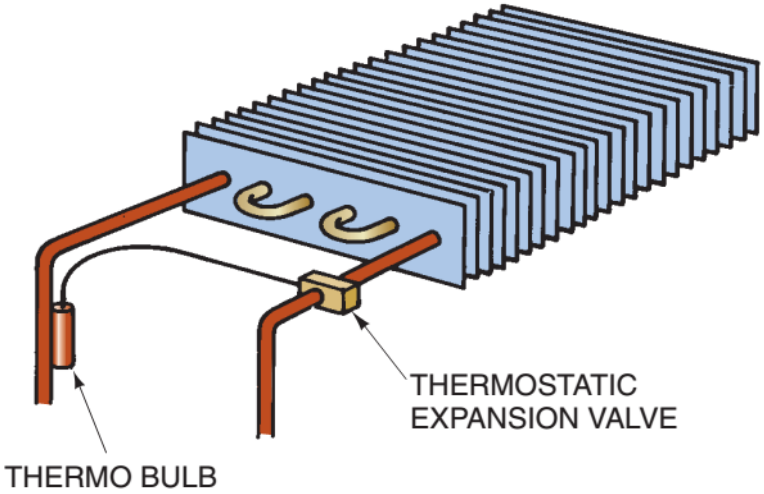

Figure 1.6. A finned evaporator
(Source: Whitman et al., 2005).

1.2.2.2. Compressors

Compressor is considered as the heart of the refrigerator. It increases the pressure and temperature of the low pressure saturated refrigerant vapor. The pressure

addition in compressor causes a pressure difference between low pressure and high pressure of the cycle, which drives the flow of refrigerant through the system (Whitman et al., 2005).

Five different types of compressors are used in refrigeration applications, they are reciprocating, screw, rotary vane, scroll and centrifugal. These types of compressors are schematically illustrated in Figure 1.7.

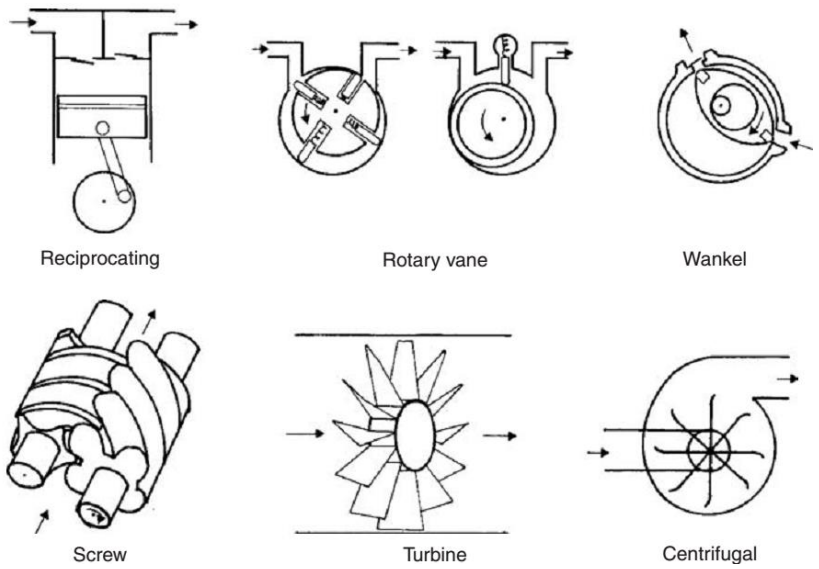

Figure 1.7. Various compressor types
(Source: Whitman et al., 2005).

Reciprocating, rotary vane and screw compressors are positive displacement compressors, whereas the turbine and centrifugal compressors are dynamic. In positive displacement compressors, compression is accomplished by a compressing member, which is a piston in reciprocating compressor, rotary blade or vane in rotary vane compressor, or rotary screws in screw compressor. In dynamic compressors, compression is achieved by means of centrifugal forces created by axial or centrifugal impellers (Dossat, 1961).

The positive displacement compressors, especially the reciprocating compressor are the widely used for refrigeration applications, since they can provide the necessary flow rate, pressure difference and operating temperature requirements. Dynamic compressors also have some areas of usage especially for large applications.

All types of compressors shown in Figure 1.7. can be categorized as open, hermetic and semi – hermetic, according to their housing types and drive mechanisms between the motor and shaft of compressor.

1.2.2.2.1. Hermetic Compressors

In hermetic compressors, motor and compressor crankshaft share the same shaft. All parts are enclosed in a single housing and this housing is fully welded and impossible to open unless it is cut, meaning that no later service is possible in the case of a malfunction.

Almost all compressors used in domestic refrigerators are hermetic reciprocating type. A section view of a hermetic reciprocating domestic refrigerator compressor can be seen in Figure 1.8.

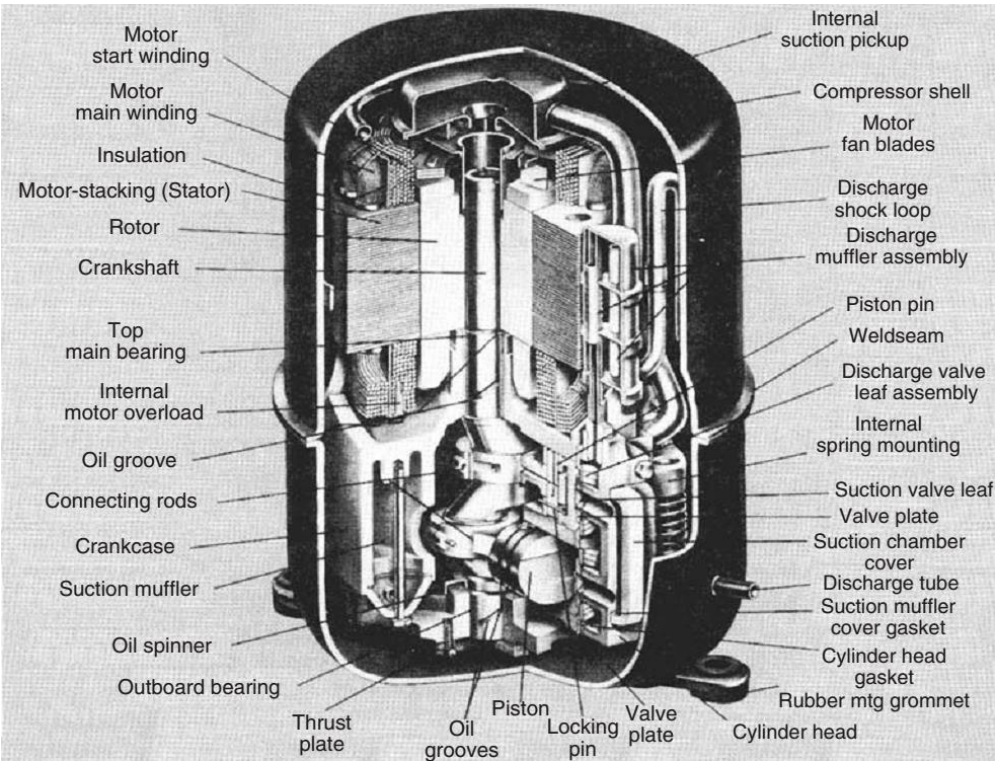

Figure 1.8. Section view of a hermetic reciprocating compressor (Source: Dincer & Kanoglu, 2011).

1.2.2.2.2. Semi – Hermetic Compressors

In semi – hermetic (or serviceable hermetic) compressors, all components of compressor are enclosed in a single housing that has two parts bolted together, which makes their later maintenance possible. The motor and crankshaft combination of these compressors are similar to the hermetic compressors, they both share the same shaft.

Although the serviceability of semi – hermetic type compressors is a major advantage over hermetic compressor, the main drawback is cost and this makes the semi – hermetic type compressors more suitable in larger sizes of cooling applications. The section view of a semi – hermetic reciprocating compressor can be seen in Figure 1.9 .

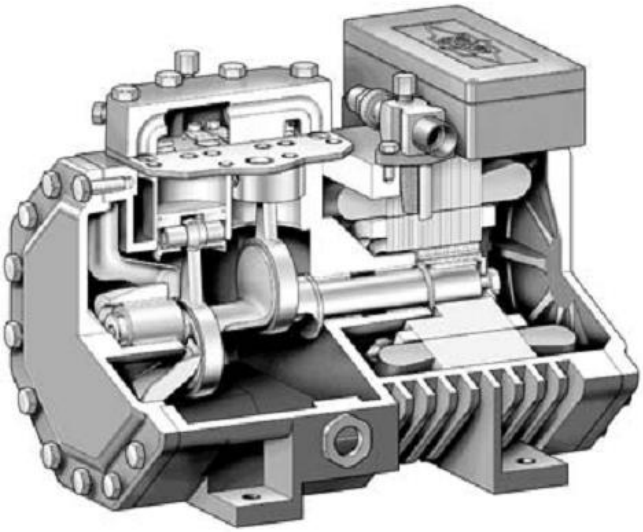

Figure 1.9. Section view of a semi – hermetic reciprocating compressor (Source: Dincer & Kanoglu, 2011).

1.2.2.2.3. Open Compressors

In open compressors, the parts of compressor and the motor are not in the same casing. Since motor is placed externally in these type of compressors, a shaft seal is a vital component to prevent refrigerant and oil leakage. Casing of open compressors are bolted as well, so maintenance is possible like in semi – hermetic compressors.

According to the connection type between the motor and compressor shaft, open compressors can be divided into two, belted drive compressors and direct drive compressors. In belted drive compressors, motor and compressor shafts are placed in parallel and transmission is provided by a belt. In direct drive compressors, motor and compressor shafts are placed collinear and the connection is butt joint, provided by a coupling. In Figure 1.10., a belted and a direct drive compressors side by side can be seen.

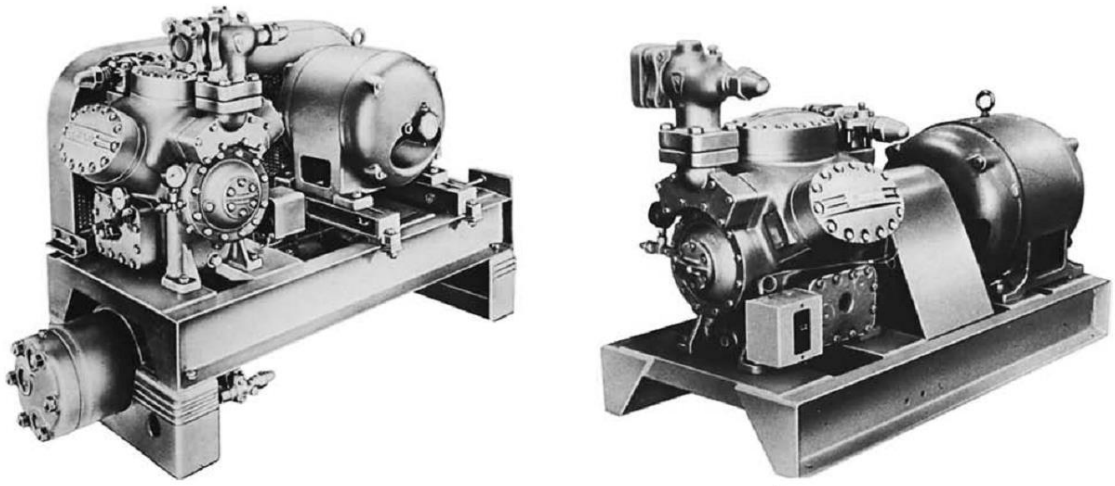

Figure 1.10. (a) belted, (b) direct drive open compressors
(Source: Dincer & Kanoglu, 2011).

1.2.2.3. Condensers

Condensation is the process of liquidification of a gas by rejecting heat. The rejected heat is the sum of sensible heat and latent heat. The high pressure superheated refrigerant carrying the heat absorbed from evaporator and work from the compressor is condensed to the high pressure saturated liquid in the condenser. By this, the heat energy absorbed from the evaporator is pumped to the ambient and cooling the refrigerated space is accomplished.

Instead of using condenser to reject the heat, the superheated refrigerant could be discharged to the atmosphere which is usually done in outer earth space programs where the heat rejection medium is not available. However, this is usually impractical for regular users. Condensing the refrigerant allows reusing it at the beginning of next cycle (Dincer & Kanoglu, 2011).

There are three types of condensers in cooling applications, air cooled, water cooled and evaporative condensers. Air cooled condensers, as the name implies, uses air as the heat rejection media. They are used in most refrigerating applicarions, from domestic to large industrial refrigeration. Like air cooled condenser, water is used as the heat rejection media in water cooled condensers. Water cooled condensers are used in large heat capacity refrigerating and chilling applications. Evaporative condensers use both air stream and water spray for heat rejection.

1.2.2.4. Expansion Valves

The high pressure refrigerant liquid has to be brought into the beginning of the cycle. This is accomplished by a throttling device such as a valve, orifice plate, or a capillary tube. By this way, the refrigerant undergoes an expansion process and its pressure is reduced. After this process, the refrigerant becomes a low quality saturated fluid and brought into the evaporator to absorb heat. Unlike the compressors, condensers and evaporators, the expansion devices are smaller in size, hidden somewhere in evaporator compartment and generally not visible to an ordinary observer.

The common types of expansion valves are as follows, thermostatic expansion valves (TXV), constant pressure (automatic) expansion valves (or AXVs), float valves and capillary tubes.

1.2.2.4.1. Thermostatic Expansion Valves (TXVs)

The TXVs control the flow of refrigerant to the evaporator that matches the cooling capacity of the system by measuring the temperature of superheated refrigerant leaving the evaporator. As a response to this temperature, the valve is opened or closed and by this way a small amount of constant superheat at the exit of evaporator is provided. In Figure 1.11., the complete refrigeration cycle can be seen with all components including TXV.

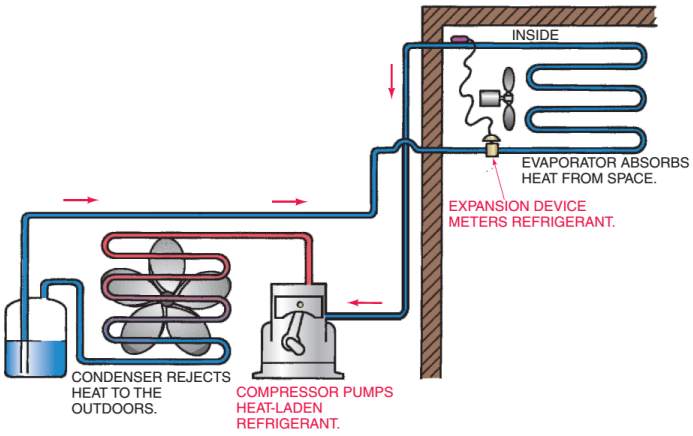

Figure 1.11. Complete refrigeration cycle with all four basic components. (Source: Whitman et al., 2005)

1.2.2.4.2. Constant Pressure Expansion Valves

Consant pressure expansion valves, (or automatic expansion valves, or AXVs) are precessor of TXVs. AXVs are much the same with TXVs, however, they don't use temperature measuring unit. They sense the pressure at the evaporator and maintain a constant evaporator pressure by controlling flow of refrigerant, without noticing the superheting at the outlet. When the pressure at the evaporator drops for some reason, they are opened, allowing more refrigerant to enter to the evaporator to catch the required pressure (Whitman et al., 2005).

1.2.2.4.3. Float Valves

Float valves are employed to control the flow of refrigerant in flooded type evaporators, allowing the level of refrigerant liquid in a preset value (Dincer & Kanoglu, 2011).

1.2.2.4.4. Capillary Tubes

Capillary tubes are the cheapest and simplest way to control the refrigerant flow in a vapor – compression cycle. They are tubes in which the refrigerant throttles to the evaporation pressure having an inside diameter small enough and a length high enough for the necessary pressure drop (having an internal diameter of 0.4 – 3 mm and length of 1.5 – 5m).

Its role in vapor compression cycle is similar to a garden hose. Lower hose diameter yields less water at the exit in a certain hose inlet pressure. Likewise, longer hose will also yield less water and lower outlet pressure because of the pressure drop across length of hose (Whitman et al., 2005).

The capillary tube does not measure neither the evaporator pressure, nor the evaporator exit temperature. It is a fixed bore device without any valve and can not adjust itself in cases of load change. Because of this, it is used in applications where load is low without any large fluctuations, such as household refrigerators. It is desingned to maintain a certain pressure drop specified by the manufacturer and allows

adequate refrigerant to flow to the evaporator according to this pressure drop. Since this device does not have any valve and does not stop the flow of refrigerant to the low pressure side during the period when the cycle is off, the pressures between condenser and evaporator will be equalized (Whitman et al., 2005). This maldistribution of refrigerant increases the required motor torque at the next start and causes an efficency drop. In Figure 1.12. a capillary tube can be seen.

Figure 1.12. A Capillary Tube
(Source: Whitman et al., 2005)

1.3. Household Refrigerators

The components that form the vapor – compression cycle explained above are called as "cold production system" when they are installed to a refrigerator (M.M. Farid, 2010). In Figure 1.13., the cold production system installed to a domestic refrigerator with all units can be seen.

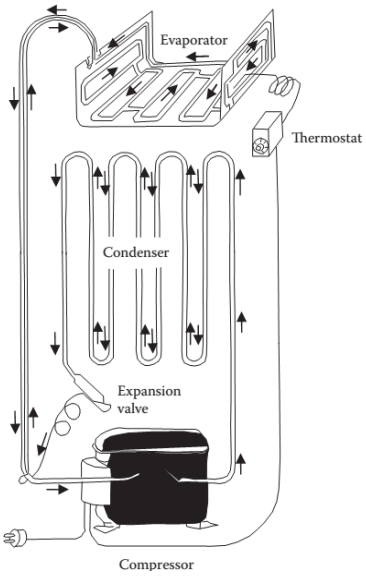

Figure 1.13. Cold production system of a domestic refrigerator
(Source: M.M. Farid, 2010).

Currently, there are 3 kinds of household refrigerators according to their heat transfer and airflow mechanisms between the evaporator and refrigerator cabin. They are static type, brewed type and no frost type refrigerators. In static type refrigerators, airflow and heat transfer is provided by natural convection, with an evaporator placed at the back wall. In brewed type refrigerator, airflow is accelerated by a fan, placed usually at the top and in no – frost type refrigerators, air is cooled by a finned evaporator placed in a separate location and sprayed to the refrigerated space.

Today, the widespread usage of household refrigerators is necessary to preserve the food from spoilage. According to statistics in the year of 2002, there are approximately 700 – 1000 million of household refrigerators are in operation worldwide (IIR, 2002). Today's household refrigerators have a size of approximately 60 cm depth and 60 cm width. The length can be between 90 cm and over 200 cm. The composition of walls are polystyrene (inner wall) steel sheet (outer wall) and an insulating material between these two (polyurethane), having a thickness of about 4 cm (O. Laguerre & Flick, 2004).

1.3.1. Static Type Refrigerators

In static type refrigerators, which this thesis is mainly related, the evaporator is mounted to any wall of refrigerator cabin (generally to the back wall) and directly exposed to the refrigerated space. Heat transfer occurs with natural convection and the airflow is formed by the effects of buoyancy. Advantages of static type refrigerators are their simplicity and cheapness. The main disadvantage of these refrigerators is the temperature heterogeneity between bottom and top zones is high due to the low airflow (Ben Amara, Laguerre, Charrier-Mojtabi, Lartigue, & Flick, 2008).

1.3.2. Brewed Type Refrigerators

The brewed type refrigerators are static refrigerators equipped with a fan generally at the top. The fan accelerates the air flow inside the cabin and this makes the air temperature distribution inside the refrigerator cabin more homogeneous, but the energy consumption is slightly higher due to this (Ben Amara et al., 2008).

1.3.3. No – Frost Refrigerators

The refrigerated food is not exposed to the evaporator directly in the no – frost refrigerators, rather the evaporator is placed in a separate chamber. By this way, frost cannot be formed in the refrigerated space, it is accumulated on the fins of evaporator.

Air flow is driven by a fan. This fan transports the warm and humid air inside the refrigerator cabin to the evaporator fins. The air blown through evaporator compartment is cooled and dehumidified by rejecting its latent and sensible heat to the refrigerant fluid. After cooling and dehumidifying, the cold air is carried through ducts and sprayed to the refrigerator cabin via nozzles. This air removes heat and moisture from the refrigerated products and becomes warm and humid again, and then blown through the evaporator fins, becomes cold and dry. This cycle repeats over the whole operation of refrigerator (Gupta, Ram Gopal, & Chakraborty, 2007).

The main advantage of no – frost refrigerators is the defrost mechanism. Also, the air temperature field in no – frost type refrigerators is the most homogeneous among the other types. Disadvantages of no – frost type refrigerators are high energy consumption, high price and drying of foods (Ben Amara et al., 2008).

In no – frost type refrigerator, a defrost heater is mounted just below of the evaporator. This heater removes the frost formed on the evaporator coils by heating it in a periodic manner. Defrosting is done manually by the user in static and brewed type of refrigerators, by switching off the refrigerator and allowing the frost in refrigerated cabin melt. This process is automatized in no – frost refrigerators, thanks to the defrost mechanism. (Gupta et al., 2007)

The schematic view of these refrigerator types can be seen on Figure 1.14. The air flow patterns of these refrigerators can also be seen on this figure.

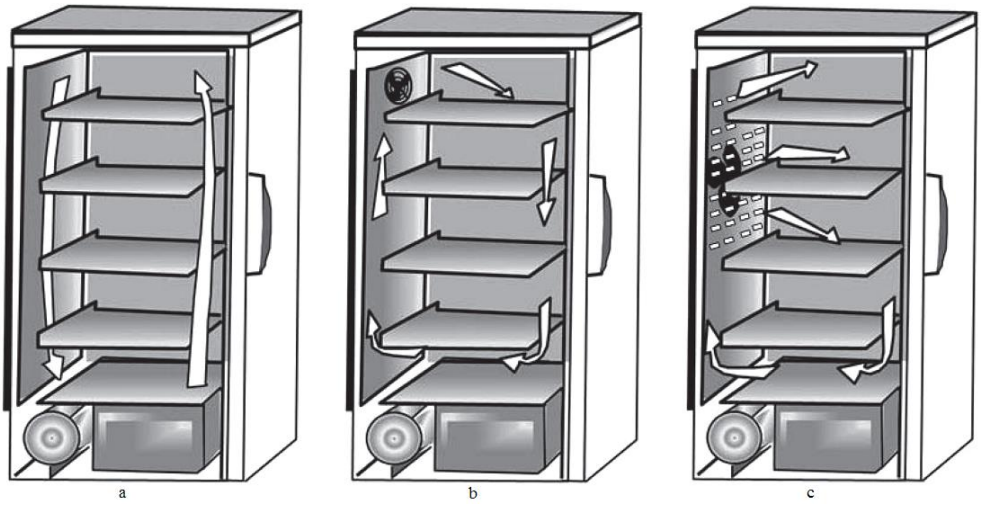

Figure 1.14. Schematic views of (a) static, (b) brewed, (c) no – frost types of refrigerators (Source: M.M. Farid, 2010)

1.4. Airflow and Heat Transfer Mechanisms in Static Refrigerators

It is shown by a number of studies that the temperature and air distribution inside a household refrigerator directly affects the quality of food products inside the refrigerator cabin. Any uncontrolled rise (too frequent door openings, electric blackouts etc.) may also deteriorate food, even the mean temperature inside the cabin is low enough for preservation (Gupta et al., 2007). The reasons of high temperature fluctuations of storage compartments in commercial freezers and refrigerators can be listed as, heat loads gained by ambient, frequent door openings by customers, heat generated by the defrost system (if the refrigerator is a no – frost type) and electrical power failures

According to some surveys conducted in several European countries, many domestic refrigerators operate at higher temperatures than the temperatures indicated in the regulations of countries. For example in France, it is found that the average temperature is higher than $8^{O}C$ for %26 of the domestic refrigerators, while the specified average air temperature in standards is $4^{O}C$ (Onrawee Laguerre, Derens, & Palagos, 2002). Also, implications from several researches show that, strong temperature heterogeneity is observed especially in static type unventilated refrigerators, due to the very low air circulation. The temperatures are high in some zones, where sanitary risk can be observed, and too low, where freezing can happen. Therefore, it is absolutely necessary to understand the mechanism of heat transfer in

refrigerators and take some precautions to control it. This is important for customers for food quality control (O. Laguerre, Ben Amara, Moureh, & Flick, 2007).

As mentioned in 1.3.1, in static refrigerators heat transfer happens with natural convection and the airflow is formed by the effects of buoyancy, which can occur due to the variations of density. These variations are related with the temperature and humidity gradients. The vertical force resulting from the density and humidity gradients is ascendant if the air is humid and hot, and descendant if the opposite case is valid (dry and cold air is heavier than the humid and hot air).

The temperature distribution is dependent on the position of evaporator inside the refrigerated compartment When the evaporator is mounted on the bottom horizontal wall of refrigerator and that wall becomes the cold wall, a stratified temperature profile is expected where the bottom is cold and top is hot and there is no airflow, since the heavier and dry air is already at the bottom. However, when the ceiling of refrigerator is the cold wall, an unsteady flow can be observed, since the heavier air at top and lighter air at bottom. After a critical density gradient is exceeded, a spontaneous and steady, cellular – like flow results (Figure 1.17). When one of the vertical walls is cold, which is similar to the domestic static type refrigerators, circular flow is also observed along walls and the air at the center is nearly stagnant (O. Laguerre & Flick, 2004).

To describe the heat transfer between the evaporator and air in unventilated static type refrigerators, the simplest approach that can be applied is to consider the refrigerator cabin as a rectangular cavity with one vertical wall is colder than the others (the wall with evaporator). The air circulation in this case can be seen in Figure 1.15 (O. Laguerre & Flick, 2004).

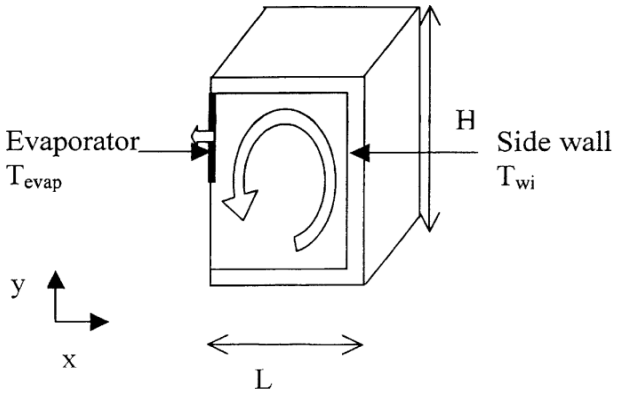

Figure 1.15. Air circulation in an empty closed cavity
(Source: O. Laguerre & Flick, 2004).

As can be seen on Figure 1.15., a circular air circulation is established in an empty closed cabinet. Cold air near the evaporator mounted wall goes downward, and the hot air near the door wall goes upright. To characterize this kind of flow and to get some qualitative information about the thermal and hydraulic boundary layers, a dimensionless number called Rayleigh number (*Ra*) is used. Up to $Ra=10^9$, the flow is assumed to be laminar (O. Laguerre & Flick, 2004).

$$Ra = \frac{g\beta(T_S - T_\infty)x^3}{\nu\alpha} \tag{1.1}$$

The geometry of the cavity, especially the aspect ratio (H/L), and the Rayleigh number strongly affect this air flow pattern. When the Rayleigh number is small, such as $Ra \leq 10^3$, the effects of buoyancy is weak and the heat transfer occurs mostly by conduction. At intermediate levels of *Ra*, such that $10^3<Ra<10^9$, buoyancy effects becomes effective and a celluar flow structure is formed near walls. The core region becomes nearly stagnant, and the effects of turbulence at the boundary layers near side walls can be visible. The thermal and hydraulic boundary layer structures for small and intermediate Rayleigh numbers can be seen at Figure 1.16 and Figure 1.17 respectively (O. Laguerre & Flick, 2004). For a regular static type refrigerator, the Rayleigh number is in a magnitude of $10^7 – 10^8$, which is in upper limits of intermediate levels.

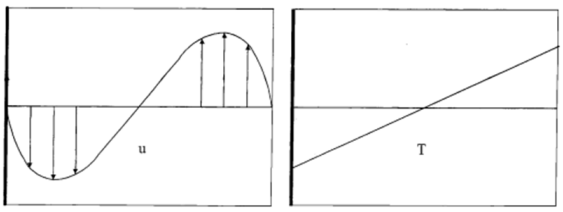

a b

Figure 1.16. (a) Hydraulic and (b) Thermal boundary layer structures at low Rayleigh numbers (Source: O. Laguerre & Flick, 2004).

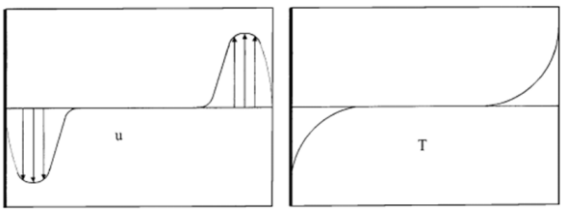

a b

Figure 1.17. (a) Hydraulic and (b) Thermal boundary layer structures at intermediate Rayleigh numbers (Source: O. Laguerre & Flick, 2004).

As seen on Figure 1.16 and Figure 1.17, as the Rayleigh number gets higher, both thermal and hydraulic boundary layers becomes steeper, velocities near wall region becomes higher and the core region becomes nearly stagnant.

If we take a closer look to the near a wall of the cavity, we come up with the theory of natural convection near vertical walls. In this context, the heat transfer inside a static refrigerator can be modeled with the natural convection phenomena between air and vertical plates (wall with the evaporator and the side walls). If we visualize the flow near a vertical cold wall ($T_w<T_\infty$) by injecting a tracer, then we see the air flow behaviour can be seen in Figure 1.18. (O. Laguerre & Flick, 2004).

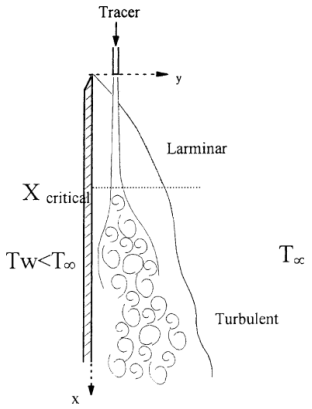

Figure 1.18. Air flow by natural convection near a vertical wall
(Source: Padet, 1997).

Here in Figure 1.18, the natural convection flow in boundary layer with the transition from laminar flow to turbulent flow can be seen. The heat transfer between wall with evaporator and the air is similar to this case when the other limiting walls are neglected. Heat transfer correlations can be derived for both laminar and turbulent cases. For most of the engineering calculations, these heat transfer correlations can be generalized with the form shown in Equation (1.2).

$$Nu = a.Ra^{b} \tag{1.2}$$

In Equation (1.2), values of "*a*" and "*b*" are dependent on the flow regime. For most turbulent flows ($10^9<Ra<10^{13}$) a and b might be taken as 0.59 and 0.25 respectively. For laminar flows where Rayleigh number is between 10^4 and 10^9 *a* and *b* might be taken as 0.10 and 1/3 respectively. For more extensive range of Rayleigh numbers, more accurate correlations can be found in the literature (Incropera, 2006).

There are two kinds of boundary layers in convective heat transfer problems, hydrodynamic and thermal boundary layers. For natural convection flows, air velocity is zero at both the wall surface and at the end of hydrodynamic boundary layer. The temperature increases from the wall temperature (T_w) to the ambient temperature (T_∞) inside the thermal boundary layer. (O. Laguerre & Flick, 2004).

The temperature and velocity profiles under the hydrodynamic and thermal boundary layers can be seen in Figure 1.19.

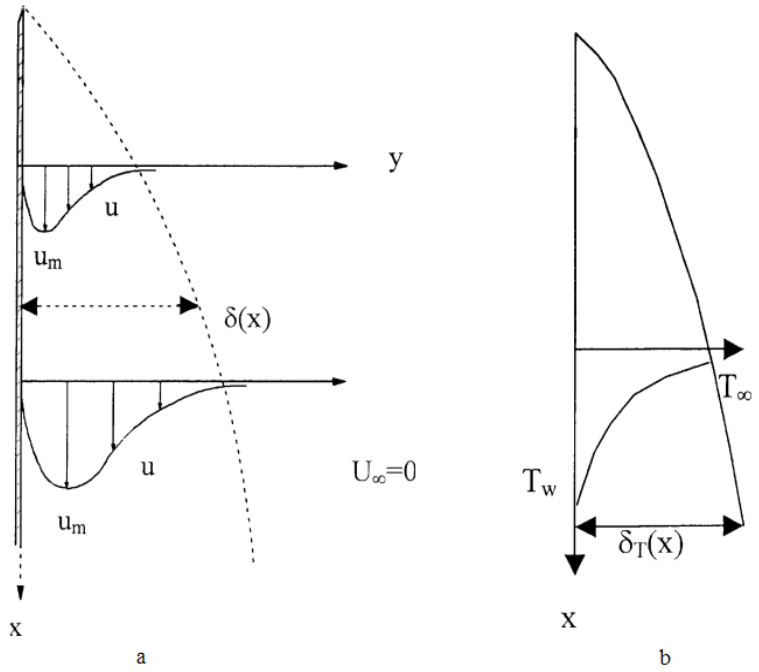

Figure 1.19. (a) Velocity profile and (b) Temperature profile in hydrodynamic and thermal boundary layers (Source: O. Laguerre & Flick, 2004).

In Figure 1.19.(a), the air velocity (u) is zero both at the surface and at the end of the boundary layer. As the distance increases from the surface, it increases suddenly at first and reaches to a maximum value (u_{max}) and decrease gradually to zero at the end. The zone with non – zero velocity is known as Hydrodynamic boundary layer.

In Figure 1.19.(b), the air temperature is between the wall temperature (T_w) and ambient temperature (T_∞) where T_w is lower than the T_∞. The zone where the temperature increases from T_w to T_∞ is called as Thermal boundary layer. Both thermal and hydrodynamic boundary layer thicknesses increase in the flow direction.

The relationship between the thermal and hydraulic boundary layer thicknesses is designated by a dimensionless number, known as Prandtl number (Pr). Prandtl number can be defined as the ratio of viscous diffusion rate (ν) to the thermal diffusion

rate (α) The formulation of Prandtl Number can be seen on Equation (1.3). For fluids which have Prandtl number near 1 such as air, the both boundary layer thicknesses have the same order of magnitude.

$$\Pr = \frac{\nu}{\alpha} = \frac{C_p \mu}{k} \tag{1.3}$$

In the refrigerator which is under consideration in this study, the Rayleigh number based on the distance between two shelves of the refrigerator is estimated as $2x10^7$ The film temperature is -6.45^{o}C and the distance between the shelves is about 0.26m. The Prandtl number at -6.45^{o}C film temperature is 0.71.

If convective and radiative heat transfer coefficients between evaporator and other vertical walls are determined, one can notice that these heat transfer coefficients have the same order of magnitude, which makes is necessary to take notice of radiation between evaporator wall and other walls. As an example, O. Laguerre and Flick (2004) developed a mathematical model by considering an empty refrigerator as a combination of vertical plates. They first calculated the Rayleigh number based on the evaporator length, by using the measured temperatures of evaporator and bulk air, which is $2x10^7$. Since this value is less than 10^9, they estimated both convective and radiative heat transfer coefficients by using correlations for laminar flow. They found that the convective and equivalent radiative heat transfer coefficients between air and evaporator as $h_{c,\ evap}$ = 3.28 W/m^{2}K, and $h_{r,\ evap}$= 3.85 W/m^{2}K respectively, which are in the same order of magnitude. So, radiation should be taken into account when analyzing the heat transfer inside a static type domestic refrigerator. (O. Laguerre & Flick, 2004).

1.4.1. Temperatures in a Static Refrigerator

The compressor of any refrigerator is operated according to the temperature information obtained from the thermostat inside of the refrigerated space. According to this, the compressor is either operated or stopped. When this temperature at thermostat exceeds a certain value, compressor is started, and when this temperature is below another certain value, compressor stops. The maximum and minimum temperature limits of thermostat are specified by the manufacturer. This “on” and “off” operation

principle of compressor causes temperature fluctuations inside the refrigerated space (M.M. Farid, 2010).

An experimental investigation by Farid (2010) presents the temperatures of an empty refrigerator with one door and one compressor. The internal dimensions of the refrigerator is 50 x 50 x 90 cm (width x depth x height). The walls have a 4 cm of thickness and 0.027 W/m.K of overall thermal conductivity. The thermostat temperature is 6^{o}C. Evaporator is mounted to the back vertical wall and its dimensions are 50 x 30 cm (width x height). The evaporator wall temperatures, air temperatures at top, middle and bottom positions in the centerline of refrigerated space and wall temperatures are obtained.

The results of this experimental study show that the air temperature is heterogeneous in the refrigerated space. The evaporator wall temperature varies between +7 and -12^{o}C with an average of -1.2^{o}C. The mean air temperature is 6.7^{o}C with a minimum value of 3.8^{o}C and a maximum value of 8.3^{o}C. The air temperature variations at top, middle and bottom positions can be seen in Figure 1.20. The mean vertical wall temperatures are 9.1^{o}C at the top level, 5.4^{o}C at the middle level and 5.7^{o}C at the bottom level (M.M. Farid, 2010).

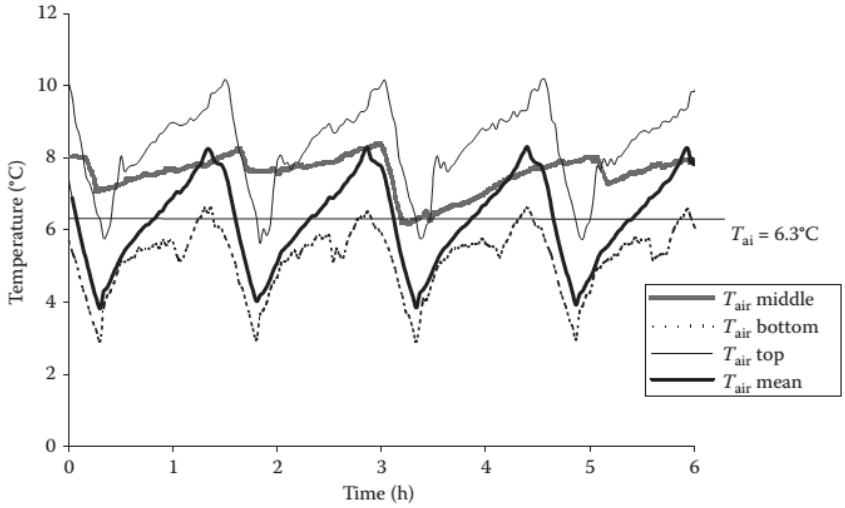

Figure 1.20. Example of air temperature variations in a static refrigerator (Source: M.M. Farid, 2010).

As it can be seen in Figure 1.20., the air temperatures inside the refrigerated space fluctuates about the thermostat setting, with cold air at the bottom and warm air at

the top. The results of this experimental study confirm that the main heat transfer mode in a static type refrigerator is natural convection.

The main problem that this thesis is intended to approach is, how to increase the temperature performance of a static type household refrigerator by employing phase change materials (PCM). Temperature stabilization and compressor efficiency is crucial for refrigerating applications and it is supposed that employing PCMs in a household refrigerator could reduce the temperature fluctuations and decrease the temperatures, and may increase energy grade of refrigerator.

PCMs are materials, which absorbs and releases heat energy as latent heat between its solidus and liquidus temperatures. Since most pure materials and some mixtures have almost equal solidus and liquidus points, these materials are capable of storing energy in large amounts, without high fluctuations in its temperature. By exploiting this feature, employing these materials in practical applications involving heat transfer should stabilize and decrease the temperatures and improve the heat pump efficiency of those applications.

In the following chapters, a literature survey covering some studies, some basic properties of PCMs, the CFD basics, the modelling details of refrigerator, results of CFD analyses are explained, and finally conclusions are made and possible future works are described.

CHAPTER 2

LITERATURE SURVEY

The application of PCMs on household refrigerators has showed some benefits in different ways. Since it stores a high amount of heat energy, it can keep the cold energy further and prolongs the compressor off time and reduces the number of on – off cycles. Reducing the number of on – of cycles of compressor is beneficial in terms of efficiency, because the maldistribution of refrigerant fluid decreases the efficiency of refrigerator at the next start of compressor, until the balance of refrigerant fluid is reestablished. Also, PCMs have an effect of stabilizing the temperatures of refrigerator by reducing the fluctuations caused by on – off cycles, which has a dramatic negative effect of frozen foods.

The studies about application of PCMs on household refrigerators can broadly be divided in two parts, experimental and numerical. The numerical studies are validated by test data. The type of PCMs in this studies are generally water, or eutectic mixtures of water and salt which have a phase change temperature below $0^{o}C$, making it suitable for keeping cold energy. As an exception, Wen – Long Cheng et al. used a high temperature PCM on condenser coils, and stored the heat dissipated from the condenser (2011). In this section, some of the studies are summarized.

In 2005, K. Azzouz et al. investigated the effect of phase change materials applied to the evaporator of a household refrigerator. They developed a simple mathematical model based on conservation equations for the cases with and without PCMs. According to their study, the coefficient of performance and the energy efficiency of this new design increased significantly. The thermal storage of PCMs caused a 10 hours or more continuous operation without electric supply and this reduces the overloading problem to the electrical distribution grid during peak loads (K. Azzouz, Leducq, D., Guilpart, J., Gobin, D., 2005).

A static type refrigerator without a freezer compartment is considered in this study. The performance of this refrigerator is specified in terms of cooling capacity (500 W.h for $4^{o}C$ and $20^{o}C$ internal and external temperatures respectively), electric consumption, evaporation and condensation temperatures. The measured global heat

transfer coefficient of the walls of refrigerator is 0.34 W/m^{2}K. The type of used PCMs are eutectic salt solutions, whose phase change temperatures are between -6 and 0^{o}C. The size of PCM is 0.03 x 0.5 x 0.5 m, having a volume of 0.0075m^3. The location of PCM slab in the refrigerator, and the presentation of energy balance of the evaporator and with PCM can be seen in Figure 2.1.

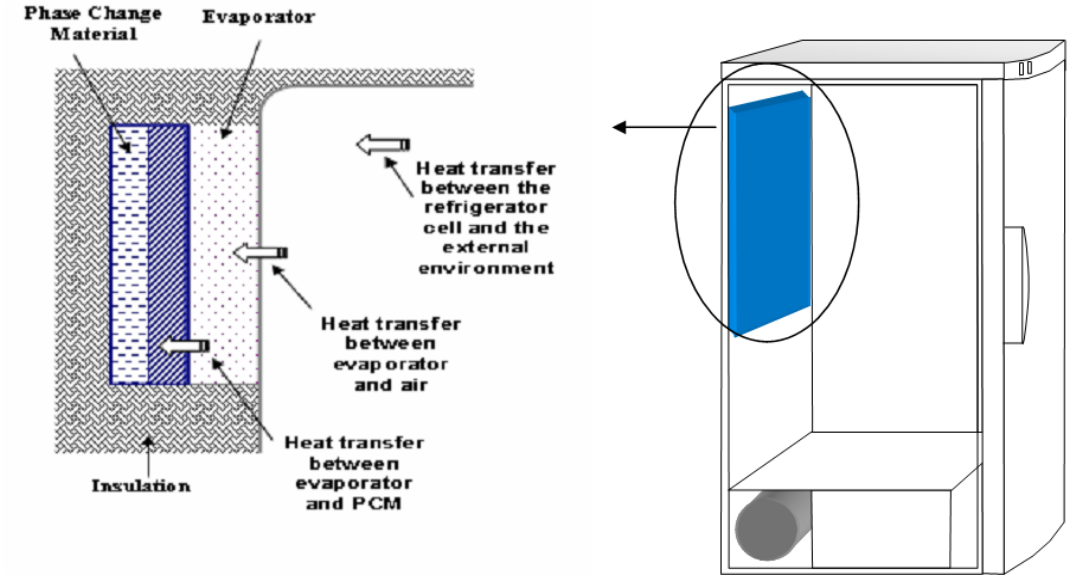

Figure 2.1. Location of PCM in the refrigerator and the representation of energy balance in PCM (Source: K. Azzouz, Leducq, D., Guilpart, J., Gobin, D., 2005)

To see the effect of different phase change temperatures, PCM slab thicknesses and ambient temperatures, many simulations are carried out. According to the study, the addition of PCM slab significantly increased the coefficient of performance (COP) and the cooling capacity. The heat transfer at the evaporator is increased by %86. The evaporation temperature is increased from -19 to -7^{o}C. The decrease of evaporation temperature results a reduction of pressure compression ratio, thus a lower power consumption. The COP increased from 1.09 to 1.9. In Figure 2.2. and Figure 2.3., evolution of evaporation temperatures and cooling capacity with and without PCM slab can be seen respectively. As it can be seen from these figures, the minimum evaporator temperature is increased from -20^{o}C to -7 ^{o}C. The maximum cooling capacity is almost doubled (70W to 135W) by the addition of PCM.

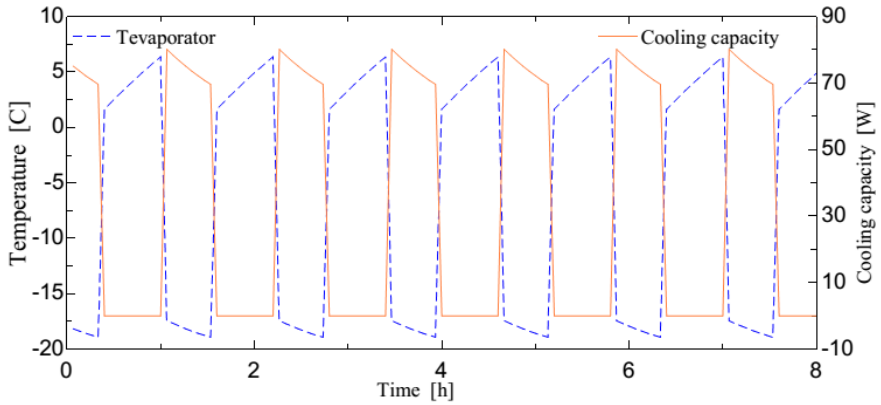

Figure 2.2. Evaporator temperature and cooling capacity (without PCM) (Source: K. Azzouz, Leducq, D., Guilpart, J., Gobin, D., 2005).

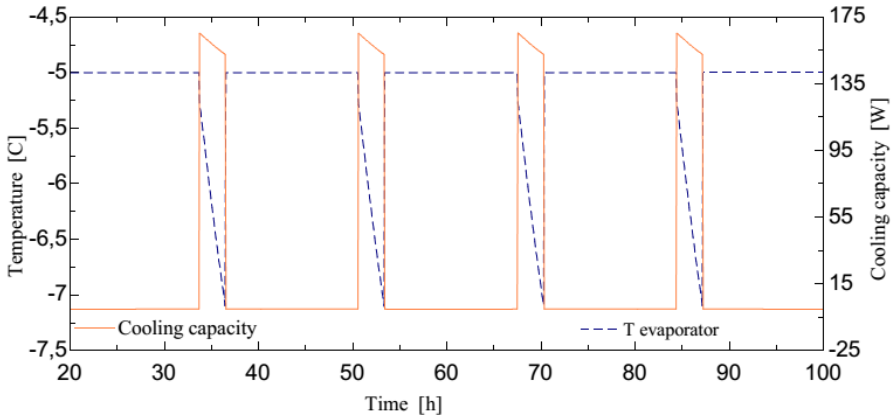

Figure 2.3. Evaporator temperature and cooling capacity (with PCM) (Source: K. Azzouz, Leducq, D., Guilpart, J., Gobin, D., 2005).

In another study by K. Azzouz et al. (2008), the mathematical model in their previous study is supported by experiments. They used the same refrigerator and PCMs. They validated their model by experimental measurements for the cases with and without PCM. After the model is validated, they did a series of simulations to perform a parametric study with different phase change temperatures from -9 to 0^{o}C, various PCM thicknesses and various thermal loads. Like in the previous study, the PCM slab is located at the back side of the evaporator. The surface area of PCM slab is 0.48 m^{2}. In experiments, ambient temperature was 20^{o}C and cabinet temperature was 5^{o}C. After the tests, numerical simulations were conducted with the same operating conditions, and it was seen that the numerical and experimental results are in good agreement (K. Azzouz, Leducq, & Gobin, 2008).

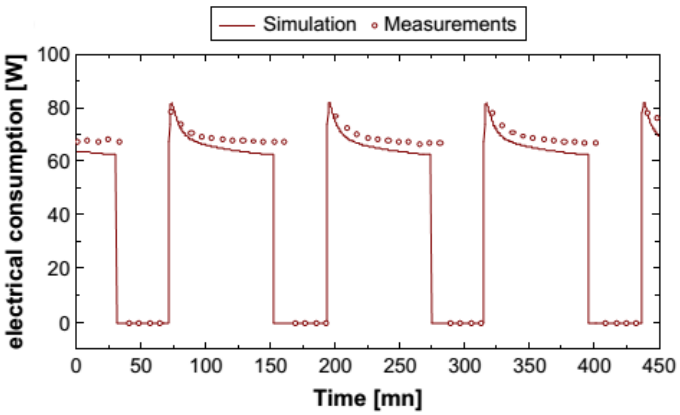

Figure 2.4. Electric consumption of compressor for the case of without PCM (Source: K. Azzouz et al., 2008).

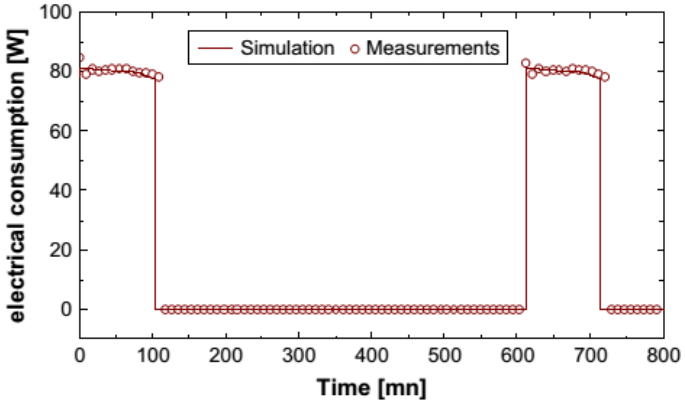

Figure 2.5. Electric consumption of compressor for the case of with PCM (Source: K. Azzouz et al., 2008).

In Figure 2.4. and Figure 2.5., the electric consumptions of compressor with and without PCM can be seen respectively. As it can be seen from these figures, the results of numerical analyses and experiments are in good agreement. The mean electric consumption is decreased significantly with the application of PCM. (K. Azzouz et al., 2008).

To describe the effect of PCM slab on the evaporator more clearly by experiments, K. Azzouz et al. conducted another experimental study in 2009. In this study, water and an eutectic mixture having a phase change temperature of -3^{o}C is used for a variety of operating conditions (PCM thickness, ambient temperature and thermal load). This study suggests some options to improve the efficiency of a refrigerator and the option of improving the efficiency of heat exchangers (evaporator and condenser) by using latent heat with PCMs to the evaporator is investigated thoroughly, which is a cheap and effective solution.

The experimental device used in previous studies by K. Azzouz remained unchanged in this study, and the PCM slab is also located at the back side of the evaporator. Two setups with different PCM quantities are prepared, having thicknesses of 5 and 10 mm. Temperatures at various locations, such as compressor, condenser, evaporator, PCM slab and refrigerated space are measured with thermocouples. The uncertainity is estimated to be 0.5^{o}C. In the experimental setup, 45 thermocouples are located regularly inside of the PCM slab to get the spatial temperature distribution inside the PCM. Also, 3 thermocouples are used to measure the refrigerated space temperature. Evaporator and condenser pressures are measured at compressor inlet and outlet with two pressure transducers. Electric consumption is measured by a wattmeter.

The experimental procedure is started with calculating the overall thermal conductance of the refrigerator cabinet. To evaluate the performance and cool storage capacity by PCMs, a variety of experiments are done with the cases of no PCM, water as PCM and eutectic mixture as PCM. The data is collected by measurement instruments in a frequency of 1 minute (K. Azzouz, Leducq, & Gobin, 2009).

The air temperature results of the experiments with water can be seen in Figure 2.6. The air temperature here is the temperature average of 3 thermocouples located inside the refrigerated space.

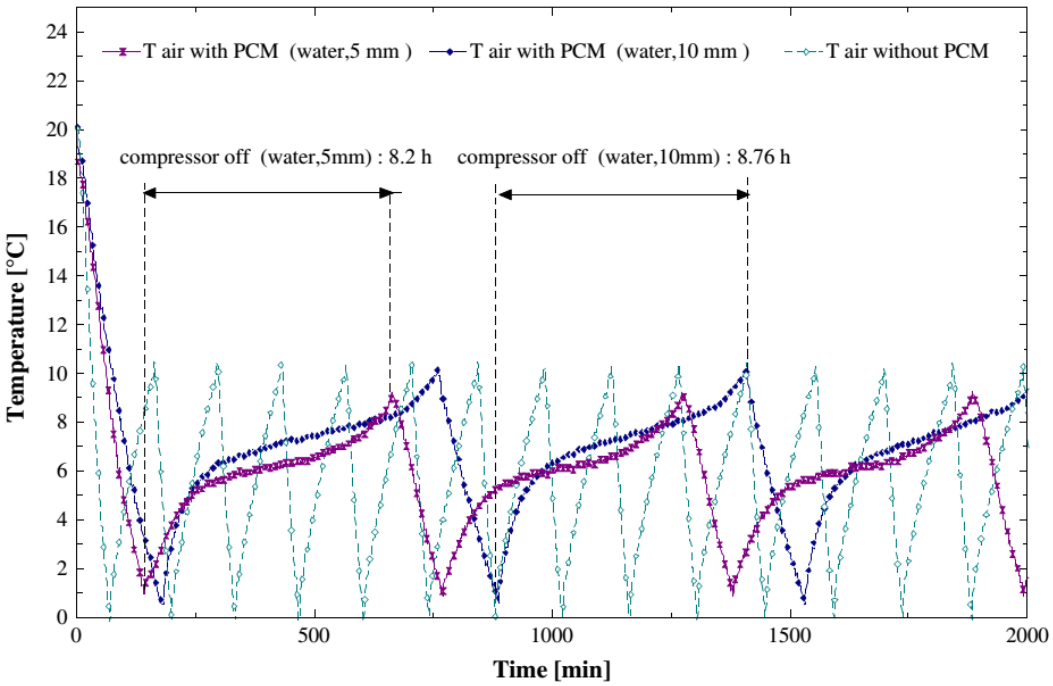

Figure 2.6. Time evolution of air temperatures of refrigerated cabin, with water as PCM (Source: K. Azzouz et al., 2009).

In Figure 2.6., the ambient temperature is 20°C and thermal load is zero. The influence of the PCM on the cabinet temperature and start and stop number of compressor is very clear. The percentage of runtime of the compressor is much lower with PCM slab, which allows 5 – 9 hours of continuous operation without electric supply (K. Azzouz et al., 2009). In Figure 2.7., the average air temperature with eutectic aqueous solution and the comparison with water in terms of operation without electric can be seen.

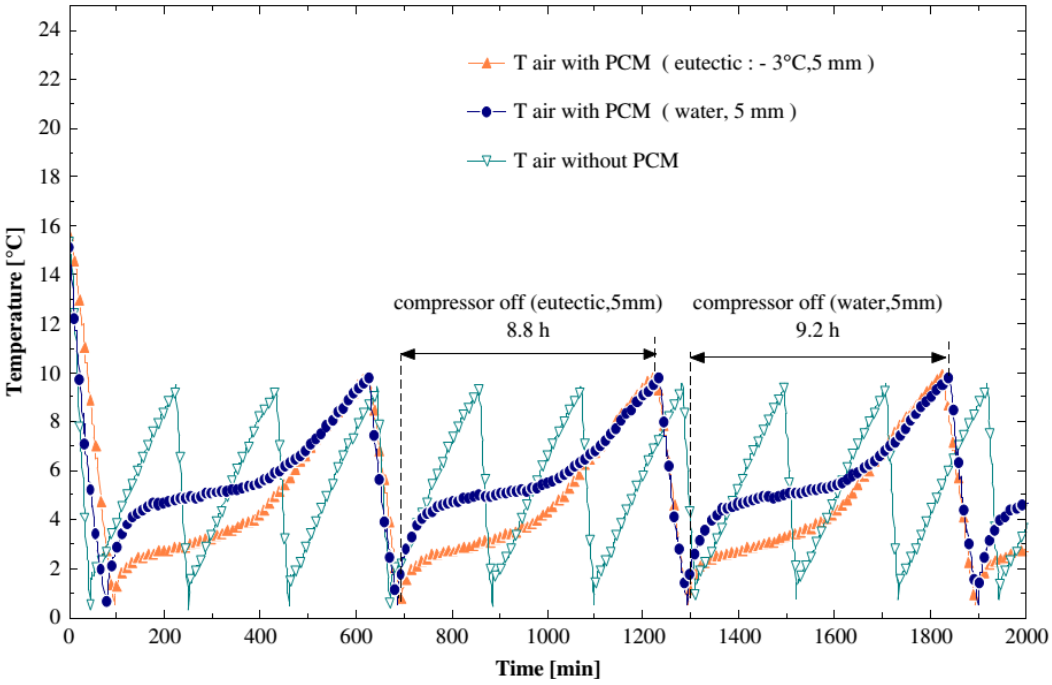

Figure 2.7. Time evolution of air temperatures of refrigerated cabin, with eutectic solution as PCM (Source: K. Azzouz et al., 2009).

As it can be seen in Figure 2.7., the storage capacity of eutectic solution is slightly less than the water. This is because of the latent heat capacity of solution, which is lower than the water (310 and 330 kJ/kg, for solution and water respectively). Although the storage capacity of eutectic solution is lower, its advantage is maintaining a lower temperature in refrigerated space, since its phase change temperature is lower. The other benefit of employing PCM arises in COP. According to the experiments, the COP increase is between %10 and 30, depending on the thermal load and the type of PCM used.

In another study by A.C. Marques et al. analyzed a static type thermal energy storage refrigerator numerically to compare the temperature stability with using different type PCMs. Three scenarios about the location of PCMs are included and the

most effective one is evaluated, vertical position at the backside of storage compartment, horizontal position at the top of the compartment, and the combination of these two (vertical and horizontal). In the numerical model, only the half of the refrigerator compartment is included because of the symmetric geometry. The model is solved with a mesh of 455000 cells with a finer mesh structure near wall to solve the boundary layers better. The Rayleigh numbers are calculated according to the scenarios explained above and it is found less than 10^9 for all cases, so the effects of turbulence is neglected. To solve the effects of density variation, Boussinesq approach is employed. Discrete ordinate (DO) radiation model is used since radiation heat transfer coefficient has the same order of magnitude with the convection. The biggest assumption in this study is, the solidification and melting cycles of the PCMs are not included. Instead, the PCM surfaces are modeled as boundary condition with constant temperature corresponding to the phase change temperature of PCMs and the solution is conducted for steady state case. At first, the model was validated by using both previous studies and experiments, and then simulations are conducted. According to the simulations, vertical PCM configuration resulted a stratified temperature profile. The maximum temperature is 14.8^{o}C and the average temperature is 11.2^{o}C. The airflow is circular and air is nearly stagnant at the center. Horizontal PCM configuration resulted more homogeneous temperature profile, with 2.4^{o}C average temperature lower than previous case. The most homogeneous air temperature profile is observed in the third case, combined vertical and horizontal PCM configuration. The average temperature is also lowest, which is 6.1^{o}C (Marques, Davies, Evans, Maidment, & Wood, 2013).

A.C. Marques et al. conducted another study in 2013. In this study, the efficiency gain caused by a larger compressor change is resulted a more frequent start – stop cycles of the compressor. To lower the start – stop number of the compressor and increase the efficiency even more, a method is proposed which offer accumulating the cold energy capacity of compressor in a PCM, which is assumed to reduce the number of start – stop cycles. Numerical modelling and experimental prototyping was undertaken. Encapsulated ice was used as energy storage media in this study. One surface of slabs containing ice is in thermal contact with the evaporator, while another surface is subjected to natural convection from the refrigerated space. To conduct the numerical part, a mathematical model is used to find the heat transfer during the phase change, with conservation of energy equations for liquid and solid phases discretized on a fixed grid and solved with finite difference method. It was assumed that the

conduction is the only heat transfer mechanism inside the PCM and walls are assumed to be insulated except the ones in contact with evaporator and refrigerated space. 2, 3, 4 and 5 mm of PCM slabs, 20, 25 and 30^{o}C of ambient temperatures and -15 and -10^{o}C of evaporating temperatures were used to investigate the effects of these variations. Numerical model was validated with an experimental rig having a 5 mm thickness of PCM slab. According to the numerical analyses and experiments, increasing the displacement of compressor from 4 cm^3 to 8 cm^3 reduced the energy requirement by %19.5. By employing a 5 mm of PCM slab into the refrigerator increases this energy efficiency even more by allowing the refrigerator to operate 3 or 5 hours without power supply, depending on the thermal load inside the refrigerator thanks to the latent heat storage. The numerical model is found in good agreement with the experiments, showing an error margin less than %5 (Marques, Davies, Maidment, Evans, & Wood, 2014).

Pradip Radhakrishnan Subramaniam et al. presented a method and design of a dual evaporator refrigerator equipped with PCMs in 2010. They made a mathematical model and simulation program of a refrigerator with a freezer – fresh food type domestic refrigerator to simulate the energy consumption of this new design. The used PCM is an eutectic mixture having a phase change temperature below 0^{o}C. The simulation program is developed in MS Excel macros with Visual Basic programming language. This program predicts and optimizes the new design refrigerator by calculating the energy requirements. According to this model, they also prepared a experimental refrigerator prototype. The simulations are resulted a COP increase from 1.5624 to 1.808 when PCM is discharging and 2.007 when PCM is charging (Subramaniam, 2010).

In 2011, Wen – Long Cheng took a different approach about applying phase change materials into the household refrigerators. They did not apply the material near evaporator or to the walls of refrigerated cabin, instead they wrapped PCMs around the condenser coils and investigated the performance of this new refrigerator experimentally. For this new refrigerator, part of condensation heat is stored into the PCMs during the working time of compressor, and this heat is dissipated to the environment during off – time of the compressor. This makes the condensation temperature lower, the evaporating temperature higher and the overall heat transfer performance is increased. In this paper, an ordinary double door static type household refrigerator was used in experiments. The used PCM was prepared with paraffin, high

density polyethylene and expanded graphite, whose phase change temperature matched to the condensation temperature. Both the new and ordinary refrigerators were tested with the same procedure and the test room was kept at 25^{o}C. According to the experiments, compared to the ordinary refrigerator, the novel refrigerator dissipates heat from the condenser in a continuous manner during whole cycle, resulting in a lower condensation temperature. Also, the total cycle time (between two successive starts) of the new refrigerator is much shorter, while the ratio of on time to the total working time is higher. Under the stable operating conditions, the energy consumptions of the new and ordinary refrigerators are 0.51 kWh and 0.45 kWh respectively, meaning a %12 in energy savings (Cheng, Mei, Liu, Huang, & Yuan, 2011).

Since investigating the effects of PCM on the condenser coils experimentally requires much time and money, the working characteristics of the new refrigerator explained in the previous study is studied numerically by Wen – Long Cheng and Xu – Dong Duan in 2014. A dynamic simulation model is established for these purposes according to the ISO standards and the model is computed against the experimental results. The model is based on the refrigerator in their previous study in 2011 and the same PCM is used. The results of simulations agreed well with experiments. The energy savings caused by the PCM was analyzed more deeply by means of refrigerating capacity, the power and the heat leakage from ambient to the refrigerated cabin by this model. According to the results of the simulations, the refrigerating capacity of the new refrigerator is obviously higher than the ordinary one. The increase in COP is %18, from 1.34 to 1.59. The energy consumption is decreased from 0.502 kWh/24h to 0.441 kWh/24h, which is a %12 decrease. The simulations are conducted at different ambient temperatures (15, 20, 25 and 30^{o}C), different freezer air temperatures (-6, -12 and -18 ^{o}C) and different phase change temperatures to see the effects of these parameters. According to the results, the increasing ambient temperature results a decrease in the COP and an increase in the energy consumption. However, when PCMs are in action, the COP increases and this increase gets higher as the ambient temperature increases. When the phase change temperature is 49^{o}C, it is found that the energy consumption is minimum (Cheng & Yuan, 2013).

In 2012, Oro et al. conducted an experimental study, aiming to increase the thermal performance of commercial freezers by PCMs usually used in supermarkets, by decreasing the temperature fluctuations inside the freezer, under the cases of electrical failure or frequent door openings. Their main motivation was to increase the lifetime

and quality of frozen food, which have to be kept under -18^{o}C. A commercial PCM (Climsel C-18 by Climator) is employed for this purpose, having a melting point of -18^{o}C. The used freezer is a vertical type static freezer. The evaporator tubes form the base of freezer shelves. It has a double glass door and a thermometer. The PCM is encapsulated into stainless steel plates having a thickness of 10 mm and these plates are placed at the top of evaporator coils of every shelf of freezer. The number of PCM plates is 6. During the normal freezing cycle, a fan at the top of refrigerated space circulates air. Test packages (M – packs) are used to simulate the thermal load and thermocouples are placed in the center of some M – packs to measure the temperature fluctuations of M – packs. Experiments are conducted with and without the PCMs and M – packs. Different scenarios are specified for door openings and electrical failure. During the experiments, air temperature inside the freezer, M – pack temperatures, PCM temperatures and ambient temperature is measured and monitored. According to the experiments, the temperature distribution inside the freezer reached highest values without PCM and M – packs in the case of electrical failure as expected, since thermal load is least in this case. The addition of PCM showed a great benefit to the temperature distribution inside the freezer. After a prolonged electrical failure, the use of PCM made the temperatures 4 or 6^{o}C lower. (Oró, Miró, Farid, & Cabeza, 2012).

A similar study of the Oro et al. (2012) is conducted by Benjamin Gin and Mohammed M. Farid in 2010. They placed PCM panels to the internal walls of a freezer and applied a repeated power loss to the freezer. Comparisons are made with and without PCM panels. Product analysis is also made by measuring drip loss meat and ice crystal size in ice cream blocks. A low temperature PCM, having a phase change temperature of -15.4^{o}C is placed to a vertical type freezer in this study. The PCM panels have a width of 10 mm and are installed to the internal walls, as shown in Figure 2.8.

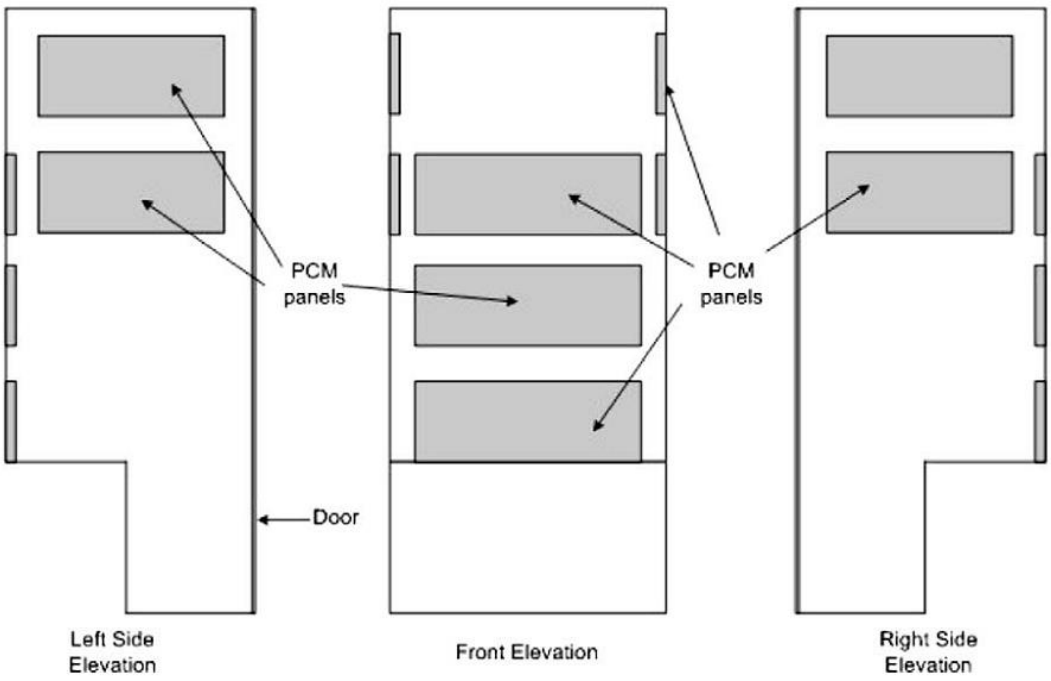

Figure 2.8. Placement of the PCM panels in the internal walls of freezer (Source: Gin & Farid, 2010).

Heat loads due to electrical power loss was investigated for 2 weeks. Samples are taken from ice cream blocks and meat and they were analyzed every 2 days. According to the experiments, while the product temperature is increased from -16^{o}C to -3^{o}C without PCM with a deviation of 13^{o}C, it increased to only -11^{o}C with PCM while the electricity is gone. Also, the ice cream crystal size remained almost constant and the drip loss in the meat is much lower with PCM (Gin & Farid, 2010).

2.1. Scope of This Study

In this thesis, as explained in the previous chapter, the effect of PCMs on the temperatures of refrigerated space is investigated numerically by using ANSYS – FLUENT commercial CFD code. A single door static type refrigerator is modelled. First, the refrigerator is simulated without PCMs for the steady state case. The evaporator temperature, ambient temperatures at compressor and condenser zones are constant in this case. The steady temperature distributions, thus the ideal zones for cold storage with PCMs are specified. Zones with a low temperature and have a large area is thought to be the ideal zones for application of PCMs. After the steady state case, transient simulations are conducted to see how the temperatures of zones specified for

PCM application changes in time. The transient boundary conditions include the variations of evaporator, condenser and compressor area temperatures caused by the stop – start cycles of compressor. As a last step, PCM slabs are placed in the appropriate places in the refrigerated space walls and transient CFD analyses are conducted to see how the temperature behavior of the refrigerator changes. Water and some commercial PCMs having phase change temperatures about $10^{o}C$ are used, since the wall temperatures are in this order of magnitude. The thermophysical properties of the PCMs are taken from the catalogues and defined in FLUENT.

CHAPTER 3

PHASE CHANGE MATERIALS (PCMs)

Storing of cold or hot heat energy can be done by thermal energy storage (TES). There are basically 2 distinct ways for TES, physical and chemical methods. Physical methods can be divided into 2, which are sensible heat storage and latent heat storage. In Figure 3.1. , these methods and the materials used can be seen in detail (Mehling & Cabeza, 2008).

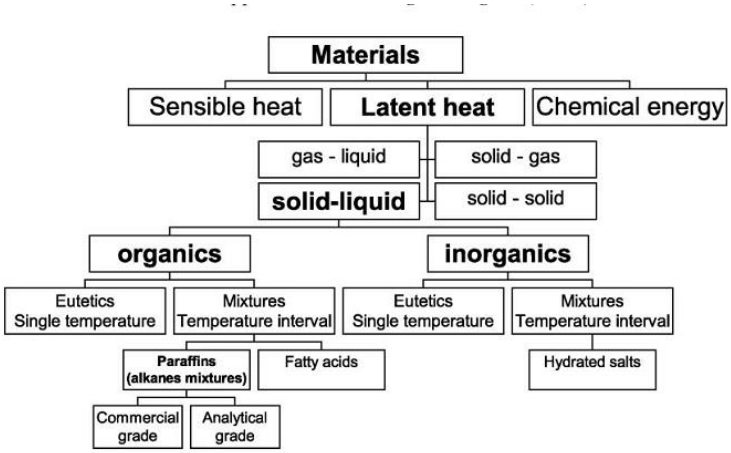

Figure 3.1. Thermal energy storage method and material classification (Source: Zalba, Marín, Cabeza, & Mehling, 2003).

3.1. Sensible Heat Storage

If the heat input to the storage media (ΔQ) provides a linear temperature increase (ΔT) of the media, then this kind of storage is called as sensible heat storage (Mehling & Cabeza, 2008).

$$\Delta Q = C\Delta T = mc_p\Delta T \tag{3.1}$$

3.2. Latent Heat Storage and Phase Change Materials

In this kind of storage, the storage media undergoes a phase change. If a proper material is selected, the solid – liquid phase change can store a large amount of heat. This makes the latent heat storage is accepted to be the most effective way of heat storage (Mehling & Cabeza, 2008). For example, while the sensible heat capacity of water in a 20^{o}C temperature interval is 84 kJ/kg, the latent heat storage capacity of water at 0^{o}C 330 kJ/kg, which is about 3.5 times of sensible heat in a 20^{o}C temperature interval.

In pure materials and eutectic mixtures, the temperature remains constant as the heat is transferred or rejected during the phase change. The heat transfer after phase change is stored as sensible heat. The amount of heat stored in the storage media can be calculated by using the enthalpy difference between solid and liquid phases. (Equation (3.2)) This enthalpy difference between solid and liquid phases is called as "melting enthalpy", or "enthalpy of fusion" (ΔH) (Mehling & Cabeza, 2008). The latent heat storage between solid and liquid phases can be seen in Figure 3.2.

$$\Delta Q = \Delta H = m\Delta h \tag{3.2}$$

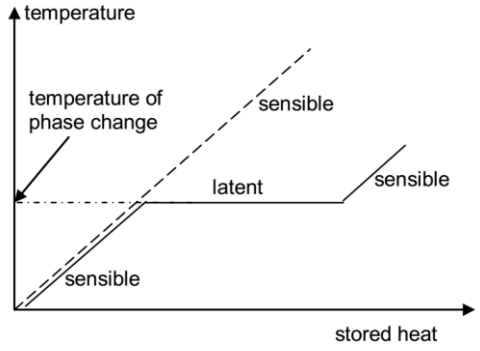

Figure 3.2. Latent heat storage
(Source: Mehling & Cabeza, 2008)

The materials that can store heat or cold energy as latent heat between its solid and liquid phase change temperatures is called as "Phase Change Materials", or PCMs. These materials can store large amounts of heat in a narrow temperature range, so it is possible to add or reject heat to these materials without much temperature change. They can be used in cases where temperature fluctuation is not desired, such as food or beverage preservation, or building indoor walls etc.

3.3. Limitations and Requirements of PCMs

A material should satisfy some requirements to be used as PCM. These requirements can be listed as follows;

- It should have a high heat of fusion and heat conductivity.
- Melt congruently with a minimum amount of subcooling. If the composition of the liquid is the same with the composition of the solid during the melting process of a compound, then it is said that the material melts conguently.
- Be chemically stable and not to be reactive with its container.
- Not to be corrosive.
- Not to be poisonous or flammable.
- Not have a high vapor pressure to not cause excessive stresses to its container.
- Its volume change during phase change must be low (Mohammed M. Farid, Khudhair, Razack, & Al-Hallaj, 2004).

Also, a PCM should be resistant to a high number of freezing and melting cycles. For example, a PCM that is used to protect a building from excessive heat during a fire only undergoes a single melting and freezing cycle. However, in the case of building cooling or heating, the number of freezing and melting cycles may be thousands (Mehling & Cabeza, 2008).

There are some limitations of PCMs, that make them difficult to use in practical engineering applications. The most significant ones are “Subcooling” and “Phase Separation”.

3.3.1. Subcooling

When a PCM reaches to its freezing point during freezing, it may not start to freeze. Lower temperatures might be required to initiate freezing. If that temperature is not reached, then the melting cannot start and the material stores only sensible heat. This reduces the latent heat storage capacity of PCM and should be considered (Kuznik, David, Johannes, & Roux, 2011). This phenomenon is called as “Subcooling” or “Supercooling” and can be seen in Figure 3.3.

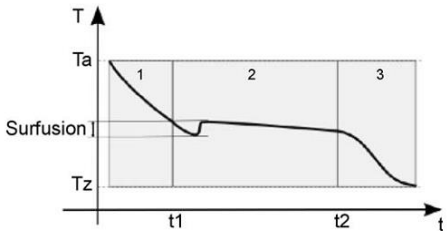

Figure 3.3. The subcooling effect
(Source: Kuznik et al., 2011)

The main reason behind subcooling can be described in molecular level. To start the solidification, there has to be at least one solid particle inside the material in liquid form, where the solidification takes place and grows. For this action, the small particle has to release its energy in heat form. For the particles that has very small radius (r), the heat released for phase change (proportional to r^3) may not be higher than the surface force (proportional to r^2) which means an energy barrier preventing the solidification until a particle having sufficient radius exists. Therefore, much lower temperatures are required to initiate solidification in subcooling (Mehling & Cabeza, 2008) .

3.3.2. Phase Separation

The most significant problem caused by the melting and freezing cycle is the phase separation. If PCM is composed by different kind of materials, these materials may separate from each other macroscopically and form different phases, which reduces the heat storage capacity of PCM (Mehling & Cabeza, 2008). In Figure 3.4, the result of phase separation seen in a water – salt solution can be seen.

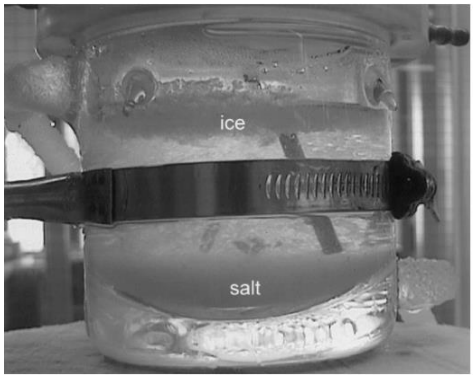

Figure 3.4. Phase Separation
(Source: CoalTech)

3.4. Types of PCMs

There are various PCMs in the market having different phase change temperatures, which are being used in different fields. The material types that are used as PCM presently are as follows, hydrated salts, paraffins, fatty acids, eutectic solutions, organic and inorganic compounds (Mohammed M. Farid et al., 2004). The working temperatures and melting enthalpies of these materials can be seen in.Figure 3.5.

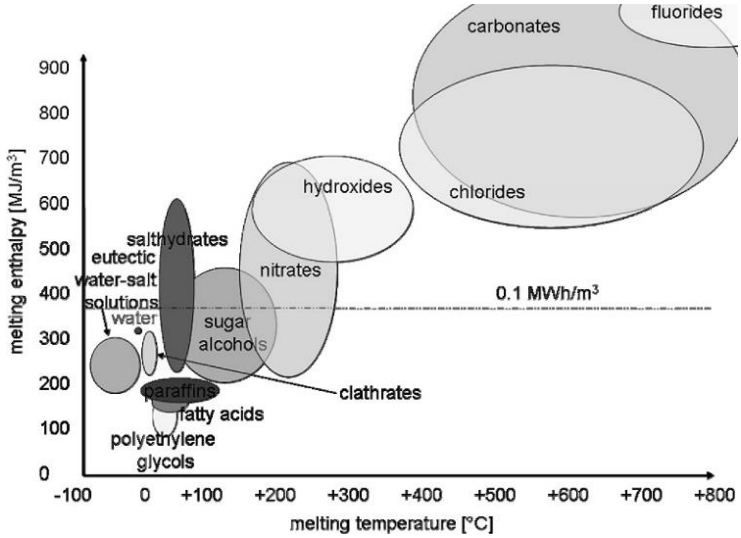

Figure 3.5. Working temperatures and melting enthalpies of different PCMs (Source: Mehling & Cabeza, 2008)

The most common PCM is water. For the temperatures less than 0^{o}C, eutectic water – salt mixtures are used. For the temperature range of 0 – 130^{o}C, salty hydrates, paraffins, fatty acids and alcohols can be used. Inorganic materials, like eutectic water – salt solutions and hydrated salts, can be used in a wide temperature range. Their most common disadvantage is they cause corrosion in metals The presence of salt makes the corrosion problem even worse (Mehling & Cabeza, 2008).

3.4.1. Eutectic Water – Salt Solutions

Eutectic mixtures are the mixtures whose components undergo phase change simultaneously at a minimum temperature. By this way, none of the components forming the solution cannot separate each other during the phase change. Since addition of salt to water decrease the phase change temperature of water below 0^{o}C, eutectic

water – salt mixtures can be used in areas of low temperature needs, so they are considered as suitable PCM for most domestic refrigerators and freezers.

In Table 3.1., thermal properties of some eutectic water – salt solutions can be seen.

Table 3.1. Some eutectic water – salt solutions and their thermal properties.

PCM	Melting Point (^oC)	Mixing Ratio	Melting Enthalpy (kJ/kg)	Density (kg/m^3)
$Al(NO_3)_3$ - H_2O	-30,6	30,5% $Al(NO_3)_3$	131	1283 (liquid) 1251 (solid)
NaCL -H_2O	-21,2	22,4% NaCl	222	1165 (liquid) 1108 (solid)
KCl - H_2O	-10,7	19,5% KCl	283	1126 (liquid) 1105 (solid)
H_2O	0		333	998 (liquid) 917 (solid)

Since there are two components in the water – salt solutions, phase separation is a possible problem. To prevent this and to increase the total number of freezing and melting cycles of the solution, it must be precisely on the "eutectic point". Eutectic water – salt solutions are also susceptible to subcooling. Like water, eutectic water – salt solutions may subcool several K's (Mehling & Cabeza, 2008).

3.4.2. Hydrated Salts

Hydrated salts are the oldest and the most studied type of PCMs. They consist of a salt and water combined in a crystalline matrix in solid form, with a general formula of $AB.nH_2O$ (A. Sharma, Tyagi, Chen, & Buddhi, 2009). They are attractive materials for heat storage within a temperature range of 0 and 130^oC (Figure 3.5). They have a high storage density with an average of 350 MJ/m^3 and relatively high thermal conductivity about 0.5 W/m.K (Mohammed M. Farid et al., 2004).

In Table 3.2., the thermal properties of low temperature salt hydrates having a phase change temperature range of 8 – 15^oC are given, which may be potential candidates in the warmer walls of domestic refrigerators. As seen on the table, lithium chlorate trihydrate (formulated by $LiClO_3.3H_2O$) has an extremely high storage capacity among the other materials and suitable for most cooling systems with its phase change temperature (Gawron & Schröder, 1977).

Table 3.2. Some salt hydrates and their thermal properties

PCM	Melting Point (^oC)	Melting Enthalpy (kJ/kg)	Density (kg/m^3)
$LiCLO_3.3H_2O$	8	253	1530 (liquid) 1720 (solid)
$NH_4CL.Na_2SO_4.10H_2O$	11	163	- -
$K_2HO_4.6H_2O$	14	108	- -

Since hydrated salts also contain more than one component, like eutectic water – salt solutions, phase separation may also happen and problems about the storage density may arise with the freezing – melting cycles. Subcooling is also a serious problem of the hydrated salts, and the amount of subcooling can be as high as 80K (Mehling & Cabeza, 2008). These disadvantages related with salt hydrates can be solved by some specific methods. For example, phase separation can be eliminated by thickening the material with gells. Subcooling is related with the difficulty of nucleation during freezing, and this can be avoided by adding some additives that accelerate nucleation to start crystal growth (S. D. Sharma & Sagara, 2005).

CHAPTER 4

NUMERICAL METHOD

In this thesis, Finite Volume based numerical schemas are employed, with the well – known commercial computational fluid dynamics (CFD) code, called FLUENT (ANSYS Corp.). A refrigerator model suitable for CFD meshing is prepared with respect to the actual 3D mechanical model, by the CAD modelling software Solidworks (Dassault Systemes SolidWorks Corp.). The model used in CFD analyses are validated by experimental data supplied by INDESIT company. After the modelling and validation of a refrigerator is completed, PCMs with suitable phase change temperature are placed in appropriate places in the model and transient simulations are conducted to see the effect of PCMs. While selecting and placing PCMs, it is considered that regions having large area and less temperature change are suitable for application of PCMs.

FLUENT has comprehensive modelling abilities used for wide range of flows. The flows including incompressible, compressible, turbulent, laminar, Newtonian or non – Newtonian can be modelled and simulated with FLUENT with complex domains. It includes mathematical models for not only engineering flows, but also transport phenomena such as chemical reactions or heat transfer, for both steady state and transient cases (ANSYS, 2011a).

In experiments conducted by INDESIT company, which are based on ISO15502 standards, thermocouples are placed at 4 temperature measurement points. 3 of them are at the centers of partitions that are separated by the shelves (T_1, T_2, T_3) and one of them is placed at the center of crisper on the right ($T_{crisper}$). These temperature measurement points can be seen on Figure 4.1. The thermocouples are placed in brass pieces to fix them and stabilize the temperature fluctuations. The cylindrical brass pieces have dimensions of 1cm diameter and 1 cm height, and their mass is approximately 6.7g. The validation of CFD simulations with the experimental data are done according to the temperature of these points.

A brief introduction to CFD method, its advantages and disadvantages and are explained in the following sections.

Figure 4.1. Temperature measurement points

4.1.1. The CFD Method

Computational Fluid Dynamics, or CFD is an analysis and simulation tool using the computer processing power used for the problems associated with fluid flow, heat transfer and other related phenomena, such as chemical reactions. Since the governing equations for these are so complex and non – linear, CFD is a powerful method to solve them. It is being used in industrial areas such as aerodynamics and aircraft vehicles, turbomachinery, cooling of electrical equipment, chemical process engineering, building and HVAC applications and so on. Commercial CFD codes contain user interfaces to input the problem variables and to study the results. The algorithms that the CFD codes employ contain three main elements, which are pre – processor, solver and post – processor (Versteeg & Malalasekera, 2007).

4.1.1.1. Pre - Processor

By using the pre – processor, user can input the computational domain, generate the mesh (or grid) which is the division of the domain into a number of infinitesimal sub

– domains (control volumes, or cells), and finally select the physical phenomena that the problem contains, define the fluid properties, and specify the boundary conditions.

4.1.1.2. Solver

Solver solves the governing equations of the physical phenomena associated with the problem in all the control volumes of the domain, by using numerical solution techniques. The numerical solution techniques are as follows, finite difference, finite element and spectral methods. CFD codes use the finite volume method, which is a special formulation of the finite difference technique. The solution of problem variables (velocity, temperature, pressure etc.) is defined at nodes at the center of each cell (or control volume) in the domain. The number of cells is associated with the accuracy of CFD solution, in general, larger number of cells yield a better solution accuracy, with a cost of higher computation time and computer hardware. So, optimizing the mesh in a non – uniform structure is crucial, with finer elements at critical locations with a large variation of flow variables and coarser elements at locations with less variation (Versteeg & Malalasekera, 2007).

In outline, any CFD code integrates the governing equations into the control volumes of the domain, discretizes the governing equations, which is the conversion of integral equations into a system of algebraic equations, and solves the algebraic equations in an iterative manner. The conservation of any flow variable φ, inside the control volume can be expressed in Equation (4.1) (Versteeg & Malalasekera, 2007).

$$\begin{bmatrix} Rate\ of\ change \\ of\ \varphi\ in\ the\ C.V \end{bmatrix} = \begin{bmatrix} Net\ rate\ of \\ increase\ of\ \varphi \\ due\ to\ convection \end{bmatrix} + \begin{bmatrix} Net\ rate\ of \\ increase\ of\ \varphi \\ due\ to\ diffusion \end{bmatrix} + \begin{bmatrix} Net\ rate\ of \\ creation \\ of\ \varphi \end{bmatrix} \qquad (4.1)$$

Equation (4.1) suggests that the net rate of change of any variable inside of a control volume is equal to the sum of convection, due to the fluid flow, diffusion due to existing gradients and creation or destruction of the variable, also known as “source terms” (Versteeg & Malalasekera, 2007).

4.1.1.3. Post – processor

Post processor is the data visualization tool of the CFD code, including domain geometry and mesh displaying, velocity vector plots, contour plots, 2D and 3D surface plots, particle tracking and so on. Post processors are also capable of creating animations, and giving alphanumeric results in addition to the graphical results (Versteeg & Malalasekera, 2007).

4.1.2. Advantages and Limitations of CFD simulations

CFD simulations provide serious advantages over the experiment based approaches for the fluid flow and heat transfer problems. They are summarized as follows;

- Great time and cost reduction in new designs. According to an estimation of cost by Versteeg & Malalasekera (2007), the total cost for CFD simulations (hardware + commercial code) is not as high as a high quality experimental set up for most cases.
- Possibility to analyze problems whose experiments might be difficult and dangerous, or impossible to perform (e.g. too large systems),
- Practically, unlimited level of detail in results (Versteeg & Malalasekera, 2007).

Apart from these advantages, CFD simulation has some limitations and disadvantages which have to be considered cautiously. First of all, the accuracy of simulations are doubted in most cases and in some situations the user gets unsuccessful results. If the user is not well – trained, he or she has the tendency to believe that the results are true and reliable. To avoid this, the results of CFD analyses have to be validated with experiments or results of other reliable CFD simulations Also, the CFD simulation has to be mesh independent, which means increasing the number of cells in mesh must not yield different results. For good CFD results, the problem has to be mathematically simplified. Better simplification yields a better accuracy. Also, there are some incomplete models to describe some physical phenomena for CFD, such as turbulence or multiphase (Patel, 2013).

CHAPTER 5

MODELLED REFRIGERATOR

In this chapter, the specifications of the refrigerator equipped with PCMs, the methodology for numerical modelling, the geometry and mesh, boundary conditions, the materials used in simulations and assumptions are mentioned in detail.

5.1. Specifications of the Refrigerator

The refrigerator, as it said before, is a static type, single door and an unventilated type. It has a single compressor and this compressor is on/off controlled. A serpentine type evaporator is installed on its rear wall. Heat transfer mechanism is pure natural convection. The specifications of this refrigerator is given in Table 5.1.

Table 5.1. Specifications of the refrigerator

Manufacturer	INDESIT Company
Model	LARDER
Width	596 mm
Depth	590 mm
Height	1731 mm
Total Volume	

The side, front and mid – section views of solid model of the refrigerator can be seen on Figure 5.1. As seen on this figure, there are 4 shelves in the compartment and 5 shelves in the door. There are also 2 crispers at the bottom.

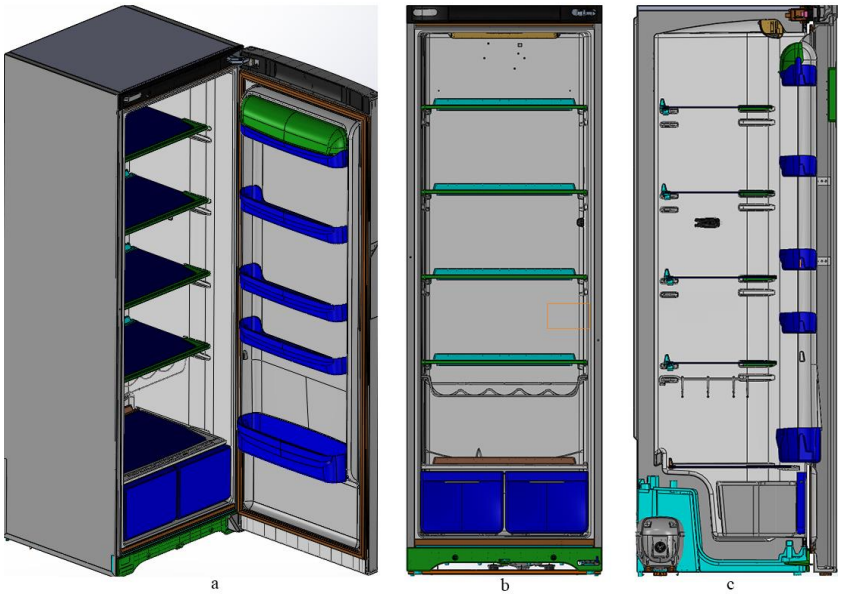

Figure 5.1. Views of the refrigerator, (a) isometric, (b) front and (c) mid – section

5.2. Geometry and Mesh

The refrigerator has a relatively complicated geometry. In order to reduce the number of cells in the mesh, which also provide a shorter calculation time during analyses, a model that is simple enough for CFD analyses is drawn based on the actual refrigerator. The fillets at the corners and edges, some details that may not affect the flow such as screw holes are omitted. Surfaces that have slight leaning (up to 10^{o}, for example) are assumed to be vertical or horizontal and surfaces which are slightly curved are assumed to be flat. The comparison of actual geometry and redrawn geometry for CFD analyses can be seen on Figure 5.2.

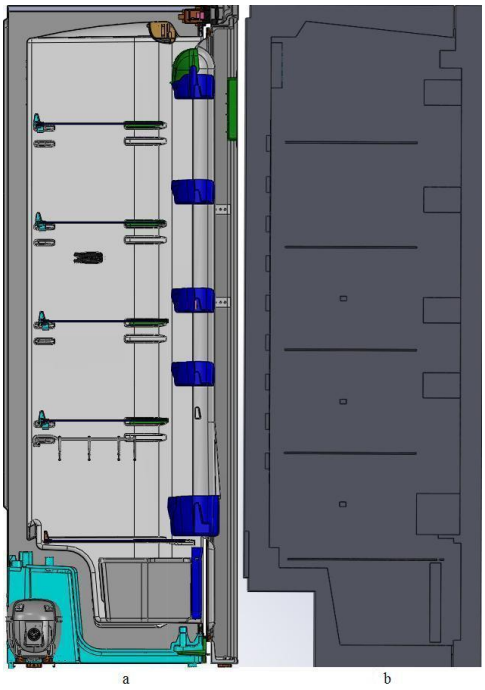

Figure 5.2. Comparison between (a) actual refrigerator model and (b) the model used in CFD analyses.

Since the geometry of the refrigerator is nearly symmetric, only half of the refrigerator is modelled and meshed and “symmetry” boundary condition is used for symmetry surfaces. While generating the mesh, the number of cells is designated to get a fast simulation without sacrificing the reliability and convergence of results.

Since the inner walls, crispers, door shelves and outer walls are in a form of thin sheet, they are not included in the model. These walls are modelled as 2D sheets and the heat transfer is modelled by a wall thickness. By this method, it is possible to solve the heat conduction in normal and tangential directions in these parts without meshing them in thickness. Since this approach eliminates the need for meshing these thin walls with a small size of cells, it reduces the number of cells in mesh greatly. After the geometry is prepared, it is transferred to ANSYS – Meshing tool and mesh is generated with Hexa cells.

Minimum and maximum mesh sizes are specified as 1 mm and 8 mm respectively. These sizes of cells are distributed such that for critical locations and narrow sections 1 – 2 mm sized cells are used and for other locations coarser cells are used having sizes of 4 – 8 mm. The total number of cells in mesh is 9941738. For near wall regions, the mesh sizes are reduced to about 0.5 mm in the normal direction with the “inflation mesh” method to solve the boundary layers better. The near wall mesh

size is crucial to solve the natural convection inside the refrigerated cabin, especially when the compressor is stopped.

The general mesh structure near wall can be seen in Figure 5.3. The near wall mesh structure can be seen in Figure 5.4., which is the area with the red circle in Figure 5.3.

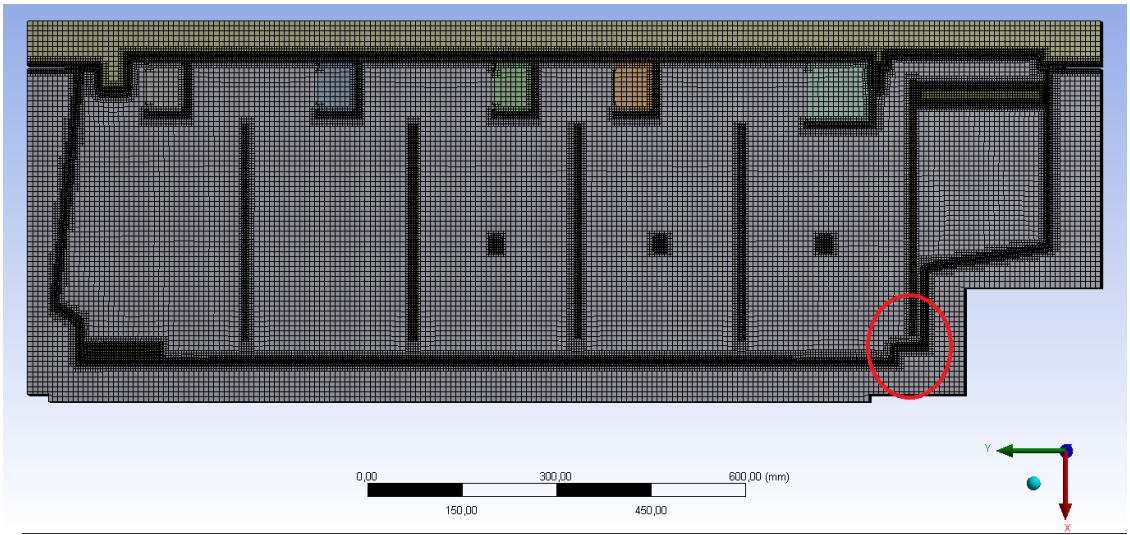

Figure 5.3. General mesh structure.

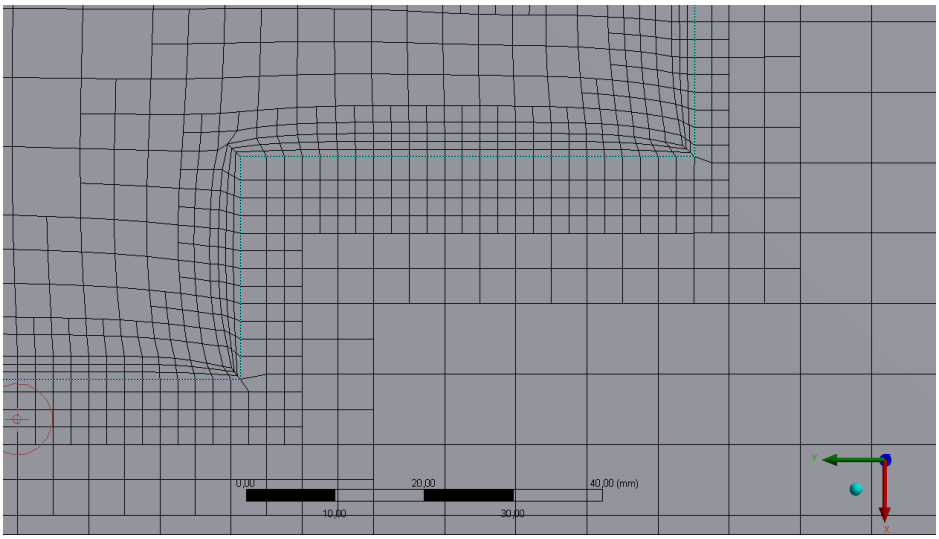

Figure 5.4. The mesh structure near a wall.

5.3. Boundary Conditions for Steady State Simulations

The boundary conditions for steady state simulations can be seen in Table 5.2. Experimental results are used while specifying the evaporator wall temperature. The

ambient temperatures (T_∞) for external walls is 25°C. For back, bottom walls and compressor area, ambient temperatures are taken 5°C higher than the other walls, since there are heat sources in these regions (compressor and condenser coils). Test conditions are used while specifying the ambient temperatures. The convective heat transfer coefficients at ambient are specified with the CFD analyses conducted before by a engineering design company for the same refrigerator.

Table 5.2. Boundary Conditions for Steady State Simulations.

Front, Side and Top Surfaces	h_c = 4.5, T_∞ = 25°C
Back and Bottom Surfaces and Compressor Region	h_c = 4.5, T_∞ = 30°C
Evaporator Temperature	T = - 23°C

The locations of these boundaries can be seen on Figure 5.5.

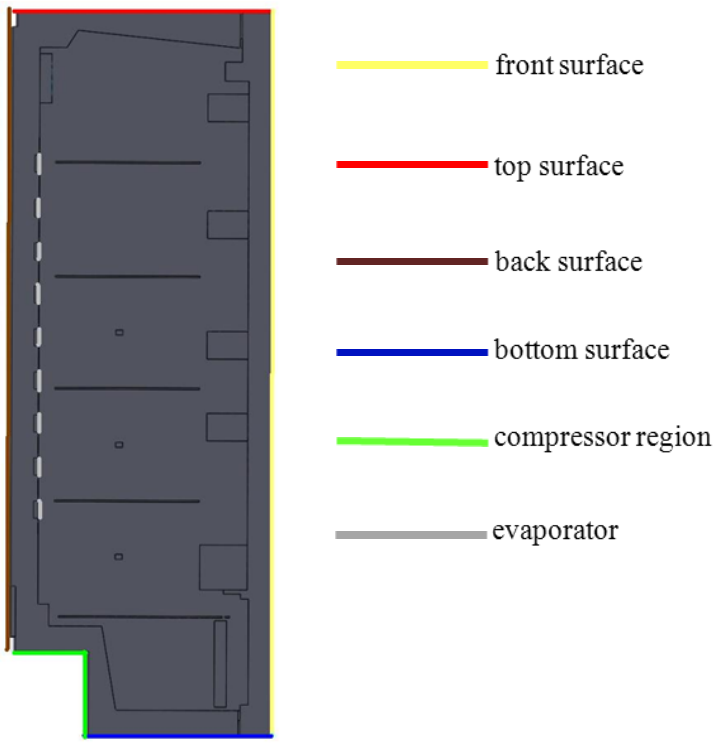

Figure 5.5. Locations of the boundaries.

The serpentine type evaporator is made by coiling the evaporator pipe and attaching the coil to an aluminum plate, which has a thickness about 0.5 mm. This system is modeled with a plate having a separate surface on it, which represents the coils of evaporator and evaporator wall temperature boundary condition is assigned to this surface. The CFD model for evaporator (the detailed view of grey area in Figure 5.5) can be seen in Figure 5.6.

Figure 5.6. CFD model for evaporator.

5.4. Boundary Conditions for Transient Simulations

A regular refrigerator, during its runtime, controls the compressor in an on/off manner with the temperature measured by the thermostat. By this control scheme, the transient stop and start cycles and temperature fluctuations arise as explained in 1.4.1. Transient CFD analyses are conducted by designating some boundary conditions variable with time. These variable boundary conditions are evaporator wall temperature, and ambient temperatures in the condenser and compressor regions. The variation of these boundary conditions are specified with the experiments conducted in INDESIT Company. To specify these boundary conditions variable with time, a user – defined function (UDF) is written.

A UDF is a computer code written in C language and loaded into FLUENT to enhance the standard features (ANSYS, 2011b). The UDF written for the transient simulations, as it is mentioned above, varies the boundary conditions in time. In this UDF, the variation of boundary conditions are defined as piecewise – linear functions. The actual variations are divided into a number of intervals, and the variations are defined as a linear function in these intervals. As an example, the evaporator wall

temperature variation of the refrigerator, and the variation defined in the UDF can be seen in Figure 5.7.

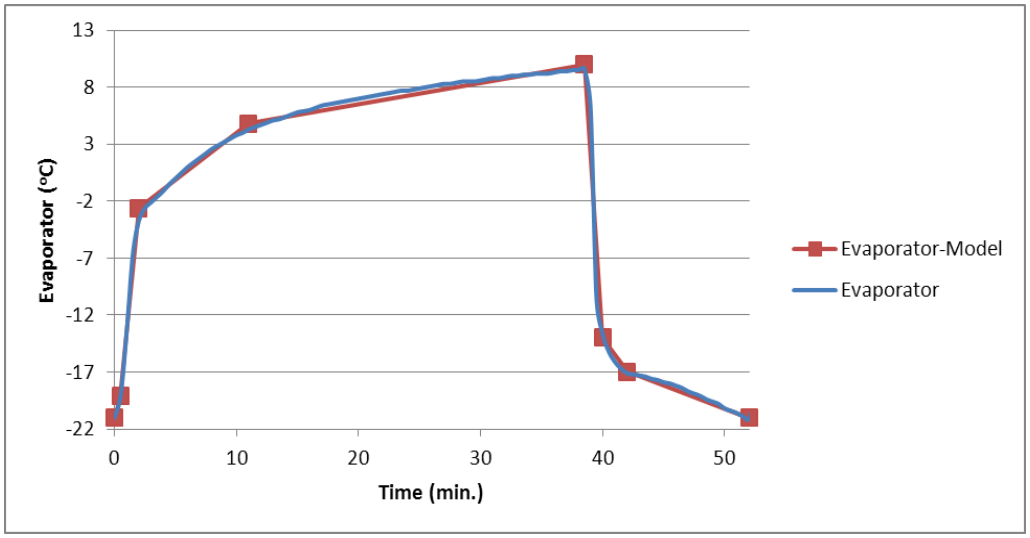

Figure 5.7. The variation of evaporator temperature with time.

In Figure 5.7., the blue plot is the actual evaporator temperature variation in test refrigerator and the red plot is the evaporator temperature variation defined in UDF. Here, the evaporator temperature shows a sharp increase from -22^{o}C to -2^{o}C in first 2 minutes. After that, it reaches to 4^{o}C at the end of next 10 minutes, continues increasing to 10^{o}C in the next 27 minutes, which is the highest evaporator temperature value. At this point, the temperature at thermostat of the test refrigerator reaches its upper limit, the compressor starts working and the evaporator temperature starts decreasing. It decreases from 10^{o}C to the temperature at the beginning, -22^{o}C in the next 13.5 minutes and the temperature in the thermostat drops to its lower limit. At this point, the compressor stops and one working cycle of the refrigerator completes.

It can be seen in this figure that, the compressor stops for first 38.5 minutes, starts working for the next 13.5 minutes and completes one cycle, which is 52 minutes. This duration is valid only in test conditions, where ambient temperature is 25^{o}C, the refrigerator is unloaded, door of the refrigerator is not opened and the transient regime reached to steady state.

The boundary conditions for transient case can be seen in Table 5.3. As it can be seen in this table, the front, side and top outer surface conditions remained unchanged. In the back, bottom and compressor region temperatures, the convection heat transfer coefficient remained unchanged, however, because there are compressor and condenser

in these regions the temperature is varied with UDF. The evaporator temperature is also varied with the UDF.

Table 5.3. Boundary Conditions for Transient Simulations

Front, Side and Top Surfaces	$h_c = 4.5$, $T_\infty = 25°C$
Back and Bottom Surfaces and Compressor Region	$h_c = 4.5$, T_∞ = UDF
Evaporator Temperature	T = UDF

As it can be seen from instructions above, the variable boundary conditions are constituted by fitting piecewise linear functions to actual temperature profiles for evaporator surface, condenser and compressor regions. While doing this, the off and on times of the compressor are assumed to be the same with test conditions (which are 38.5 and 13.5 minutes respectively). However, this may not be true for CFD simulations. The thermostat temperature of test refrigerator may reach its upper limit in 38.5 minutes but it doesn't mean that modeled refrigerator in CFD simulations will behave so. Even worse, the effect PCMs will most probably change the stop and start times dramatically. With PCMs, both stop and start times will be longer and this makes the number of total on and off cycles in a period less.

To see the on and off times of the modelled refrigerator and the effect of PCMs on total number of on – off cycles, it was crucial to model the thermostat of the refrigerator, especially in simulations with PCMs. The UDF should not works according to fixed on and off times, instead it should check the temperature of the point where thermostat was placed, and manage the on and off times according to that temperature information. Although it seems not very difficult at a first glance, we encountered many problems while writing the UDF employing this algorithm. These difficulties will be summarized in the following paragraphs.

FLUENT solver can work in 2 modes, which are "serial" and "parallel". These modes can be selected in startup window when FLUENT is executed. The serial solver manages file input and output, data storage, and flow field calculations in a single computer process. However, the parallel version allows user to calculate the solution on multiple computer processes (or "nodes") that may be on a single computer, or different computers in a network. Parallel version of FLUENT does this by splitting up the computational domain in a number of partitions and assign these to multiple processors, either on the same computer, on in different computers along a network. While the flow field calculations are done on multiple processer nodes, a "serial" node is still being

executed, to manage file input and output, data storage and other processes. (ANSYS, 2011c). Since the computational domain studied in this thesis has a complicated geometry and has a high number of cells in its mesh, it was inevitable to use the parallel version. The simulations are conducted on workstation having 8 processing units (2 processors having 4 processing cores).

The problems about the UDF capable of modelling the thermostat started at this point, when we used the new UDF with parallel version of FLUENT, it did not yield the correct temperature profile needed. When we investigated this problem deeply, we understand that the problem is about parallelizing the UDF. The UDF worked perfectly with serial FLUENT using one mesh partition. However, when the mesh is split into partitions, the computing processes measure different temperatures. Some of them can't even measure a temperature value; instead they give "indefinite" result.

When the UDF is compiled, it has to work any version of FLUENT. This requires a programming practice, referred as "parallelizing" the UDF. There are many compiler directives explained in the UDF manual of FLUENT to do this (ANSYS, 2011b). However, since this process is very complicated, requiring a deep programming experience and time is limited, we couldn't parallelize the UDF. Conducting the simulation in serial version is also useless, since it would take too much time It takes about 4 days to simulate one on – off cycle with even with parallel version, having 8 computing processes.

These problems about the UDF capable of thermostat modelling changed the roadmap of this study a little. The UDF having a fixed on – off cycle times is used in all transient simulations, both with PCM and non – PCM. The effect of PCM on temperatures of refrigerated space is investigated.

5.5. Assumptions

The assumptions that are made can be listed as follows;

- The air flow inside the refrigerator is an incompressible flow.
- Since the air flow inside the refrigerator is driven by natural convection, Boussinesq approach is used.
- Thermal properties of air are constant.
- Spalart – Allmaras turbulence model is used to solve the effects of turbulence

- Since the geometry of the refrigerator is nearly symmetric, only half of it is modelled and meshed.
- For the effects of radiation, Discrete – Ordinate method (DO) is employed.

Boussinesq approach simply says that the density variation in all directions except the direction of gravitational acceleration is negligible in natural convection flows. According to this approach, density is assumed to be constant in all governing equations, except the momentum equation in the direction of gravity. The mathematical relation of Boussinesq approach is given in Equation (5.1).

$$\left(\rho - \rho_{ref}\right)g \approx -\rho_0 \eta \left(T - T_{ref}\right)g \tag{5.1}$$

In Equation (5.1), η is thermal expansion coefficient, T_{ref} is the operational temperature, ρ_{ref} is the operational density of the flow.

Spalart – Allmaras turbulence model is a relatively new model, gaining popularity in recent years. It is a one equation model which solves a transport equation for turbulent viscosity. Since it solves one equation, it is simpler and faster than other 2 or more equation models. It can be used in engineering flows such as wall bounded aerodynamic flows and low Reynolds number flows. It is also getting popularity in turbomachinery applications. According to the observations, this turbulence model yields good results in flows where adverse pressure gradients occur in boundary layers, for example in channel flows with sudden expansions. This turbulence model is designed to get good results by employing wall functions especially in cases where mesh is coarse (ANSYS, 2011a). Therefore, it may be used in problems where solving the turbulence is not crucial and not needed to solve it in detail. Since the airflow inside refrigerated space is this kind flow and since only the effects of turbulence on heat transfer is investigated, Spalart – Allmaras method is selected for this study. It is also seen that this model yields better results than 2 equation models, such as K – epsilon or K – omega.

Discrete – Ordinate method, which is used for solving the radiative heat transfer yielded successful results to simulate the coupling of convective and radiative heat transfer in a closed cavity according to previous studies, such as (O. Laguerre et al., 2007). It can be used for heat transfer between parallel plates with participating media between them having various optical thicknesses. Effects of absorption, and both

isotropic and anistropic scattering can be solved, by entering absorption and scattering coefficients and scattering behavior as inputs to FLUENT interface.

5.6. Governing Equations

The differential equations that FLUENT solves are given below. Since the effects of turbulence is not neglected, the continuity, momentum and energy equations contain averaged and fluctuating components of variables. In these equations, the terms with an over bar indicate the average and the terms with a prime indicate the fluctuating components of the variable.

The continuity, momentum and energy equations are given below.

1. Continuity Equation:

$$\frac{\partial \overline{u_i}}{\partial x_i} = 0 \tag{5.2}$$

2. Momentum Equation:

$$\rho \overline{u_i} \frac{\partial \overline{u_i}}{\partial x_j} = -\frac{\partial \overline{P}}{\partial x_j} + \mu \frac{\partial}{\partial x_j}\left(\frac{\partial \overline{u_i}}{\partial x_j} - \rho \overline{u_i' u_j'} \right) \tag{5.3}$$

where;

$$-\rho \overline{u_i' u_j'} = 2\mu_T \left(S_{ij} - \frac{1}{3}\frac{\partial \overline{u_k}}{\partial x_k} \right) - \frac{2}{3}\rho k_T \delta_{ij} \tag{5.4}$$

3. Energy Equation:

$$\overline{u_i} \frac{\partial \overline{T}}{\partial x_i} = \frac{\partial}{\partial x_i}\left(\alpha \frac{\partial T}{\partial x_i} - \overline{u_i' T'} \right) \tag{5.5}$$

where;

$$-\overline{u_i'T} = \varepsilon_h \frac{\partial \overline{T}}{\partial x_i} \qquad \text{and;} \qquad \alpha = \frac{k}{\rho c_p} \tag{5.6}$$

The $-\rho\overline{u_i'u_j'}$ term on Equation (5.3). expresses the effects of turbulence and appears when the Navier – Stokes equations are averaged. This term can be modeled with Boussinesq approximation (Equation (5.4)). In Equation (5.4), μ_T is the turbulence viscosity and k_T is the turbulence kinetic energy. Since the turbulence kinetic energy is not solved with the Spalart – Allmaras turbulence model, the second term on the left hand side of the Equation (5.4) is omitted.

5.6.1. Radiation Equations

When radiation is enabled in the simulations, a source term including the magnitude of radiative heat transfer is included in the left hand side of Energy Equation (Equation (5.5)). The solved radiative transfer equation (RTE) for an absorbing, emitting and scattering medium in the case when radiation is enabled is as follows:

4. Radiative Transfer Equation (RTE):

$$\frac{dI(\vec{r},\vec{s})}{ds_P} + (a+\sigma_s)I(\vec{r},\vec{s}) = an^2\frac{\sigma T^4}{\pi} + \frac{\sigma_s}{4\pi}\int_0^{4\pi} I(\vec{r},\vec{s})\phi(\vec{s}.\vec{s}')d\Omega' \tag{5.7}$$

In Equation (5.7), the first term on the left hand side is the change of radiation in the medium having a thickness of ds_p (path length) and the second term I is the incoming radiation intensity, which is a function of position vector $\vec{r}$, and the direction vector $\vec{s}$. The first term on the right hand side is the emission of radiation in the medium and the second term is the addition of radiation because of scattering through the media. The path length (s_p) is the total distance that radiation intensity (I) travels.

The other terms are as follows, n is the refractive index, which is the ratio of speed of light in vacuum and the medium. For air, refractive index is 1. σ is the Stefan – Boltzmann coefficient (5.669×10^{-8} W/m^{2}K^4) and T is the local temperature of the media.

Therefore, Equation (5.7) suggests that the incoming radiation (*I*) plus the change of radiation through the participating media equals to the emission in the media and the addition of radiation due to scattering. This process can be seen schematically in Figure 5.8.

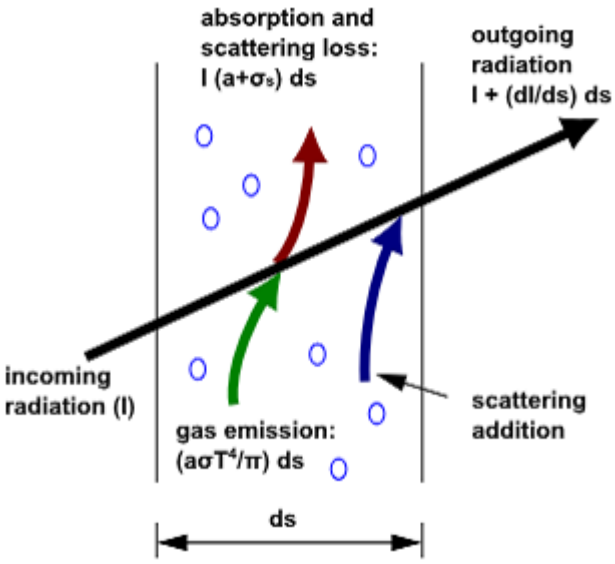

Figure 5.8. Illustration of radiative heat transfer in a participating media (Source: ANSYS, 2011a)

The *a* in the second term on the left hand side of Equation (5.7) is the absorption coefficient and σ_s is the scattering coefficient of the participating media, therefore the coefficient $(a+\sigma_s)$ on this term represents the optical thickness, or opacity of the medium and causes some loss. On the right hand side of Equation (5.7) ϕ in the second term is the scattering phase function, which is a function of direction vector ($\vec{s}$) and the scattering direction vector ($\vec{s}'$). This function appears when the participating medium include different phases, which cause anisotropic scattering of the incoming radiation.

In our simulations, both the absorption and the scattering coefficients are zero, thus the opacity of air is taken as zero. This makes the all terms of RTE except the first term on the left hand side is zero, meaning a constant *I*.

5.6.2. Turbulence Equations

The equation solved in Spalart – Allmaras turbulence model, which is used to solve the effects of turbulence is given below.

5. Spalart – Allmaras Turbulence Model Equation:

$$\frac{\partial}{\partial t}(\rho\tilde{\nu}) + \frac{\partial}{\partial x_i}(\rho\tilde{\nu}u_i) = G_\nu + \frac{1}{\sigma_{\tilde{\nu}}}\left[\frac{\partial}{\partial x_j}\left\{(\mu+\rho\tilde{\nu})\frac{\partial\tilde{\nu}}{\partial x_j}\right\} + C_{b2}\rho\left(\frac{\partial\tilde{\nu}}{\partial x_j}\right)^2\right] - Y_\nu + S_{\tilde{\nu}} \qquad (5.8)$$

The turbulent viscosity can be solved by following equation:

$$\mu_t = \rho\tilde{\nu}f_{\nu 1} \qquad (5.9)$$

where;

$$f_{\nu 1} = \frac{\chi^3}{\chi^3 + C_{\nu 1}^3} \qquad \text{and;} \qquad \chi \equiv \frac{\tilde{\nu}}{\nu} \qquad (5.10)$$

In Equation (5.8)., the term $\tilde{\nu}$ is the variable that Spalart – Allmaras turbulence model solves. By using this variable turbulent viscosity can be estimated by using Equations (5.9). and (5.10).

5.6.3. Modelling Phase Change

In the simulations with PCMs, following equations are used to model the phase change phenomena. In FLUENT, an enthalpy – porosity formulation is employed to model the phase change. In this formulation, instead of modelling the liquid – solid interface, a variable called "liquid fraction" is calculated which is the volume of liquid form in cell and this variable is updated at the end of each iteration (ANSYS, 2011a).

The enthalpy of material is the sum of sensible enthalpy (h) and latent heat (ΔH)

$$H = h + \Delta H \qquad \text{where;} \qquad h = h_{ref} + \int_{T_{ref}}^{T} c_p dT \qquad (5.11)$$

In Equation (5.11), h_{ref} is the reference enthalpy, T_{ref} is the reference temperature, c_p is the specific heat of PCM at constant pressure.

The liquid fraction of PCM is calculated according to;

$$\begin{aligned} \beta &= 0 && \text{if} && T < T_{solidys} \\ \beta &= 1 && \text{if} && T > T_{solidus} \\ \beta &= \frac{T - T_{solidus}}{T_{liquidus} - T_{solidus}} && \text{if} && T_{solidus} < T < T_{liquidus} \end{aligned} \tag{5.12}$$

According to β, the latent heat amount (ΔH) can be calculated with the following equation.

$$\Delta H = \beta L \tag{5.13}$$

In Equation (5.13), L is the latent heat of material.

In phase change problems, the energy equation is written in the following form.

$$\frac{\partial}{\partial t}(\rho H) + \nabla.(\rho \vec{v} H) = \nabla.(k \nabla T) + S \tag{5.14}$$

The temperature of PCM is solved by an iteration between equations (5.14). and (5.12). According to equations (5.12). and (5.13), the latent heat content can vary from 0 to 1 in a during the phase change. If $T_{solidus}$ and $T_{liquidus}$ are equal, which is the case for pure materials, a more general form of above formulation is used suggested by (Voller & Prakash, 1987), which is based on specific heats. (ANSYS, 2011a)

5.7. Materials

The solid materials that are used in the construction of refrigerator are defined in the FLUENT interface and they are given in Table 5.4.

Table 5.4. Materials that are used in simulations and their thermal properties

Material	Density (ρ) kg/m^3	Specific Heat (c_p) J/Kg.K	Heat Conductivity (k) W/mK	Location where it is used
Polyurethane	31,32	1500	0,025	Body and door of the refrigerator
Plastic	50	1100	0,034	Door shelves, crispers and inner walls
Aluminum	2719	871	202.4	Evaporator plate
Stainless Steel	7800	500	45	Outer walls
Gasket	160	1170	0,13	Gasket between door and body
Glass	2230	750	1,14	Shelves
Brass	8520	3770	109	T_1, T_2, T_3 and $T_{crisper}$

5.8. Solver Settings

Under – relaxation factors are used to stabilize the convergence of residuals by controlling the change of variables during iterations. To improve the residuals in the simulations, some modifications are done on the under relaxation factors. They are given in Table 5.5.

Table 5.5. Under – Relaxation Factors

Pressure	0.3
Density	1
Body Forces	1
Momentum	0.4
Modified Turbulent Viscosity	0.8
Turbulent Viscosity	1
Energy	1
Liquid Fraction Update	1
Discrete Ordinates	1

By default, FLUENT stores the calculated variables in the cell centers of the mesh. For convection terms, values at the cell faces are required instead. To interpolate the face values from the cell values, upwinding schemas are used. For a fast

convergence, First Order Upwind scheme is used for momentum. For energy and modified turbulent viscosity, Second Order Upwind scheme is used and for discrete ordinates First Order Upwind scheme is used, which are default values. PRESTO! scheme is used for pressure interpolation, which is strongly recommended for natural convection flows. SIMPLE method is used for pressure – velocity coupling. Green – Gauss Cell Based method is used to calculate the derivatives and gradients of variables.

The solution methods are tabulated in Table 5.6.

Table 5.6. Solution Methods

Pressure - Velocity Coupling	SIMPLE
Gradient	Green - Gauss Cell - Based
Pressure	PRESTO!
Momentum	First Order Upwind
Modified Turbulent Viscosity	Second Order Upwind
Energy	Second Order Upwind
Discrete Ordinates	First Order Upwind

CHAPTER 6

RESULTS AND DISCUSSIONS

In this chapter, first, the steady temperature and velocity distributions of inner walls and a mid – section, and possible places for PCM application according to these distributions are discussed for a regular refrigerator (before PCM application). Then, transient temperature variations of measurement points (T_1, T_2, T_3 and $T_{crisper}$) are discussed and the results are compared with test results. After the verification of the model with tests, PCMs are placed to appropriate places and transient simulations are conducted again to see the effect of PCMs on temperatures of measurement points and inner walls. Finally, transient liquid fraction plots of PCMs are given and the effectiveness, benefits and drawbacks of PCM application are discussed.

All simulations including steady and transient are conducted with and without radiation and the effect of radiation is also discussed.

6.1. Numerical Investigation of Regular Refrigerator and Validation

Here, the numerical investigations conducted on the refrigerator before PCM application is discussed, for steady and transient cases to see the temperature map of the refrigerator, thus to find out the possible locations for PCM application.

6.1.1. Steady Temperature and Velocity Distributions

Wall and mid – section steady temperature contours and the velocity vector plot at the mid – section can be seen in Figure 6.1., Figure 6.2., Figure 6.3., Figure 6.4. respectively. The regions where the temperature is low enough, spatially uniform, and having a large area is considered to be the best places for PCM application. This kind of regions are discussed below.

In Figure 6.1., the temperature distribution at the mid – section; in Figure 6.2., velocity vectors at the mid – section; in Figure 6.3., the temperature distribution of bottom and top inner walls and finally in Figure 6.4., the temperature distributions of front, right and back wall are given.

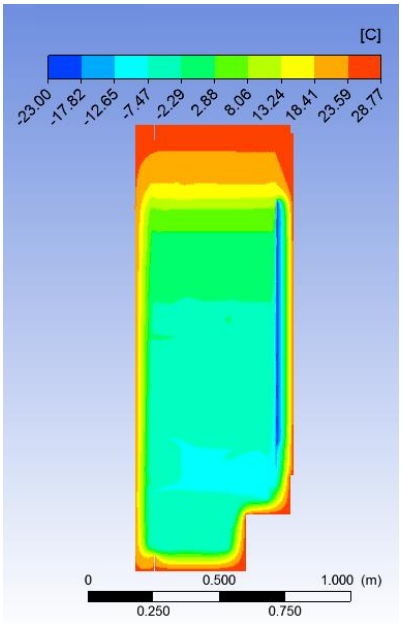

Figure 6.1. Temperature distribution at the mid section.

The left – hand side of Figure 6.1 is the front side of the refrigerator. The blue line on the back side indicates the section of serpentine type evaporator, having a temperature of -23^{o}C approximately. Since the only heat transfer mechanism is natural convection (effects of radiation between walls is not included in this case) and there is no fan to mix the air, a very high thermal stratification in vertical direction is observed. There is a region above the evaporator where the temperature is very high (in a range of 13 – 25^{o}C) and in the bottom the temperature is within a range of -7^{o}C and -2^{o}C.

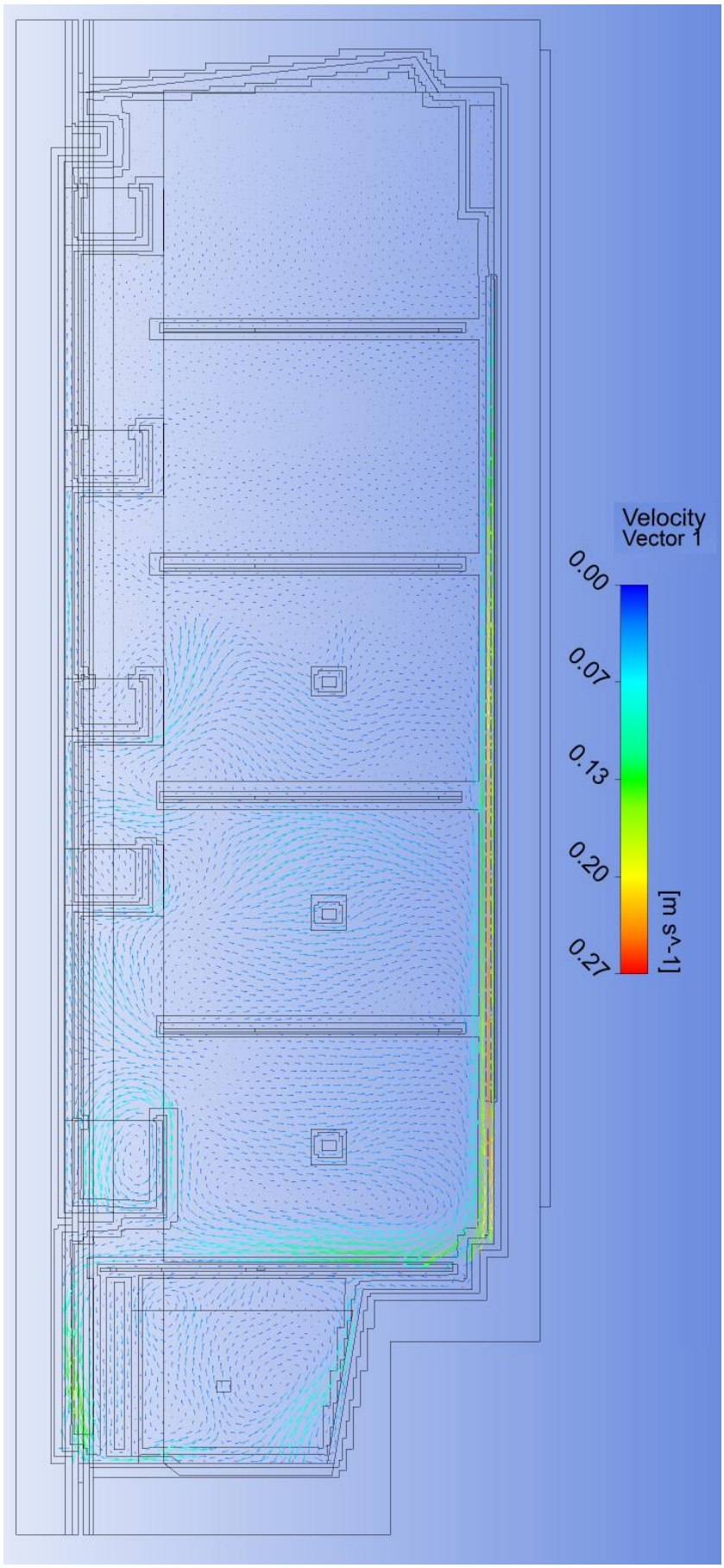

Figure 6.2. Velocity vectors at the mid section.

As seen on Figure 6.2. the air velocity above the evaporator is very low. The air layer touching the evaporator gets colder and moves to the bottom, cooling the bottom walls. Since there is no mechanism to move the air bulk above the evaporator, it stays stagnant and warm.

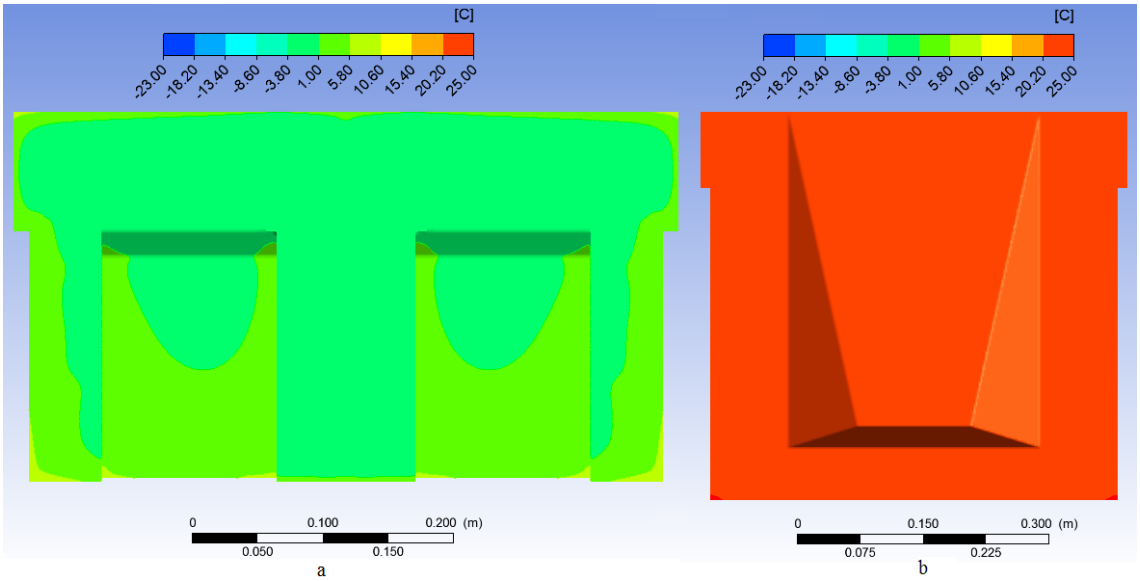

Figure 6.3. (a) Bottom and (b) Top wall temperature distributions.

In Figure 6.3., the temperature distribution at bottom and top walls can be seen. The top wall has a uniform and very high temperature because of the reasons explained above. Since the cold air coming from the vicinity of the evaporator hits the bottom wall, this wall has a relatively lower temperature compared to the other walls, having a temperature range of -4 and 5^{o}C.

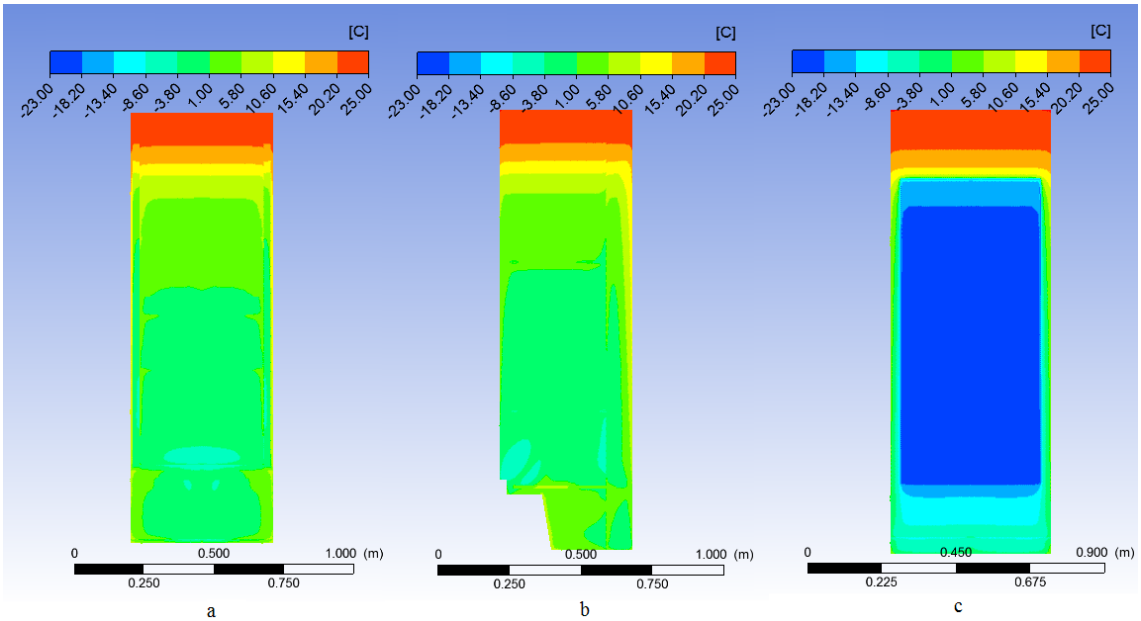

Figure 6.4. (a) front, (b) right and (c) back wall temperature distributions.

In Figure 6.4., front, right and back wall temperature distributions can be seen. Very high thermal stratification can also be observed from these figures. Back wall is the most suitable place for cool storage, since evaporator is installed here. Besides, there are large areas in front and right walls, where the temperature is approximately between -4 and 6^{o}C. PCM application can also be made to these places.

6.1.1.1. With Effects of Radiation

To see the effect of radiation in the steady temperature distributions of walls, simulation with discrete ordinates (DO) radiation model was conducted. In Figure 6.5., the temperature distribution at the mid – section; in Figure 6.7., velocity vectors at the mid – section; in Figure 6.8., the temperature distribution of bottom and top inner walls and in Figure 6.9., the temperature distributions of front, right and back wall with radiation are given.

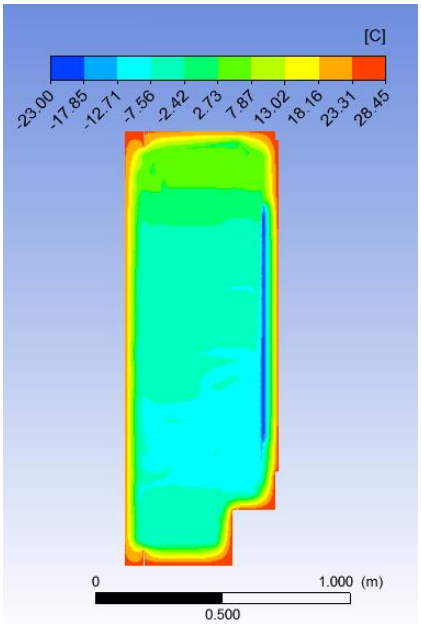

Figure 6.5. Temperature distribution at mid – section.

If Figure 6.5. is examined carefully and compared to Figure 6.1., one can notice that when the effects of radiative heat transfer is taken into account, the thermal stratification is far lower. High temperatures above the evaporator are not observed. While the temperature range above the evaporator is between 14 and 25^{o}C in Figure 6.1., it is only between 2 and 7^{o}C in Figure 6.5. This confirms the importance of the effects radiation between the walls of the refrigerated space.

To see the effect of radiation more clearly, Figure 6.1. and Figure 6.5. can be seen side by side in Figure 6.6. The comparison made by literature (O. Laguerre et al., 2007) can also be seen in this figure. O. Laguerre et. al. (2007) simulated the airflow inside a static type refrigerator with CFD. The refrigerator in that study is very similar to the refrigerator that this study deals with. They also conducted the simulations with and without radiation. Their constant evaporator temperature is 0.5^{o}C and the ambient temperature is 20^{o}C. As it can be seen in Figure 6.6, the temperature map is very similar in both studies. Very high thermal stratification in vertical direction is also observed by O. Laguerre et. al. when the radiation is off.

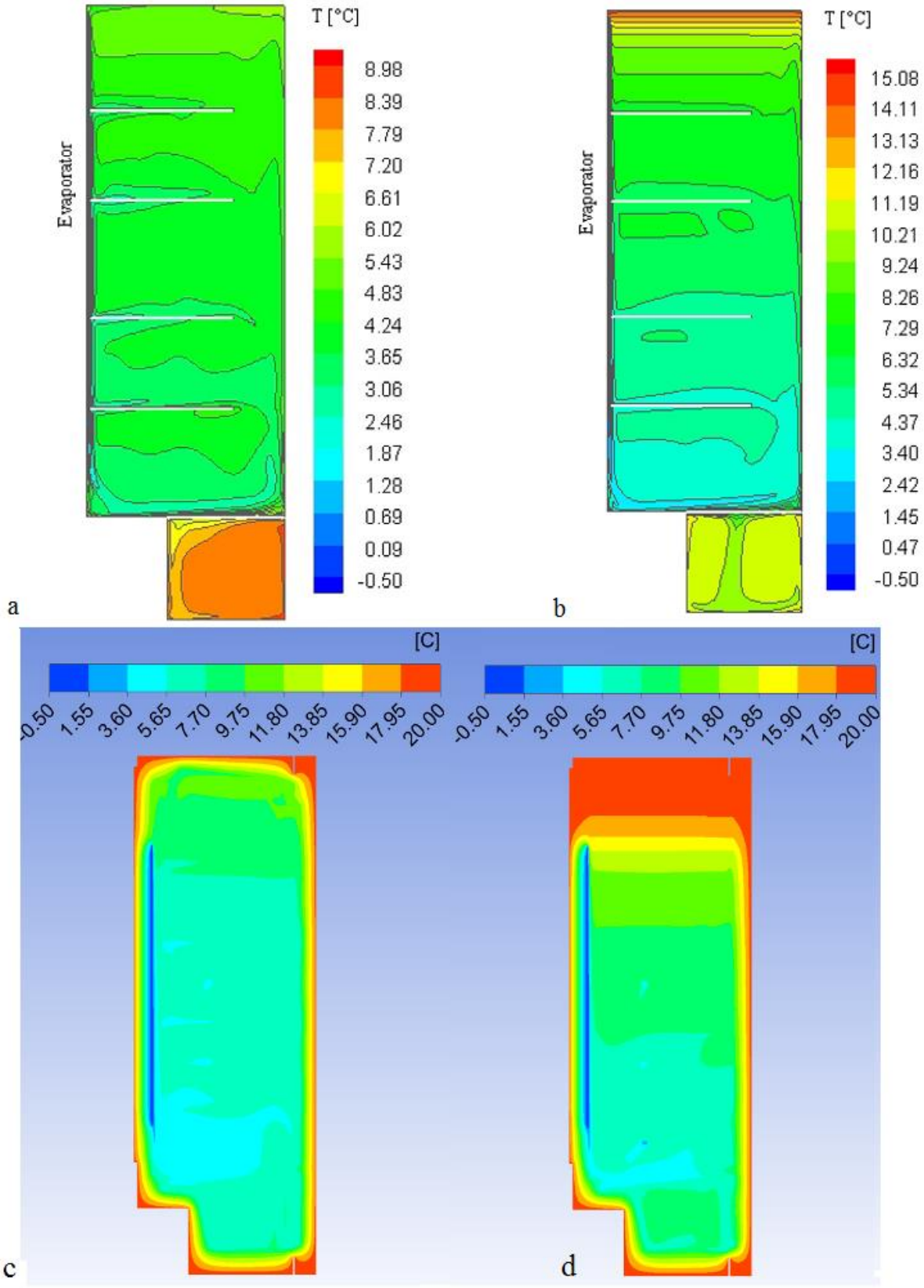

Figure 6.6. Comparison of temperature distributions at mid – section (a) O. Laguerre et. al. with radiation, (b) O. Laguerre et. al. without radiation (c) This study, with radiation, (d) This study, without radiation

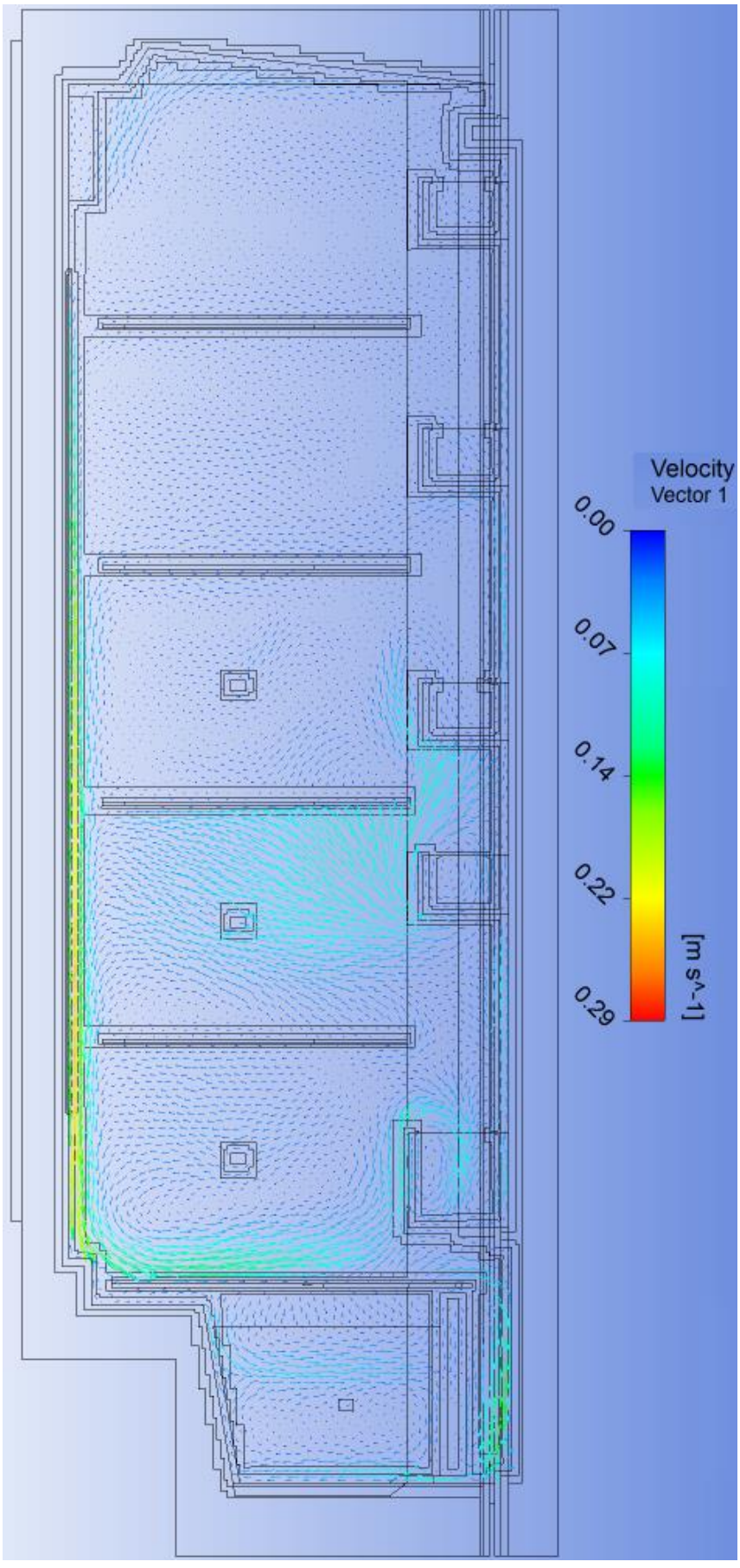

Figure 6.7. Velocity vectors at the mid – section.

In Figure 6.7. the velocity vectors when radiation is on can be seen. The air layer close to the evaporator plate on the back wall gets colder and falls, like in Figure 6.2. However, since the effects of radiation between walls is taken into account in this time, and the temperature gradient in walls is decreased, the air bulk above the evaporator starts to move as well.

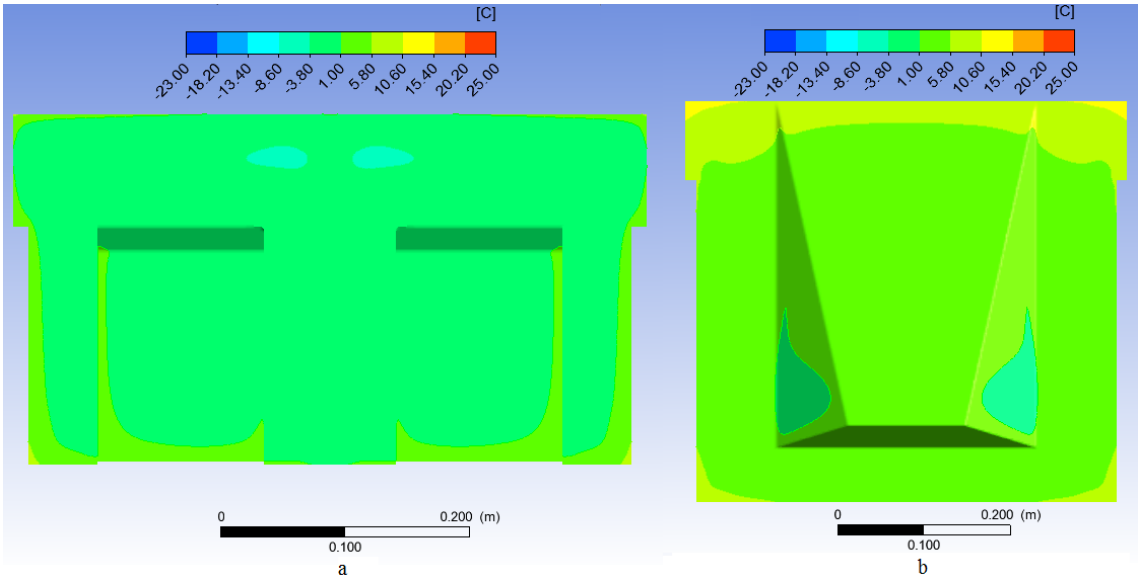

Figure 6.8. (a) Bottom and (b) Top wall temperature distributions.

In Figure 6.8., the temperature distributions of bottom and top walls with the effects of radiation can be seen If this is compared with Figure 6.3., it can be noticed that there is a big temperature decrease in top wall. While in Figure 6.3., the temperature of top wall is almost constant at about 25^{o}C., it is between 1 and 6^{o}C in Figure 6.8. The bottom wall temperature is also decreased slightly. It is between -4 and 5^{o}C in Figure 6.3. and between -4 and 1^{o}C in Figure 6.8.

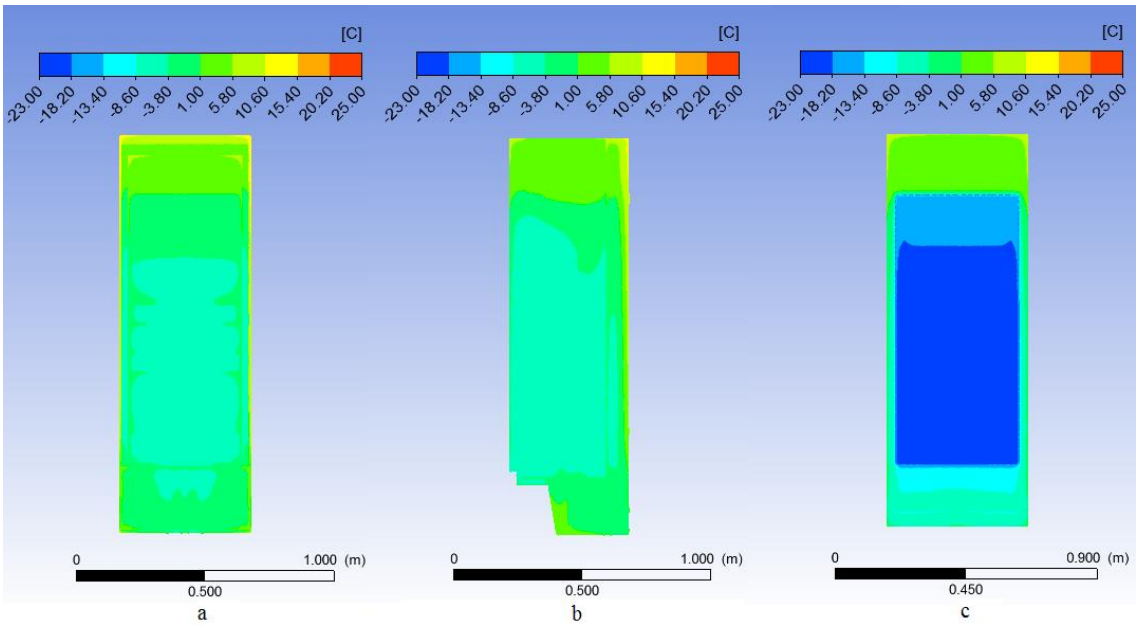

Figure 6.9. (a) front, (b) right and (c) back wall temperature distributions.

Much lower thermal stratification is also seen in Figure 6.9., when the radiation is enabled. The wall temperature is between 1 and 6^{o}C above the evaporator level.

When the vertical temperature distributions with and without effect of radiation is compared, it can be concluded that the wall temperatures are much more uniform when the radiation is enabled, especially in vertical direction. Effect of radiative heat transfer on the refrigerator temperatures is seem to be more dominant for the upper region of the refrigerator, whereas the bottom region temperatures does not seem to be too far off. If the refrigerator is divided into two equal pieces with an imaginary plane in the vertical direction, one can notice that the temperatures are almost the same when radiation is enabled in the piece at the bottom, and the temperatures are far lower in the piece above.

Table 6.1. Comparison of temperatures at measurement points

	Without Radiation	With Radiation
T_1	-1.54	-4.97
T_2	-3.76	-6.73
T_3	-5.24	-7.44
$T_{crisper}$	-1.37	-2.4
Average Cold Air Temperature	0.22	-4.95

In Table 6.1. the effect of radiation in the temperatures of measurement points and average cold air temperature can be seen. With radiation, the temperatures of T_1, T_2,

T_3 and $T_{crisper}$ decreased about 2 or 3^oC and the average air temperature decreased about 4^oC.

6.1.2. Transient Temperature Variations and Validation of CFD Model

In this section, the transient temperature profiles are presented for both walls and temperature measurement points without PCM application. The validation of CFD results with experiments can also be seen.

In Figure 6.10., the results of transient simulations can be seen. Blue lines represent the numerical simulations and red dotted lines represent the test results. The time axes starts from 53000 seconds, since it took long time to reach this steady regime. Earlier results do not contain meaningful information to present.

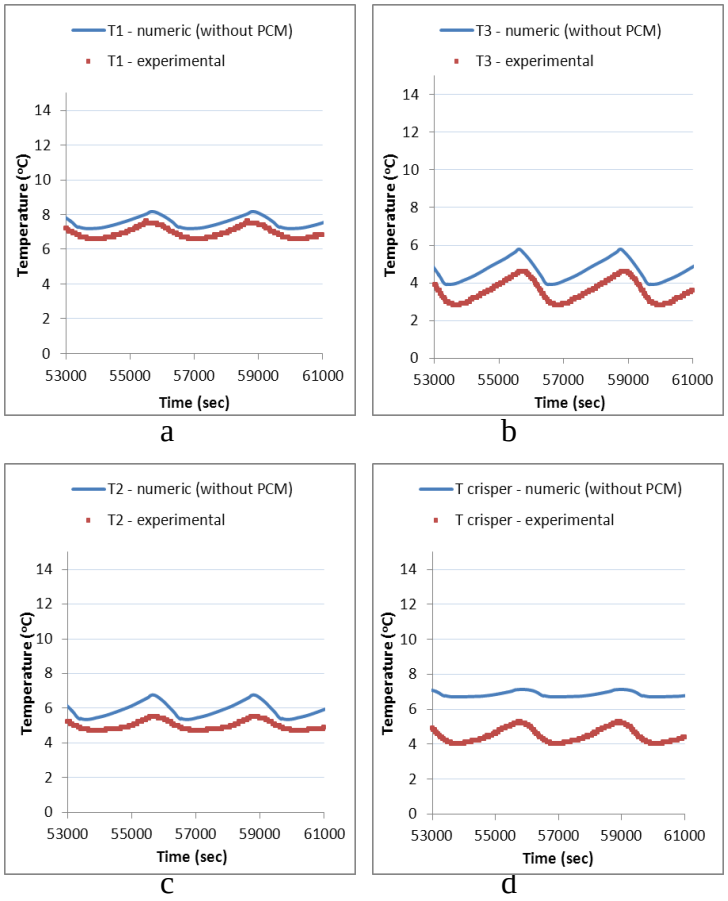

Figure 6.10. Validation of temperatures at measurement points when radiation is inactive, (a) T_1, (b) T_2, (c) T_3, (d) $T_{crisper}$

As it can be seen from Figure 6.10., the simulations showed a good agreement with test results. Temperature differences are not higher than 2°C. In T_1, the deviation between simulation and test is even less than 1°C. In T_2 and T_3, error margin is about 1°C and in $T_{crisper}$, the error margin is about 2°C.

The crisper is a plastic box placed on the bottom of refrigerated cabin. In actual refrigerator, the crisper takes some cool air from the gap between the shelf above and the crisper itself. Since it is not possible to model the air leakages from vacancies such as this, the crisper is modelled in full contact with the shelf. One possible reason of higher error margin in $T_{crisper}$ might be this.

6.1.2.1. With Effects of Radiation

In Figure 6.11., the effects of radiation on transient temperatures of measurement points can be seen. Like in Figure 6.10., the blue lines represent the simulation results, red dotted lines represent the test results.

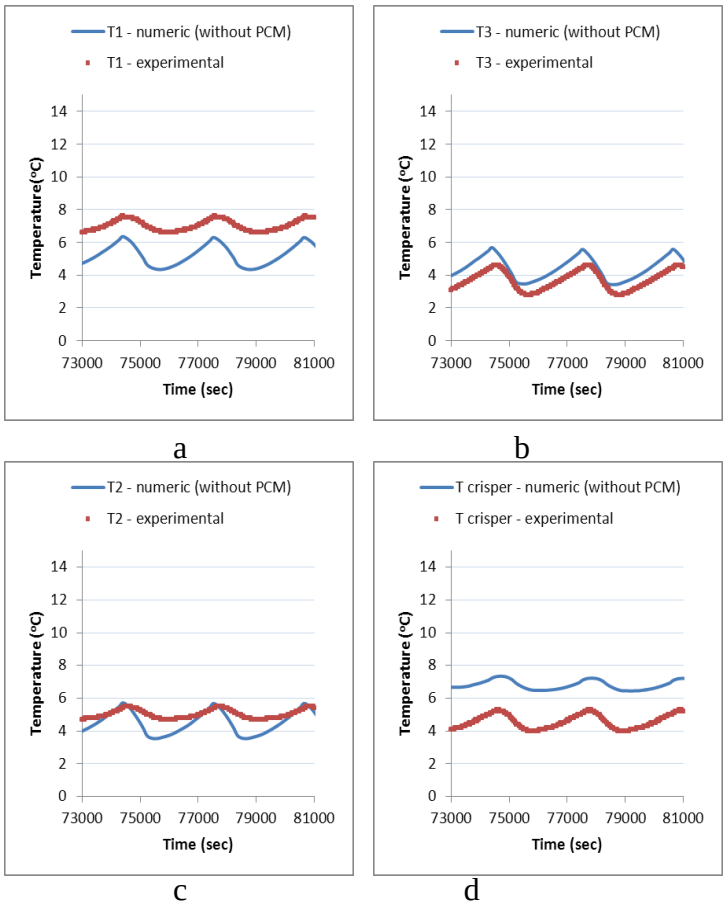

Figure 6.11. Validation of temperatures at measurement points when radiation is active, (a) T_1, (b) T_2, (c) T_3, (d) $T_{crisper}$

As it can be seen from Figure 6.11., the agreement of simulations with test results did not change much. Since the radiation reduced the high temperatures in upper half of the refrigerator (as it can be seen from steady temperature contours), the error margin between test and simulation results of T_1 increased to about 1^oC. Since the radiation model is activated later and it took some more time to reach the steady state after radiation is activated, the time axes are started from 73000 s.

If the uncertainities in tests and simulations, the assumptions and geometric simplifications before the simulations are considered, these error margins in transient results are thought to be acceptable.

6.2. Investigation the Effects of PCM

After the steady temperature map of the regular refrigerator is extracted and transient behavior of temperatures is acquired, next step was to specify the locations and specifications of PCMs and conduct the simulations again to see their effects.

6.2.1. Specification of PCMs and their locations

The specifications of PCMs are specified according to the transient wall temperatures. In the results of steady simulations, it was stated that the regions where the temperature is lower, spatially unniform and having a large area is considered to be the best places for PCM application. However, if the temperature of these regions does not vary in time, the PCM that applied to that location can't undergo phase change, thus it becomes useless.

Therefore, the locations which the temperature fluctuations are very high and exposed to higher heat transfer rates are thought to be suitable for PCM application. By this way, the heat conducted through this wall will melt the PCM and will be stored as latent heat, lowering the temperature increase rate of refrigerated space.

According to the transient simulations, an animation of temperature change of mid – section (symmetry plane) is created. By reviewing the frames of this animation,

the transient wall temperatures are estimated by using an estimation. The details of the estimation are explained below.

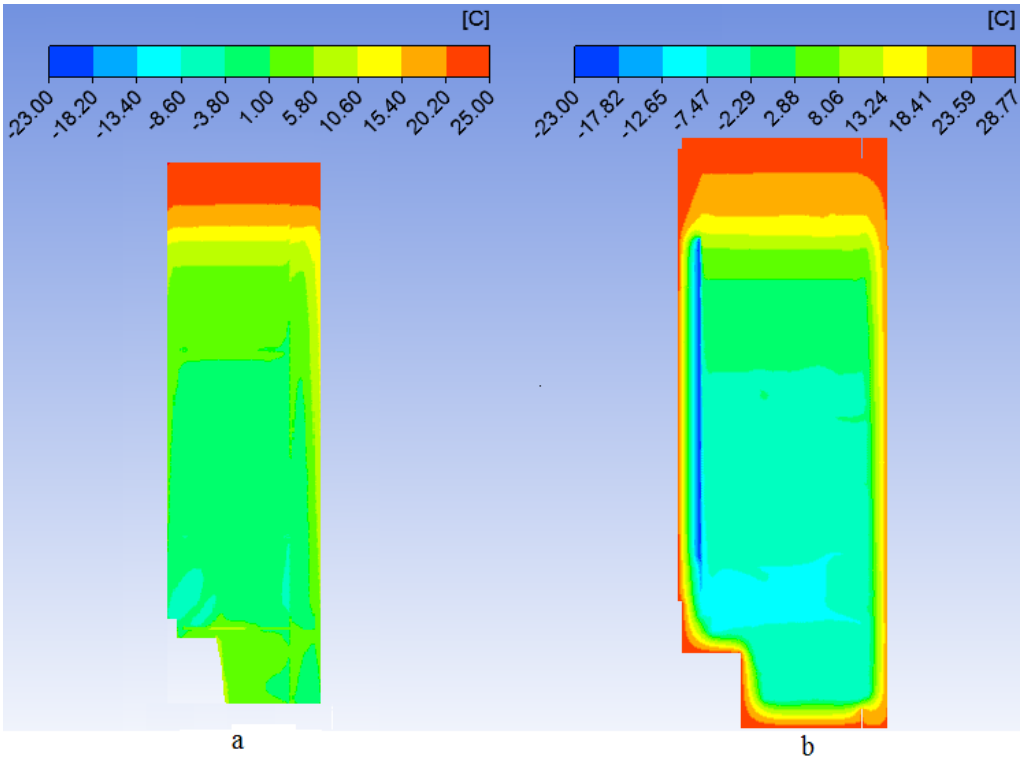

Figure 6.12. Comparison of steady temperature contours of right wall and mid – section. (a) right wall, (b) mid – section.

In Figure 6.12., the comparison of right wall and mid – section steady temperature contours are given. If those two temperature contours in Figure 6.12. are reviewed carefully, one can approximate that the temperature of right wall is nearly $2^{o}C$ higher than the mid – section and they have almost the same temperature map. By employing this approach, the right wall temperature profile is estimated by using the animation frames of mid – section transient temperature and PCM materials are specified according to time – averaged temperature of right wall. Commercially available PCM materials are selected by using the catalogue of PlusICE PCM Products Limited (PlusICE, 2013) and they are placed to appropriate places in front wall, right wall and bottom wall.

As explained in the previous chapters, the evaporator is located at the back wall of the refrigerator, so that the back wall is the coolest wall, having an average temperature of $0^{o}C$. So, pure water is applied as PCM to the back wall.

The list of selected PCMs, their thermal properties and the locations where they are used can be found on Table 6.2.

Table 6.2. Specifications of used PCMs (PlusICE, 2013)

PCM	Melting Temperature (T_{melt}) (^oC)	Enthalpy of Fusion (H_{fus}) (kj/kg)	Density (ρ) (kg/m^3)	Specific Heat (c_p) (kj/kg.K)	Heat Conductivity (k) (W/m.K)	Place where it is used
PlusICE S8	8	150	1475	1.9	0.44	Side and Front Walls
PlusICE S10	10	155	1470	1.9	0.43	Side and Front Walls
PlusICE S13	13	160	1515	1.9	0.43	Side and Front Walls, Bottom Wall
Pure Water	0	334	1000	4.18	0.60	Back Wall

The back wall (which is the coolest wall because of the evaporator), right wall, front wall and bottom wall are equipped with PCMs. Since the top wall is warmest and heat transfer rate from this wall is low, PCM was not applied to this wall. The placement of the PCMs explained in Table 6.2. can be seen on Figure 6.13.

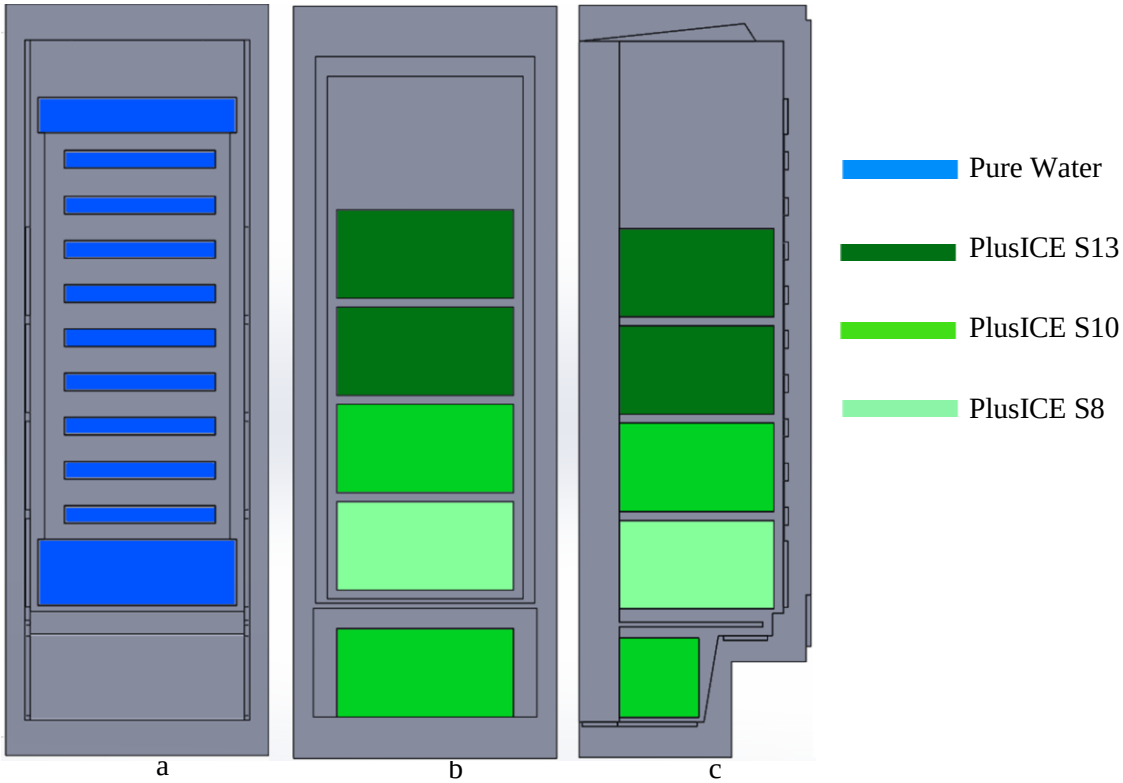

Figure 6.13. Location of PCM panels on (a) back, (b) front, (c) right walls

The detailed view of PCMs on the back of the evaporator can be seen on Figure 6.14. Here, the coiled black band represents the evaporator and the PCM panels containing pure water is placed between the evaporator coils.

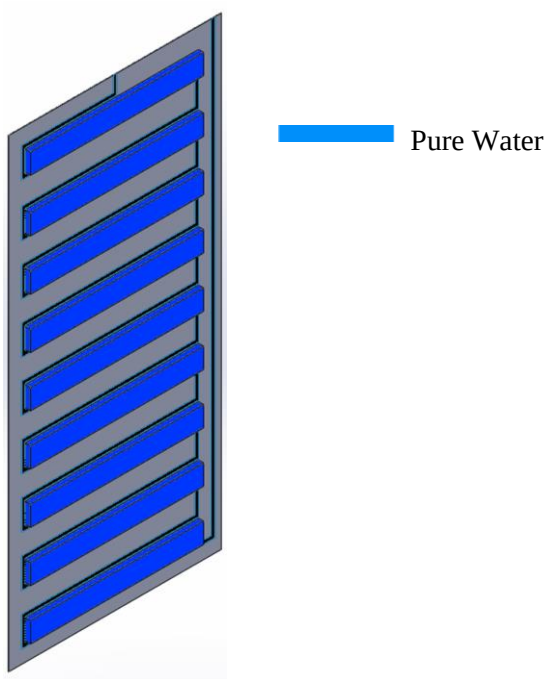

Figure 6.14. Location of PCM panels on the evaporator

These PCM slabs shown in Figure 6.13 Figure 6.14 have a thickness of 10 mm. The dimensions of five PCM slabs located on the front wall (Figure 6.14 (b)) have dimensions of 400 mm x 200 mm. On the right wall (Figure 6.14 (c)), first four PCM slabs have dimensions of 350 mm x 200 mm, because of the total width of this wall. The PCM slabs on the evaporator (Figure 6.15) have dimensions of 342 x 40 mm. In addition to the PCM slabs located on the evaporator, additional PCM slabs are placed on the top and bottom of the evaporator on the back wall, as seen on Figure 6.13 (a).

In Table 6.3., the total mass and latent heat capacity of the PCM slabs placed in each wall can be seen.

Table 6.3. Mass and latent heat capacity of PCM slabs at each wall

	Side Walls	Front Wall	Back Wall	Bottom Wall
PlusICE S13	4.242 kg 678.72 kJ	2.424 kg 387.84 kJ	-	0.833 kg 133.28 kJ
PlusICE S10	3.01 kg 466.55 kJ	2.352 kg 364.56 kJ	-	-
PlusICE S8	2.06 kg 309.75 kJ	1.180 kg 177 kJ	-	-
Pure Water	-	-	2.466 kg 823.811 kJ	-

In total, the latent heat capacity added to the regular refrigerator by means of placing PCM slabs to inner walls is 3341,5 kJ. Total PCM masses are as follows; 7.5 kg of PlusICE S13, 5.362 kg of PlusICE S10, 3.24 kg of PlusICE S8, 2.466 kg of pure water.

6.2.2. Effect on Measurement Points

In Figure 6.15., the effect of PCM slabs to the temperatures of T_1, T_2, T_3 and $T_{crisper}$ without effects of radiation can be seen.

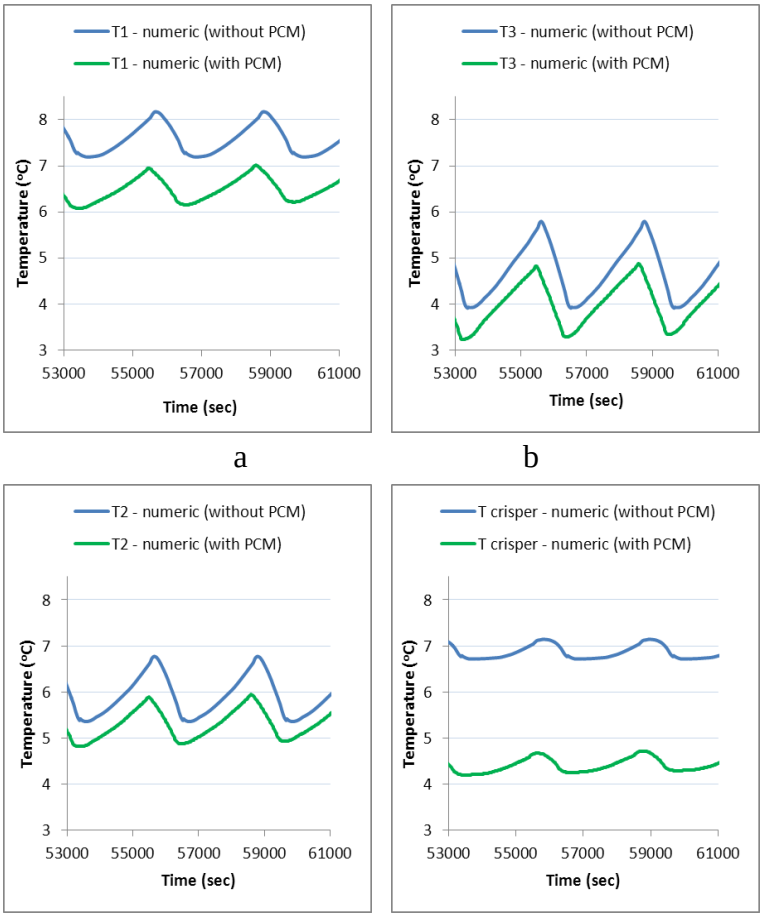

Figure 6.15. Effect of PCMs on temperatures at measurement points when radiation is inactive (a) T_1, (b) T_2, (c) T_3, (d) $T_{crisper}$

As seen on Figure 6.15., the temperature profiles are almost the same. However, the PCMs shifted the temperatures of measurement points below, thus it can be concluded that with PCM slabs, the mean air temperature in refrigerated space decreases. The decrease in temperatures is about 1^oC in T_1, T_2 and T_3 and about 2^oC in $T_{crisper}$.

6.2.2.1. With Effects of Radiation

In Figure 6.16., the effect of PCM slabs to the temperatures of T_1, T_2, T_3 and $T_{crisper}$ with effects of radiation can be seen.

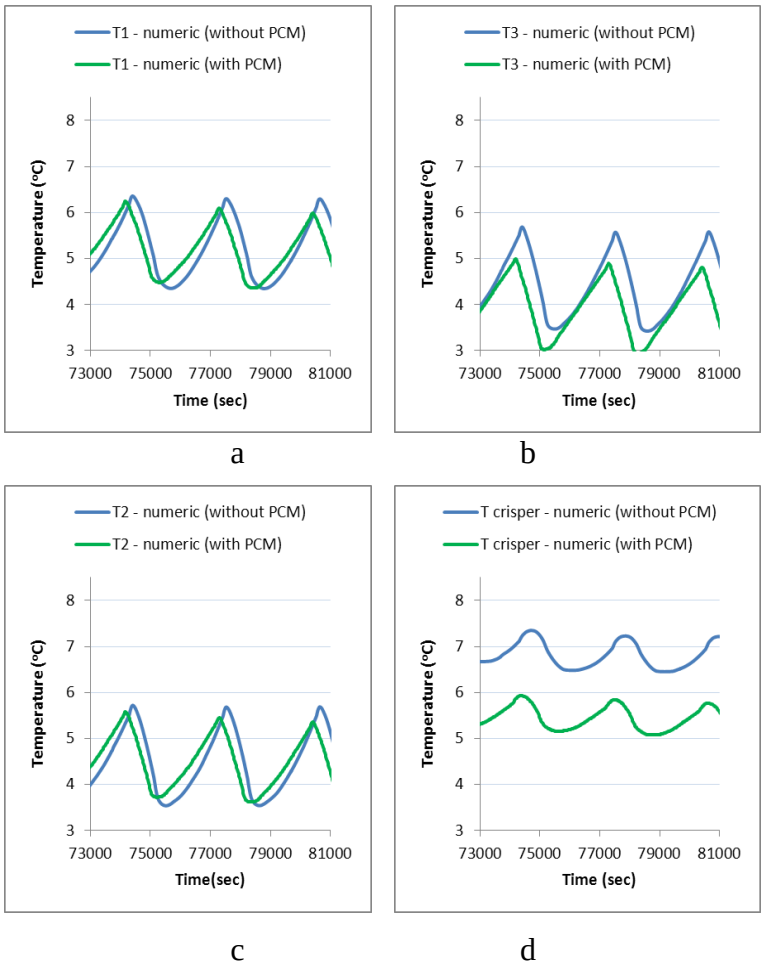

Figure 6.16. Effect of PCMs on temperatures at measurement points when radiation is active (a) T_1, (b) T_2, (c) T_3, (d) $T_{crisper}$

Here in Figure 6.16., the effects of radiation is taken into account in results of both PCM and non PCM simulations. It seems that when radiation is opened, addition of PCM slabs does not make any noticeable difference in temperatures of measurement points, especially in T_1 and T_2. If Figure 6.16. and Figure 6.15. is compared, since the main effect of radiative heat transfer is to reduce the temperatures of upper half, the results are decreased about 2 and 3^oC in T_1 and T_2 and the cases with and without PCM become almost coincident. In T_3, a slight decrease can be observed, less than 1^oC and in $T_{crisper}$, results with PCM is about 1.5^oC lower than without PCM.

If each plot in Figure 6.16. is examined carefully, one can notice that the PCMs decrease the rate of increase of the temperatures of measurement points slightly. For example, in Figure 6.17, a close look to the temperature profile of T_1 in Figure 6.16 can be seen.

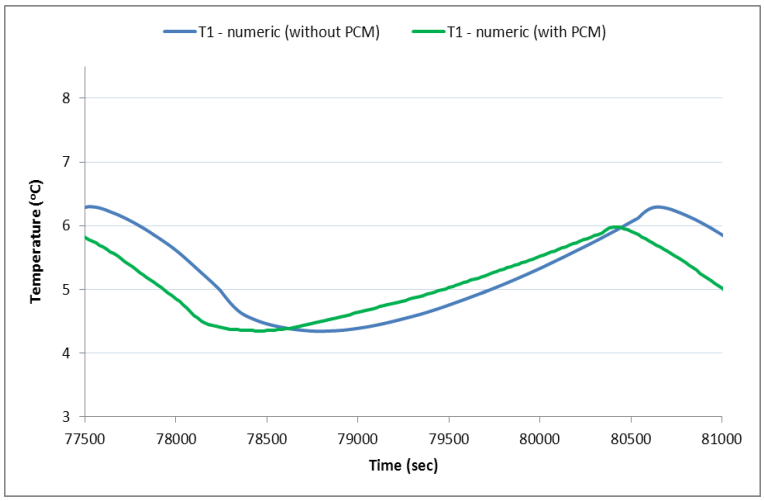

Figure 6.17. A closer look to the temperature profile of T_1

Here, it can be seen that the green plot representing the temperature with PCM has a slight lower slope than the blue plot. The minimum temperatures are the same, but there is about $0.5^{o}C$ difference between the maximum temperatures where the temperature without PCM is higher. This result is not as good as expected and bring the question to the minds that if all the PCM slabs undergo phase change.

In the following part, the effect of PCM slabs to the wall temperatures with and without radiation is discussed.

6.2.3. Effect on Wall Temperatures

In Figure 6.18., the effect of PCM slabs on wall temperatures when radiation is inactive can be seen.

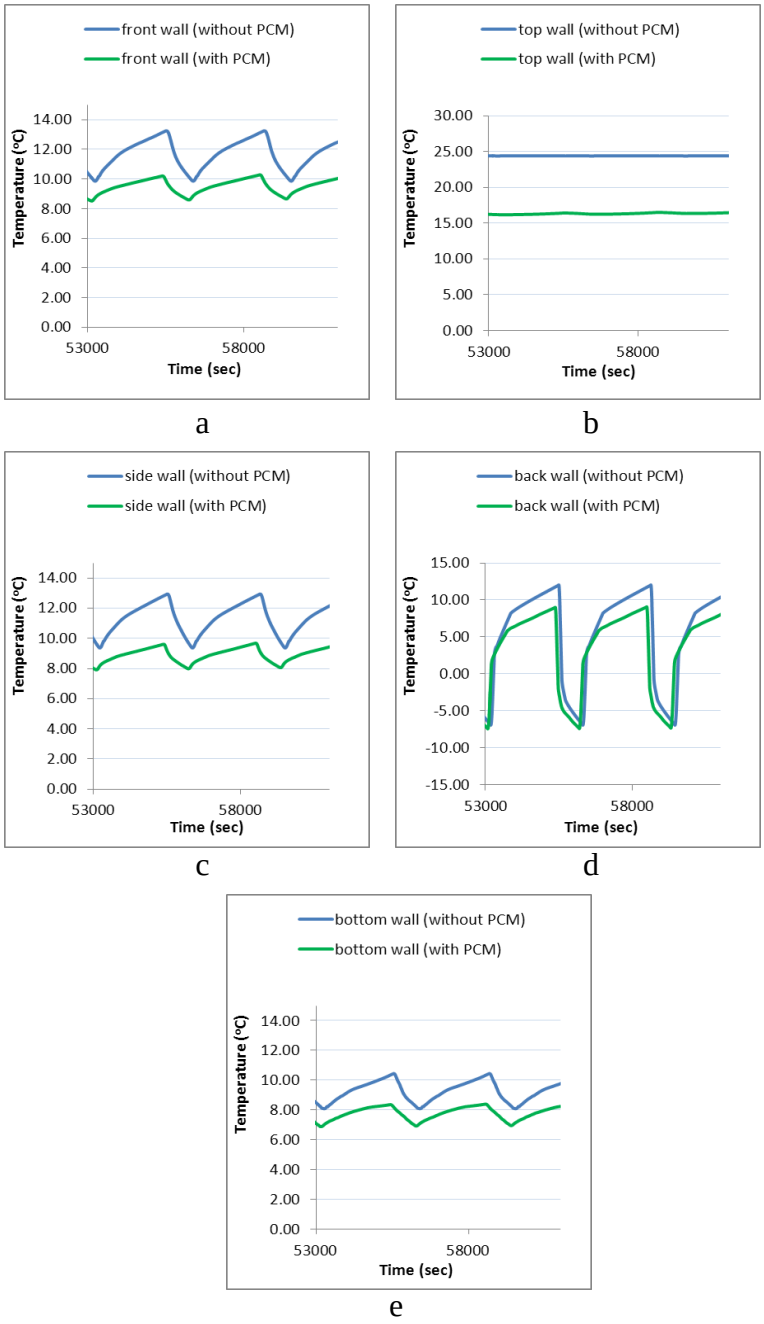

Figure 6.18. Effects of PCMs on wall temperatures when radiation is inactive, (a) front wall, (b) top wall, (c) side wall, (e) bottom wall

Here in Figure 6.18., both mean temperatures and the rates of change of temperatures of walls decrease with the application of PCM, which indicates that the PCM slabs store some amount of heat energy as latent heat, thus prevent the high temperature fluctuations. The decrease in mean temperatures are about 2^{o}C in front, side, bottom and back walls. In top wall, a big mean temperature decrease can be observed, of about 9^{o}C.

6.2.3.1. With Effects of Radiation

In Figure 6.19., the effect of PCM slabs on wall temperatures when radiation is active can be seen.

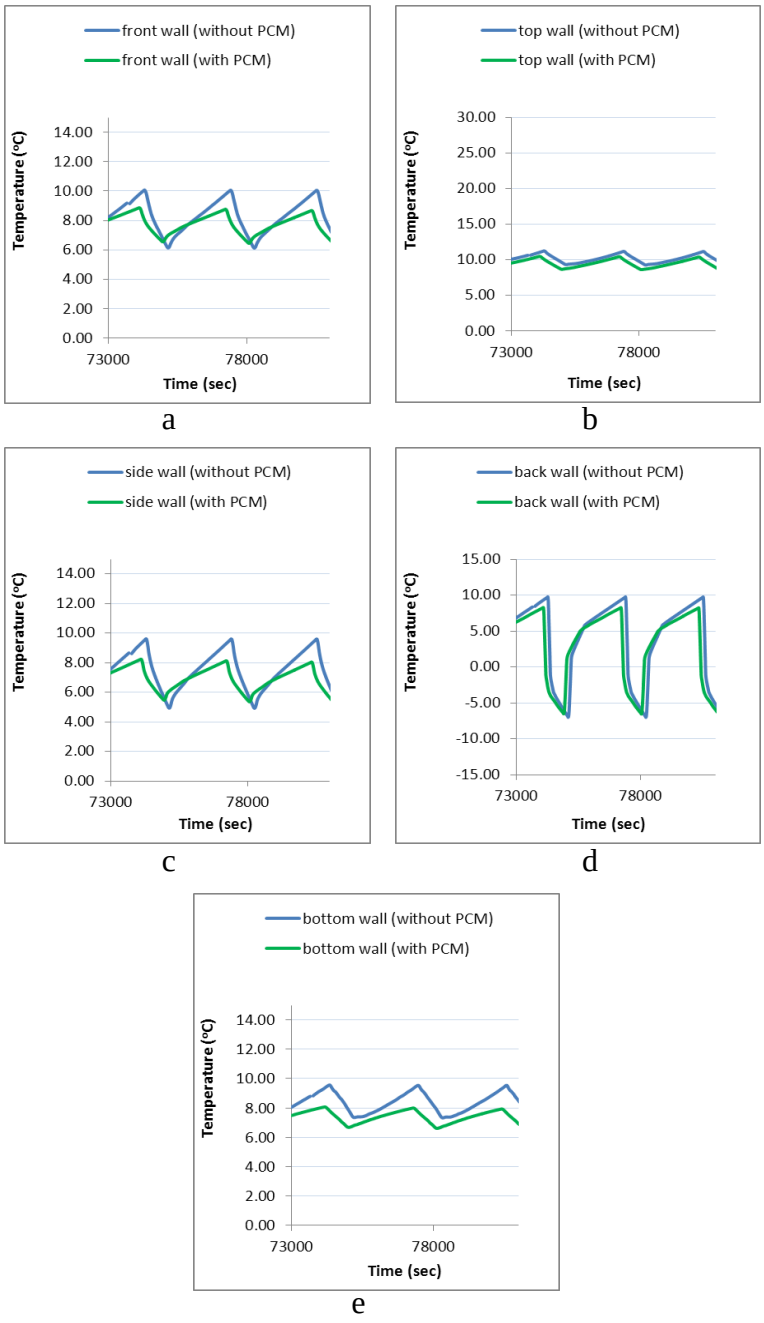

Figure 6.19. Effects of PCMs on wall temperatures when radiation is active, (a) front wall, (b) top wall, (c) side wall, (e) bottom wall

In Figure 6.19., the effect of radiation on refrigerator walls with PCM slabs can be seen. Here, the PCMs decrease not the mean wall temperatures, but the rates of

change of temperatures. There is almost no difference in the top wall, since the temperature is higher and heat transfer rate is lower at this wall.

If Figure 6.18. and Figure 6.19. are compared, one can notice that the time averaged temperatures of all walls are decreased without radiative heat transfer. The rates of changes of temperatures decrease in both cases in about the same magnitude. In this context, a conclusion may be extracted that if radiation is dominant in a refrigerator similar to this study deals with, effect of PCM slabs just decrease the rates of change of temperatures. If radiation is not dominant, where the fourth powers of wall temperature differences of refrigerator are small enough, the effect of PCM slabs decrease both time averaged temperatures and fluctuation of temperatures.

In Table 6.4. a comparison of time averaged temperatures of both measurement points and wall temperatures are given. As it was mentioned above, while the difference between front wall temperatures with and without PCM is 2.75^{o}C, this temperature difference reduces to just 0.96^{o}C while radiation is not neglected.

Table 6.4. Comparison of time averaged temperatures at various locations

		T_1 (^{o}C)	T_2 (^{o}C)	T_3 (^{o}C)	$T_{crisper}$ (^{o}C)	Front Wall (^{o}C)	Right Wall (^{o}C)	Bottom Wall (^{o}C)	Top Wall (^{o}C)	Back Wall (^{o}C)
Radiation is OFF	Without PCM	7.54	5.88	4.65	6.86	11.65	11.28	9.22	24.39	5.33
	With PCM	6.47	5.28	3.98	4.40	9.50	8.90	7.76	16.32	3.61
Radiation is ON	Without PCM	5.28	4.55	4.47	6.88	8.25	7.50	8.40	10.20	3.49
	With PCM	5.24	4.55	3.97	5.45	7.79	7.44	7.51	10.66	3.13

6.3. Solidification and Melting Rates of PCM Slabs

The discussions made above showed that the effect of PCM slabs does not make too much sense especially in measurement points when the radiative heat transfer is important. (Figure 6.16, for example) So, a question may arise in minds about the effectiveness of PCM slabs, asking that what amount of the PCM slabs undergo phase change? The liquid fraction plots of all PCM slabs can be seen in Figure 6.20.

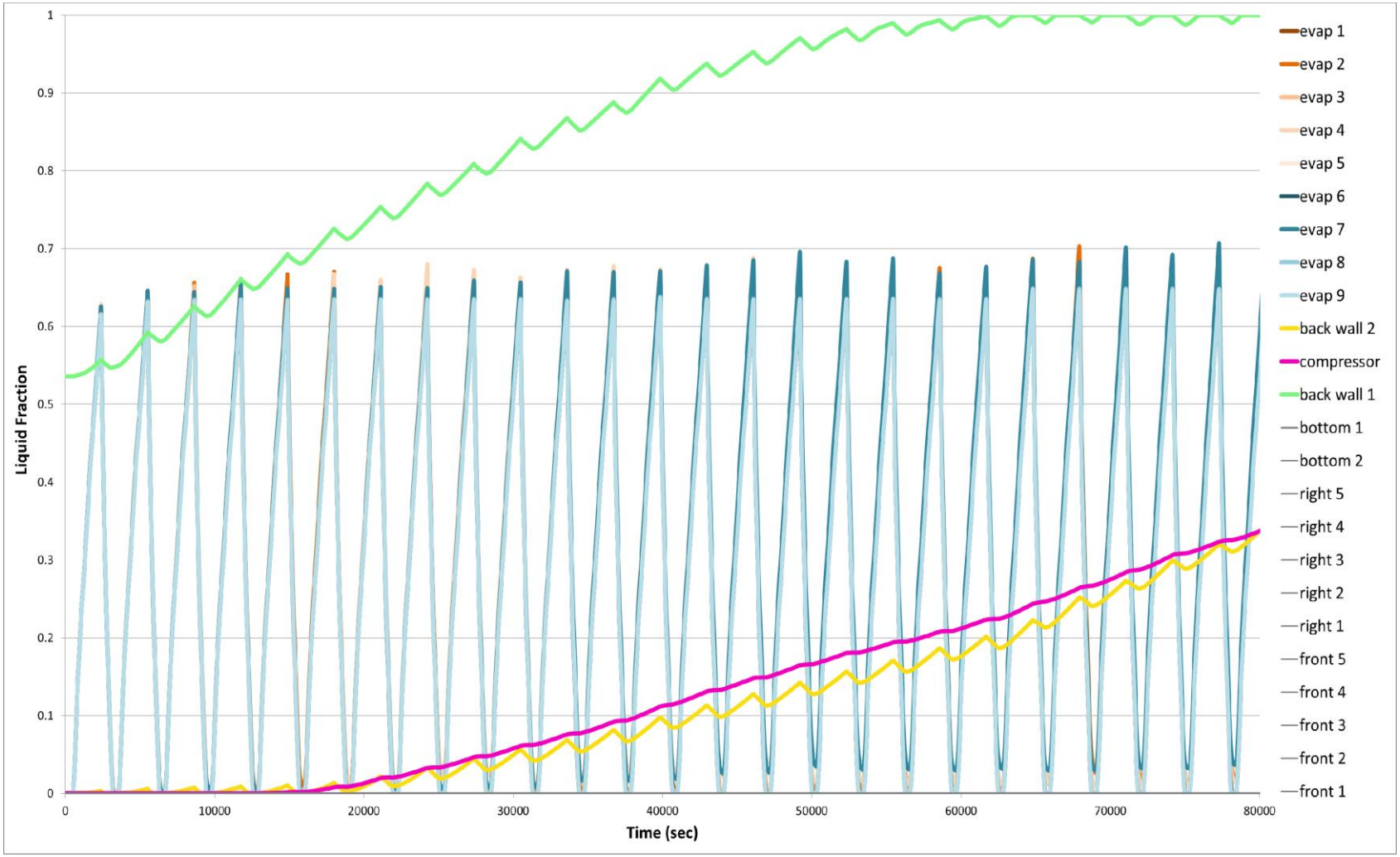

Figure 6.20. Liquid Fractions of PCM slabs

In Figure 6.20., as it can be seen, none of the PCM slabs undergo phase change on side and front walls, which have always zero liquid fraction. They are shown in black in the legend of the figure. The 9 PCM slabs containing water at the back wall, named as Evap 1, Evap 2 and so on showed some effectiveness. As it can be seen on the figure, their liquid fraction fluctuates between 0 and 0.7, which means that %70 of water in each PCM slab undergo phase change.

The other 2 PCM slabs on the back, named as “Back Wall 2” and “Compressor” could not reach the steady state regime, At the end of the simulations, they have a liquid fraction of about 0.3. Since their phase change behavior is not highly oscillatory like the slabs on the evaporator, the heat transfer on those slabs is not high enough; which implies that they are also not so effective. The slab named as “Back Wall 1”is also not effective. At the beginning of the simulation, it had a liquid fraction of 0.5, and become steady at 1, it does not even contain any latent heat, thus became useless.

As it will be mentioned in the next chapter, the most critical and highly necessary point is to study the locations and phase change temperatures of PCMs, since ineffective PCMs weaken the insulation of walls because of their higher heat conductivities.

CHAPTER 7

CONCLUSIONS

Latent energy storage with PCMs in household refrigerators are relatively new approach to increase their temperature performance and energy efficiency. This approach increases the efficiency of the refrigerator, since the heat transferred through the wall of refrigerator is stored in PCMs as latent heat, preventing the increase the temperature of refrigerated space. PCMs are interesting materials with their high latent heat storage capacities and nearly constant phase change temperatures, thus their popularity in thermal applications are getting higher in recent years.

This study is intended to see the effects of PCM application numerically on refrigerated space temperatures of a static type household refrigerator. Since an experimental study has many difficulties and requires too much time, a numerical study is conducted by using the CFD approach. ANSYS – FLUENT commercial CFD code is employed.

According to many studies found in literature, radiative heat transfer between inner walls of a refrigerator cannot be ignored. Because of this, whole numerical study is conducted with and without a radiation model and effects of radiation is validated.

According to the results, it is shown that effect of PCM lowers both the level, and the magnitude of fluctuations of temperatures. The transient fluctuations of temperature are caused by the cyclic working principle of refrigerator controlled by the thermostat. Since decreasing this fluctuation makes it longer to reach the upper limit of the thermostat, using PCM slabs on refrigerator will most probably decrease the number of stop and start cycles of the compressor in a particular amount of time, which increase the efficiency of the refrigeration cycle. This effect of PCM slabs on the number of stop and start cycles in a certain time period could not be modelled numerically, since there are many difficulties on implementation of boundary conditions.

The favorable effect of PCM slabs applied on inner walls of the refrigerator comes up only when all of the PCM slabs undergo phase change completely. If the PCM does not change its phase, the latent heat storage feature of PCM slabs will be lost and since their heat conductivity is higher than the insulation material used in the wall

of the refrigerator, the refrigerated space temperatures will be affected adversely. Therefore, designation of the locations, total mass and phase change temperatures of PCM slabs are highly critical.

According to these, some complementary future works for this study may be proposed as follows:

- The algorithm that implementing the thermostat of the refrigerator should be introduced in the boundary conditions to see the decreasing the number of stop and start cycles of the compressor.
- Different mesh types and meshes containing different cell numbers should be employed in simulations to see the effect of mesh on results more clearly.
- Different scenarios should be applied with PCMs. The masses and phase change temperatures of PCMs should be optimized to suppress the negative effects of PCMs when they do not undergo phase change.
- A more powerful computer must be used in CFD simulations to gain time and to simulate more cases in a limited time period.

REFERENCES

ANSYS. (2011a). ANSYS FLUENT Theory Guide.

ANSYS. (2011b). ANSYS FLUENT UDF Manual.

ANSYS. (2011c). ANSYS FLUENT User's Guide.

Azzouz, K., Leducq, D., & Gobin, D. (2008). Performance enhancement of a household refrigerator by addition of latent heat storage. *International Journal of Refrigeration, 31*(5), 892-901. doi: 10.1016/j.ijrefrig.2007.09.007

Azzouz, K., Leducq, D., & Gobin, D. (2009). Enhancing the performance of household refrigerators with latent heat storage: An experimental investigation. *International Journal of Refrigeration, 32*(7), 1634-1644. doi: 10.1016/j.ijrefrig.2009.03.012

Azzouz, K., Leducq, D., Guilpart, J., Gobin, D. (2005). *Improving the energy efficiency of a vapor compression system using a phase change material*. Paper presented at the Proceedings of Second Conference on Phase Change Material & Slurry, Yverdon les Bains, Switzerland.

Ben Amara, S., Laguerre, O., Charrier-Mojtabi, M. C., Lartigue, B., & Flick, D. (2008). PIV measurement of the flow field in a domestic refrigerator model: Comparison with 3D simulations. *International Journal of Refrigeration, 31*(8), 1328-1340. doi: 10.1016/j.ijrefrig.2008.04.005

Cheng, Wen-Long, Mei, Bao-Jun, Liu, Yi-Ning, Huang, Yong-Hua, & Yuan, Xu-Dong. (2011). A novel household refrigerator with shape-stabilized PCM (Phase Change Material) heat storage condensers: An experimental investigation. *Energy, 36*(10), 5797-5804. doi: 10.1016/j.energy.2011.08.050

Cheng, Wen-Long, & Yuan, Xu-Dong. (2013). Numerical analysis of a novel household refrigerator with shape-stabilized PCM (phase change material) heat storage condensers. *Energy, 59*, 265-276. doi: 10.1016/j.energy.2013.06.045

CoalTech. (August 2008). *CoalTech News, Volume 1*.

Dincer, I., & Kanoglu, M. (2011). *Refrigeration Systems and Applications*: Wiley.

Dossat, R.J. (1961). *Principles of refrigeration*: Wiley.

Farid, M.M. (2010). *Mathematical Modeling of Food Processing*: Taylor & Francis.

Farid, Mohammed M., Khudhair, Amar M., Razack, Siddique Ali K., & Al-Hallaj, Said. (2004). A review on phase change energy storage: materials and applications. *Energy Conversion and Management, 45*(9-10), 1597-1615. doi: 10.1016/j.enconman.2003.09.015

Gawron, K., & Schröder, J. (1977). Properties of some salt hydrates for latent heat storage. *International Journal of Energy Research, 1*(4), 351-363. doi: 10.1002/er.4440010407

Gin, Benjamin, & Farid, Mohammed M. (2010). The use of PCM panels to improve storage condition of frozen food. *Journal of Food Engineering, 100*(2), 372-376. doi: 10.1016/j.jfoodeng.2010.04.016

Gupta, J. K., Ram Gopal, M., & Chakraborty, S. (2007). Modeling of a domestic frost-free refrigerator. *International Journal of Refrigeration, 30*(2), 311-322. doi: 10.1016/j.ijrefrig.2006.06.006

IIR. (2002). Report on Refrigeration Sector Achievements amd Challenges. *International Institute of Refrigeration*.

Incropera, Frank P. (2006). *Fundamentals of Heat and Mass Transfer*: John Wiley \\& Sons.

Kuznik, Frédéric, David, Damien, Johannes, Kevyn, & Roux, Jean-Jacques. (2011). A review on phase change materials integrated in building walls. *Renewable and Sustainable Energy Reviews, 15*(1), 379-391. doi: 10.1016/j.rser.2010.08.019

Laguerre, O., Ben Amara, S., Moureh, J., & Flick, D. (2007). Numerical simulation of air flow and heat transfer in domestic refrigerators. *Journal of Food Engineering, 81*(1), 144-156. doi: 10.1016/j.jfoodeng.2006.10.029

Laguerre, O., & Flick, D. (2004). Heat transfer by natural convection in domestic refrigerators. *Journal of Food Engineering, 62*(1), 79-88. doi: 10.1016/s0260-8774(03)00173-0

Laguerre, Onrawee, Derens, Evelyne, & Palagos, Bernard. (2002). Study of domestic refrigerator temperature and analysis of factors affecting temperature: a French survey. *International Journal of Refrigeration, 25*(5), 653-659. doi: http://dx.doi.org/10.1016/S0140-7007(01)00047-0

Marques, A. C., Davies, G. F., Evans, J. A., Maidment, G. G., & Wood, I. D. (2013). Theoretical modelling and experimental investigation of a thermal energy storage refrigerator. *Energy, 55*, 457-465. doi: 10.1016/j.energy.2013.03.091

Marques, A. C., Davies, G. F., Maidment, G. G., Evans, J. A., & Wood, I. D. (2014). Novel design and performance enhancement of domestic refrigerators with thermal storage. *Applied Thermal Engineering, 63*(2), 511-519. doi: 10.1016/j.applthermaleng.2013.11.043

Mehling, H., & Cabeza, L.F. (2008). *Heat and cold storage with PCM: An up to date introduction into basics and applications*: Springer.

Oró, E., Miró, L., Farid, M. M., & Cabeza, L. F. (2012). Improving thermal performance of freezers using phase change materials. *International Journal of Refrigeration, 35*(4), 984-991. doi: 10.1016/j.ijrefrig.2012.01.004

Padet, J. (1997). *Principes des transferts convectifs*: Polytechnica.

Patel, Mehul. (2013). 4 Advantages and Disadvantages of CFD. Retrieved 28.04.2014, from http://cfdmodelingservices.wordpress.com/2013/06/12/4-advantages-and-disadvantages-of-cfd/

PlusICE. (2013). PlusICE Phase Change Materials.

Sharma, Atul, Tyagi, V. V., Chen, C. R., & Buddhi, D. (2009). Review on thermal energy storage with phase change materials and applications. *Renewable and Sustainable Energy Reviews, 13*(2), 318-345. doi: 10.1016/j.rser.2007.10.005

Sharma, S. D., & Sagara, Kazunobu. (2005). Latent Heat Storage Materials and Systems: A Review. *International Journal of Green Energy, 2*(1), 1-56. doi: 10.1081/ge-200051299

Subramaniam, P. R., Tulapurkar, C., Thagamani, G., Thiyagarajan, R.,. (2010). *Phase Change Materials For Domestic Refrigerators To Improve Food Quality And Prolong Compressor Off Time.* Paper presented at the International Refrigeration and Air Conditioning Conference.

Versteeg, H.K., & Malalasekera, W. (2007). *An Introduction to Computational Fluid Dynamics: The Finite Volume Method*: Pearson Education Limited.

Voller, V. R., & Prakash, C. (1987). A fixed grid numerical modelling methodology for convection-diffusion mushy region phase-change problems. *International Journal of Heat and Mass Transfer, 30*(8), 1709-1719. doi: http://dx.doi.org/10.1016/0017-9310(87)90317-6

Whitman, W.C., Johnson, W.M., & Tomczyk, J. (2005). *Refrigeration & Air Conditioning Technology*: Delmar Cengage Learning.

Zalba, Belén, Marín, José Ma, Cabeza, Luisa F., & Mehling, Harald. (2003). Review on thermal energy storage with phase change: materials, heat transfer analysis and applications. *Applied Thermal Engineering, 23*(3), 251-283. doi: http://dx.doi.org/10.1016/S1359-4311(02)00192-8